High-precision measurement of the W boson mass with the CDF II detector

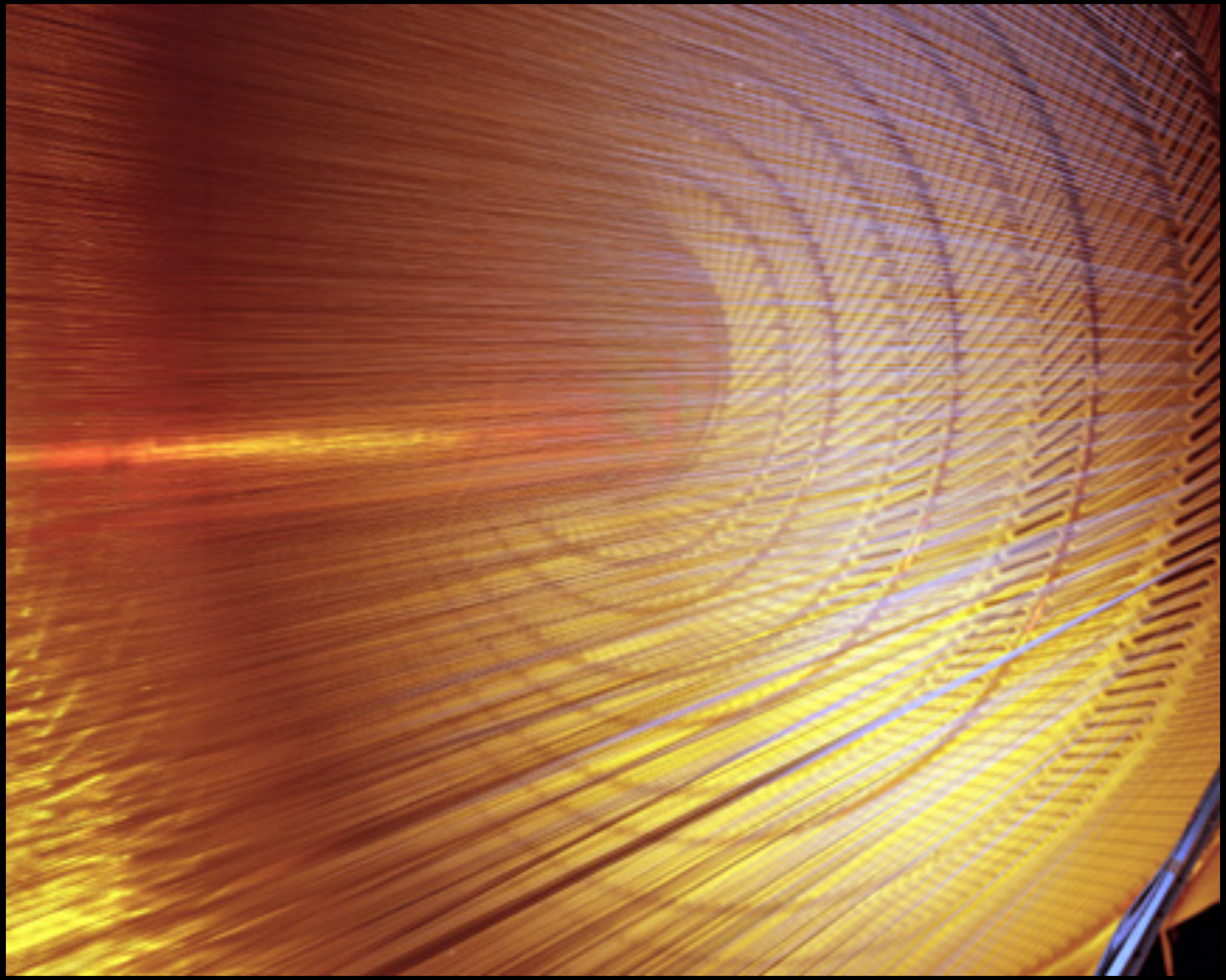

Chris Hays, Oxford University

Science & Technology Facilities Council
Rutherford Appleton Laboratory

RAL seminar
4 May, 2022

Electroweak gauge boson masses

In a gauge-symmetric theory the phase of a matter field does not affect physical processes

QED: $\mathscr{L} = D_\mu \phi D^\mu \phi - \frac{1}{4} F_{\mu\nu} F^{\mu\nu},$

$$\phi' = e^{ie\alpha(x)}\phi, \quad A'^{\mu} = A^\mu - \partial^\mu \alpha(x)$$

$$\mathscr{L}' = \mathscr{L}$$

The gauge field transports the matter field according to the gauge field strength (curvature)

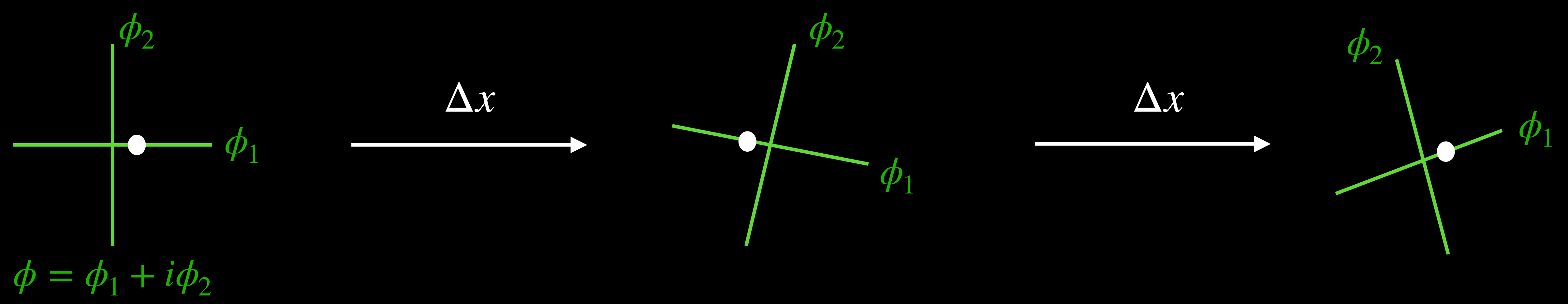

The gauge symmetry allows a choice of axes that removes the phase

Electroweak gauge boson masses

The weak gauge symmetry SU(2) transports the phase through three fields W_1, W_2, W_3

$$\mathscr{L} = D_\mu \phi^a D^\mu \phi^a + \mu^2 \phi^\dagger \phi - \lambda(\phi^\dagger \phi)^2 - \frac{1}{4} F^a_{\mu\nu} F^{a,\mu\nu}$$

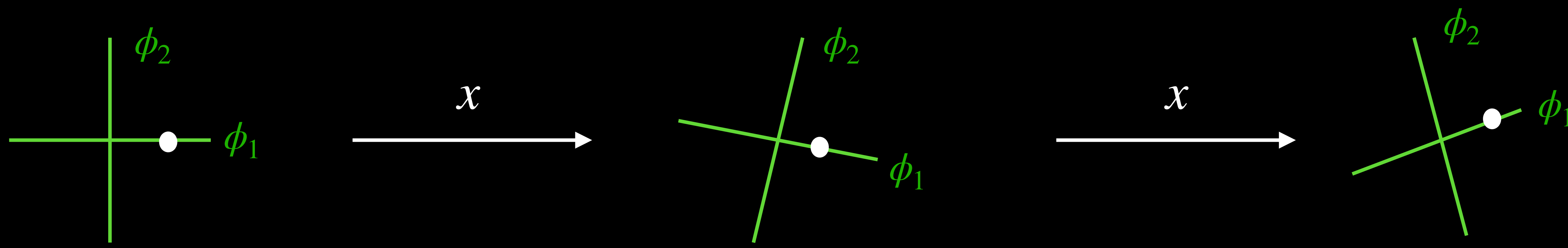

The expectation value of the scalar (Higgs) field creates an energetically favorable direction

Still free to choose coordinates but perpendicular oscillations raise the gauge field energy

Results in massive gauge bosons with a scalar (spin-0) component

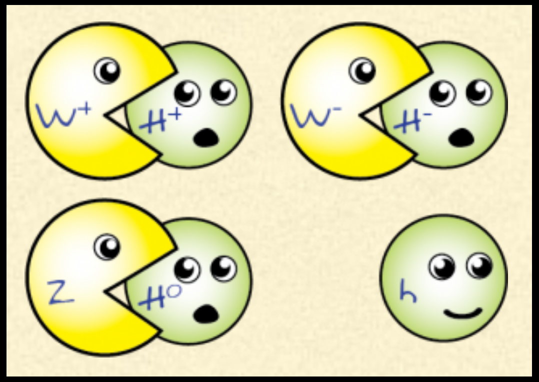

Higgs boson mass

Higgs field potential

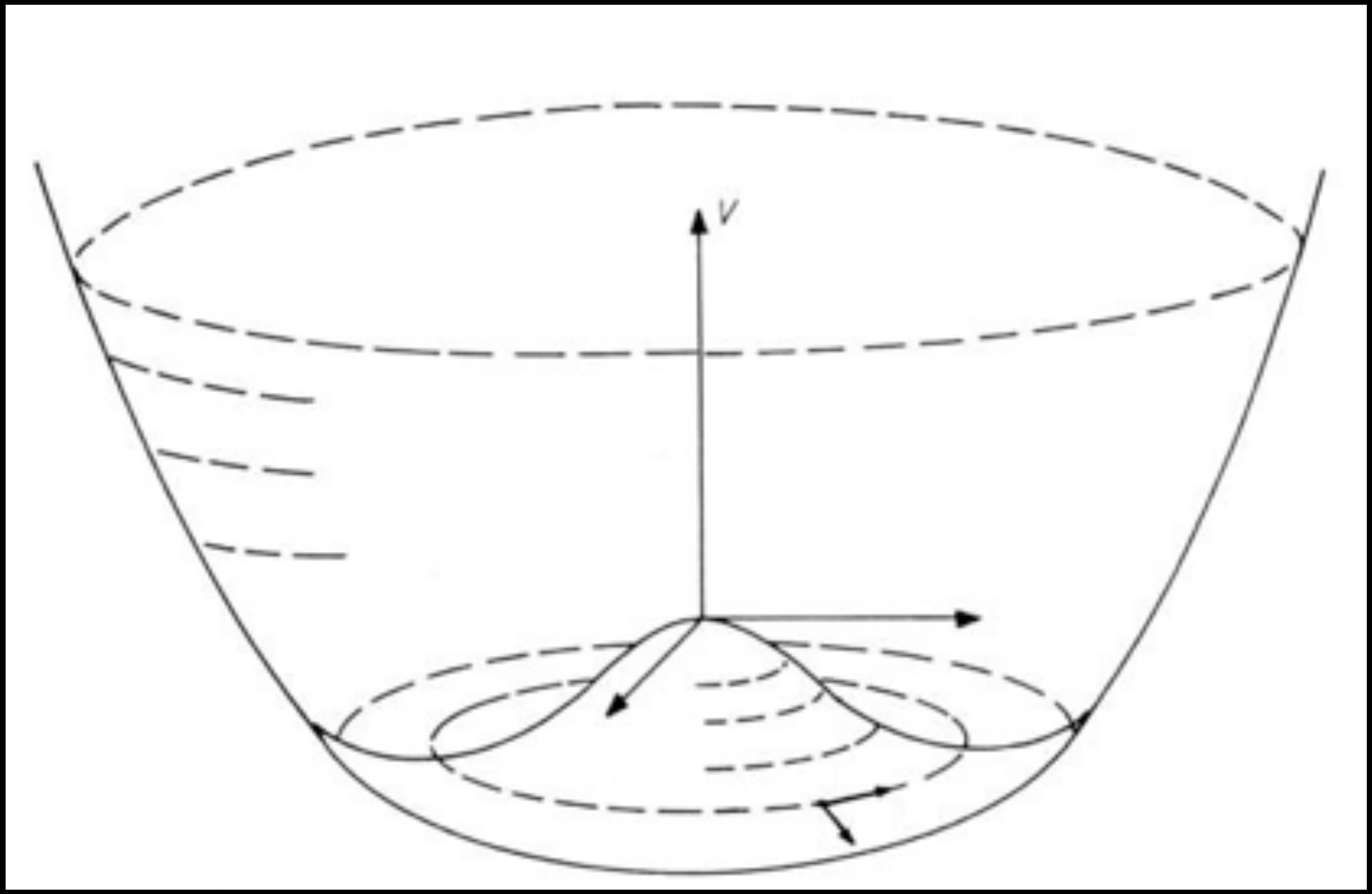

$$m_H = v\sqrt{2\lambda} = 125 \text{ GeV}$$

$$\lambda \approx 0.1$$

Quantum corrections

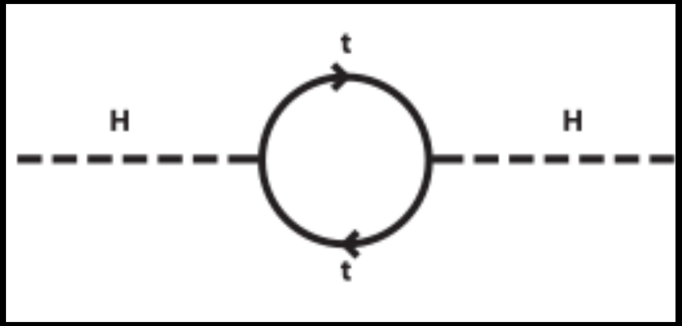

Naively integrating to a cutoff scale Λ:

$$\Delta m_H = \frac{3g^2 m_t^2}{16\pi^2 m_W^2}\Lambda^2$$

If there is no new physics up to scale Λ then we need 'fine-tuning' to cancel the quantum corrections

1% fine tuning: $\Lambda = 6.6$ **TeV**

Motivates TeV-scale new physics

Electroweak gauge boson masses

Gauge field potential

$$V = -\frac{g^2 v^2}{8}[(W_\mu^+)^2 + (W_\mu^-)^2] - \frac{v^2(g^2 + g'^2)}{8} Z^\mu Z_\mu$$

$$m_W = \frac{v}{2} g$$

$$m_Z = \frac{v}{2}\sqrt{g^2 + g'^2}$$

$v = 246$ GeV and $g = 0.64$:

$m_W = 78.7$ GeV

Quantum corrections

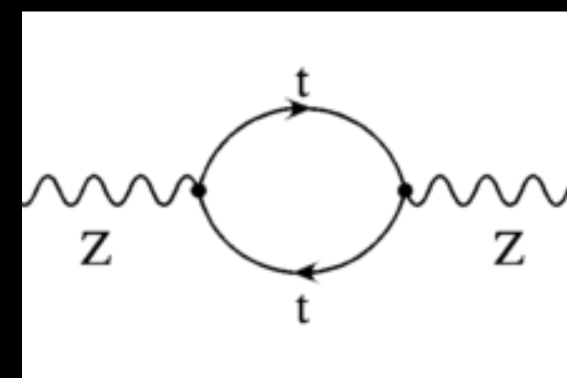

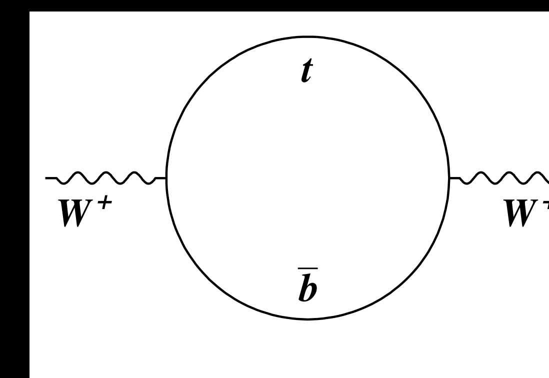

$$m_W^2 = \frac{\hbar^3}{c} \frac{\pi \alpha_{EM}}{\sqrt{2} G_F (1 - m_W^2/m_Z^2)(1 - \Delta r)}$$

$$\Delta r_{tb} = \frac{c}{\hbar^3} \frac{-3 G_F m_W^2}{8\sqrt{2}\pi^2 (m_Z^2 - m_W^2)} \times \left[m_t^2 + m_b^2 - \frac{2 m_t^2 m_b^2}{m_t^2 - m_b^2} \ln(m_t^2/m_b^2) \right]$$

Global fit to SM measurements yields indirect W boson mass of 81354 ± 7 MeV

W boson mass and naturalness

The W boson mass is the most sensitive observable to sources of ‘naturalness’

Classic example: **Supersymmetry**

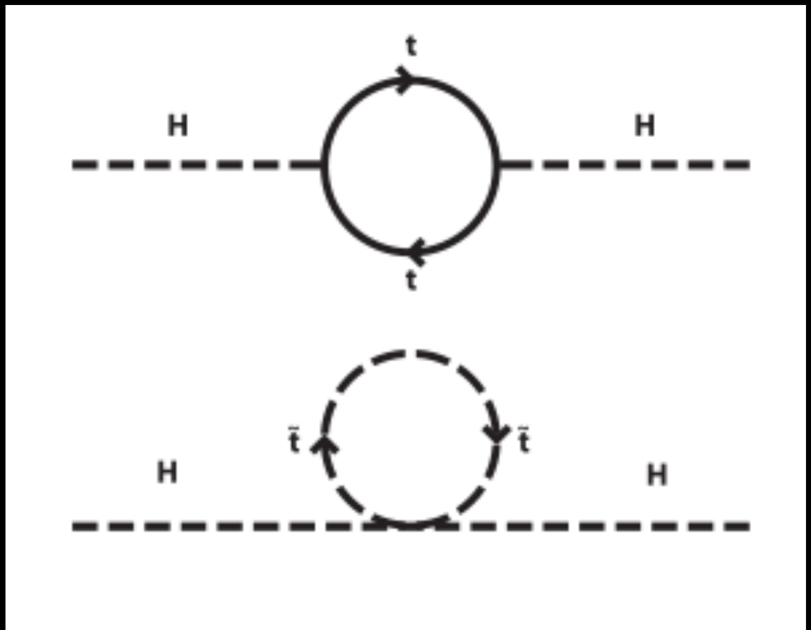

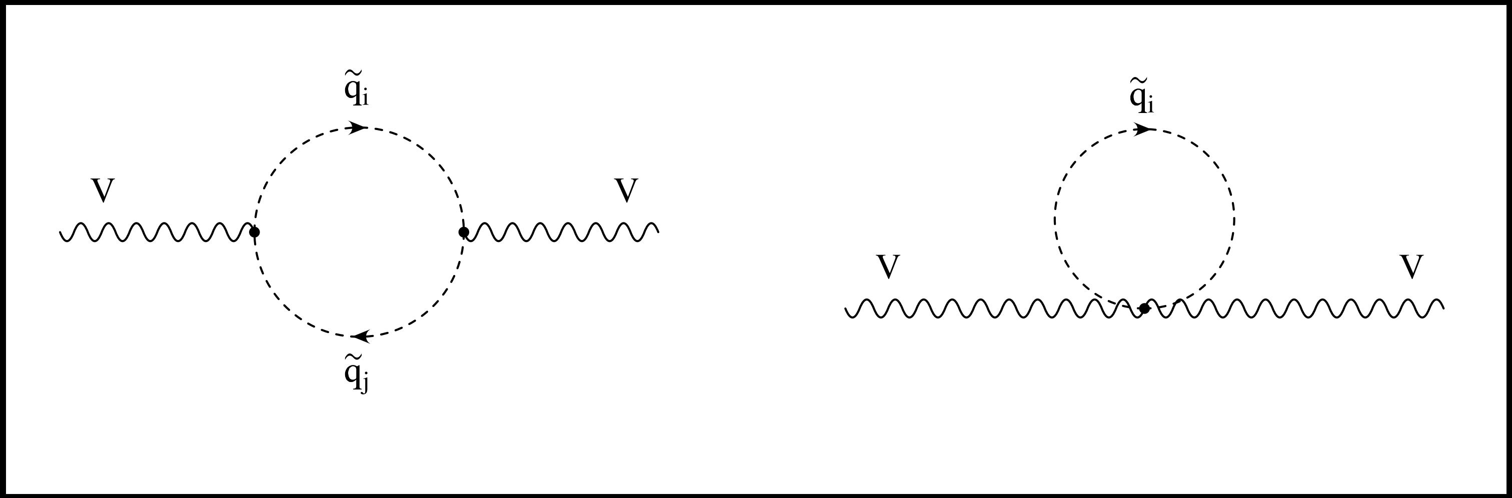

Mass splittings in supersymmetric isospin doublets: different mass shifts for W & Z bosons

W boson mass and naturalness

Difference in corrections to W and Z propagators encapsulated by ρ parameter

$$\Delta\rho = \frac{\Sigma^Z(0)}{M_Z^2} - \frac{\Sigma^W(0)}{M_W^2}$$

$$\Delta\rho_0^{\rm SUSY} = \frac{3\,G_\mu}{8\sqrt{2}\,\pi^2}\Big[-\sin^2\theta_{\tilde t}\cos^2\theta_{\tilde t}F_0(m_{\tilde t_1}^2, m_{\tilde t_2}^2) - \sin^2\theta_{\tilde b}\cos^2\theta_{\tilde b}F_0(m_{\tilde b_1}^2, m_{\tilde b_2}^2) + \cos^2\theta_{\tilde t}\cos^2\theta_{\tilde b}F_0(m_{\tilde t_1}^2, m_{\tilde b_1}^2) + \cos^2\theta_{\tilde t}\sin^2\theta_{\tilde b}F_0(m_{\tilde t_1}^2, m_{\tilde b_2}^2) + \sin^2\theta_{\tilde t}\cos^2\theta_{\tilde b}F_0(m_{\tilde t_2}^2, m_{\tilde b_1}^2) + \sin^2\theta_{\tilde t}\sin^2\theta_{\tilde b}F_0(m_{\tilde t_2}^2, m_{\tilde b_2}^2) \Big].$$

$$\delta M_W \approx \frac{M_W}{2}\frac{c_W^2}{c_W^2 - s_W^2}\Delta\rho$$

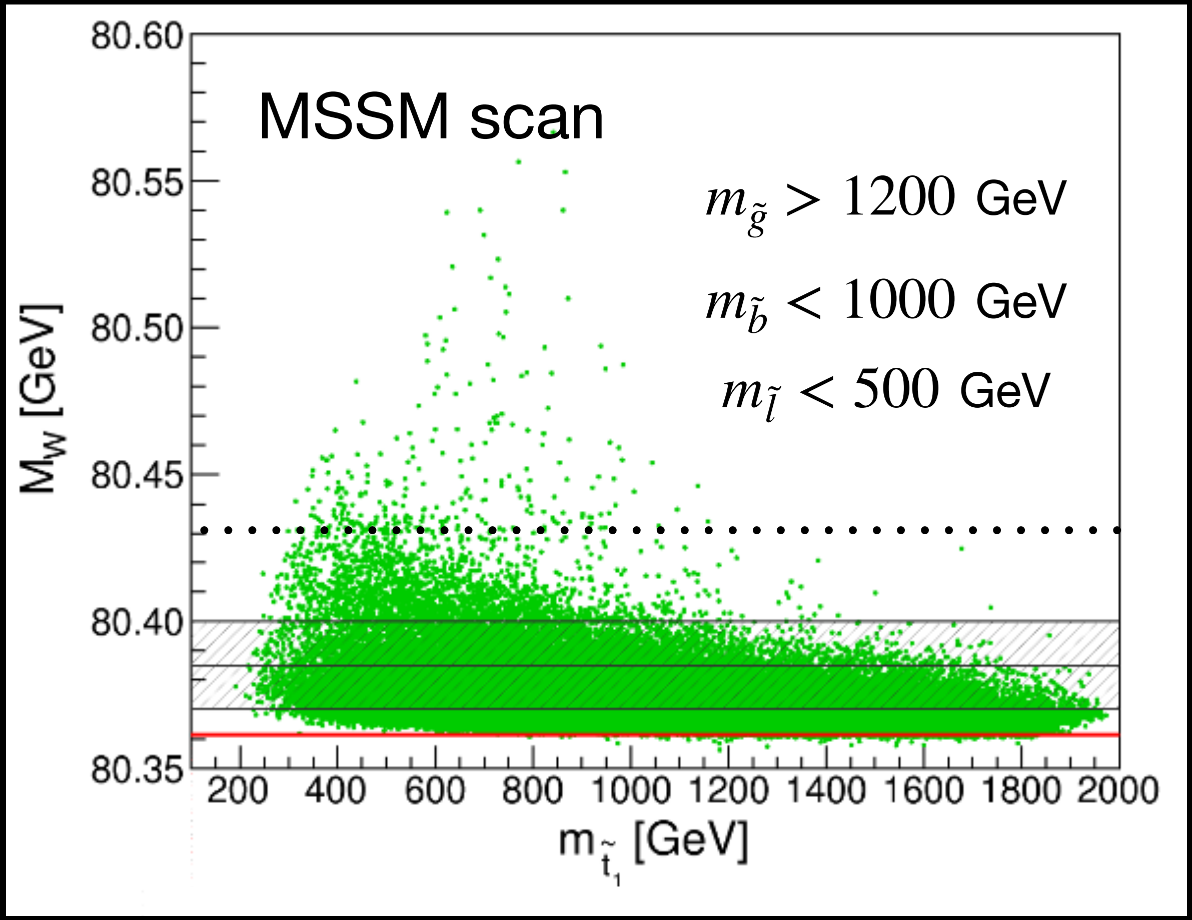

Heinemeyer, Hollik, Weiglein
Phys Rep 425, 265 (2006)

Heinemeyer, Hollik, Weiglein, Zeune
JHEP 12 (2013) 084

W boson mass and naturalness

More generally the SM effective field theory parameterizes high-scale effects

$$\mathcal{L}_{SMEFT} = \mathcal{L}_{SM} + \mathcal{L}^{(5)} + \mathcal{L}^{(6)} + \mathcal{L}^{(7)} + \cdots, \qquad \mathcal{L}^{(d)} = \sum_{i=1}^{n_d} \frac{C_i^{(d)}}{\Lambda^{d-4}} Q_i^{(d)} \quad \text{for } d > 4.$$

I. Brivio and M. Trott, Phys. Rep. 793 (2019) 1

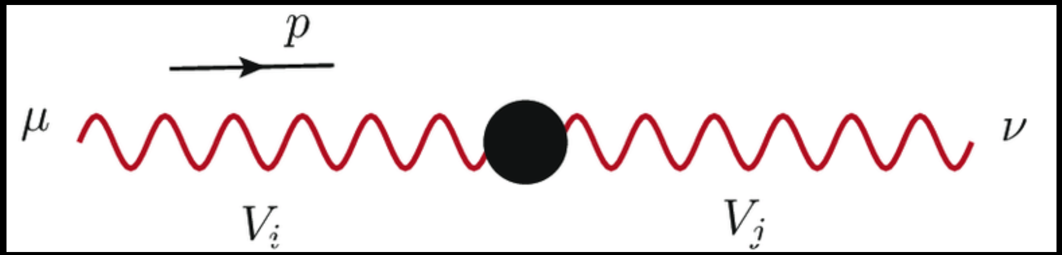

$$\frac{\delta m_W}{m_W} = \left(0.34 c_{HD} + 0.72 c_{HWB} + 0.37 c_{Hl3} - 0.19 c_{ll1}\right) \frac{v^2}{\Lambda^2}$$

For $\delta m_W / m_W = 0.1\ \%$ and $c_{HD}=1$, $\Lambda = 4.5$ TeV

e.g. Z' boson

For $\delta m_W / m_W = 0.1\ \%$ and $c_{HWB}=1$, $\Lambda = 6.6$ TeV

e.g. compositeness

Smaller $c_i \rightarrow$ smaller Λ

W boson mass measurements

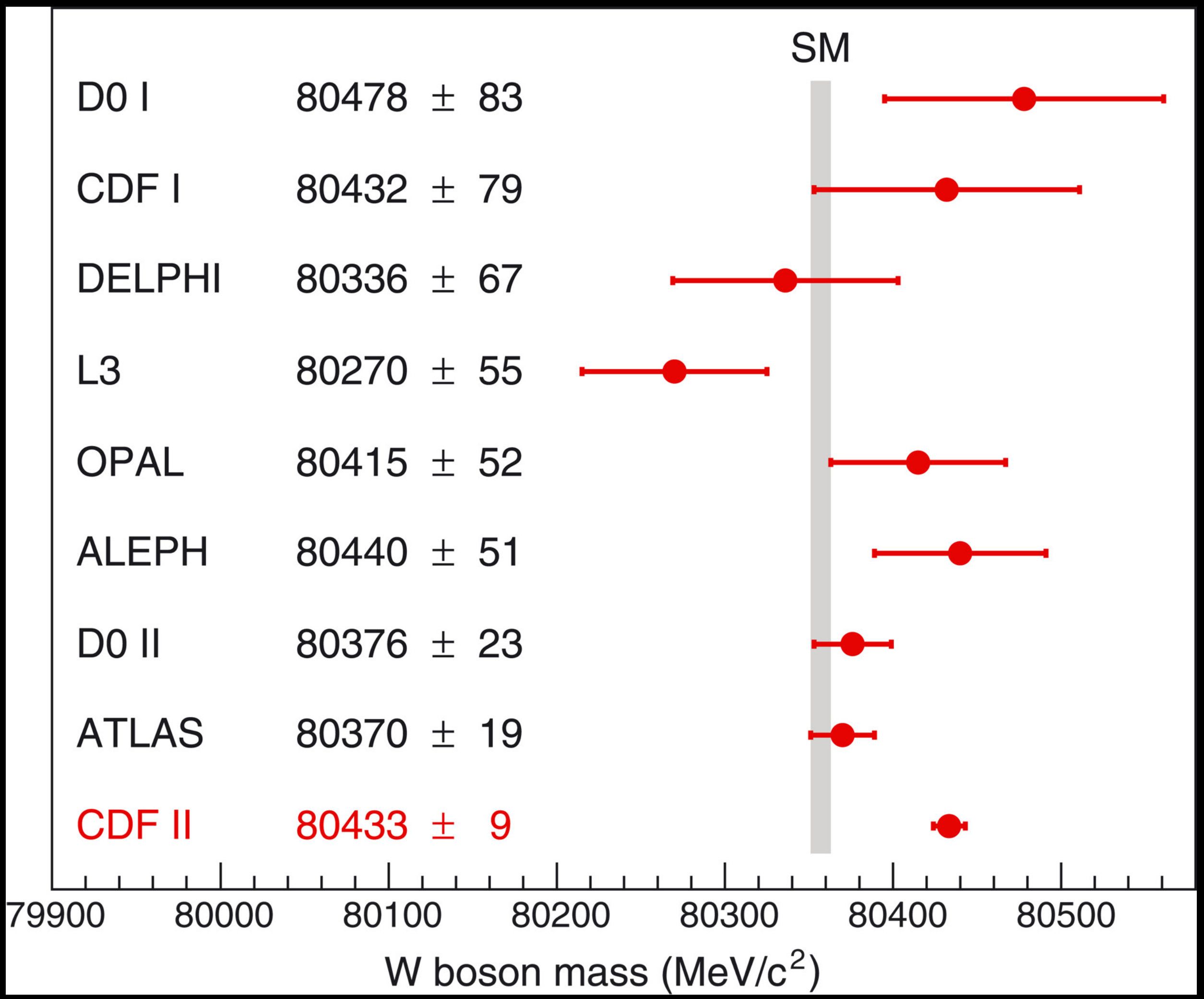

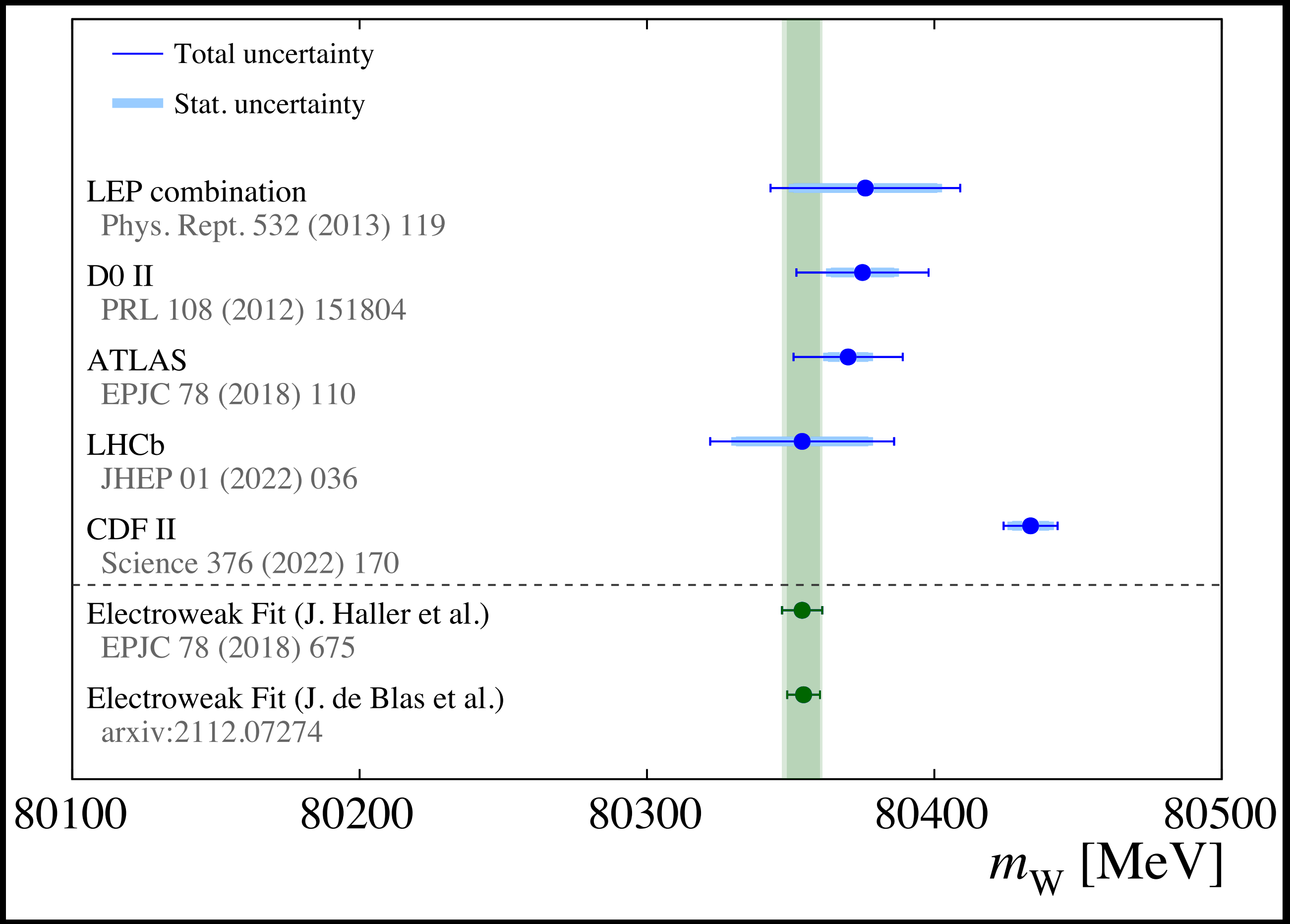

CDF II measurement of the W boson mass

$\sqrt{s} = 1.96$ TeV proton-antiproton collisions from the Fermilab Tevatron

CDF II detector consists of

silicon vertex detector

large drift chamber

coarse calorimeter towers

outer muon chambers

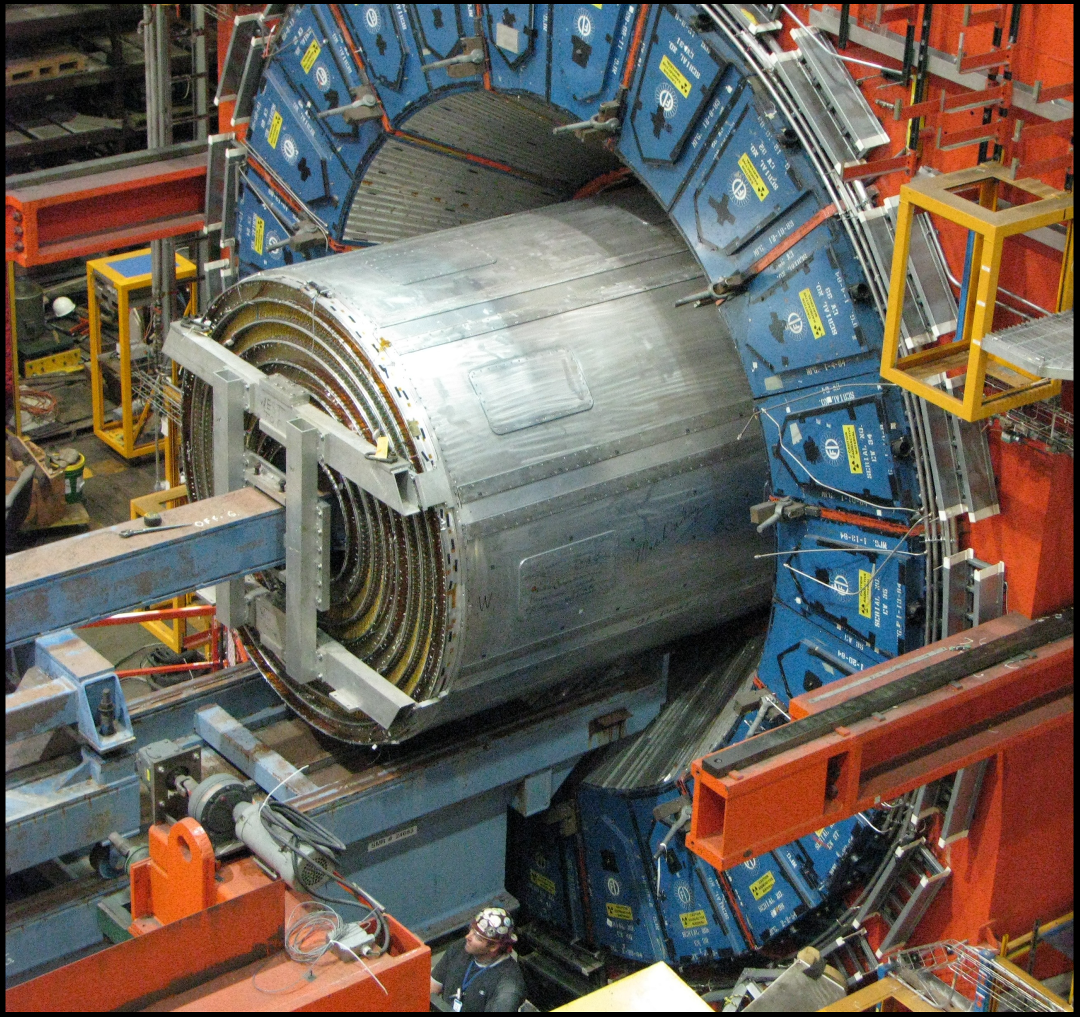

CDF II measurement of the W boson mass

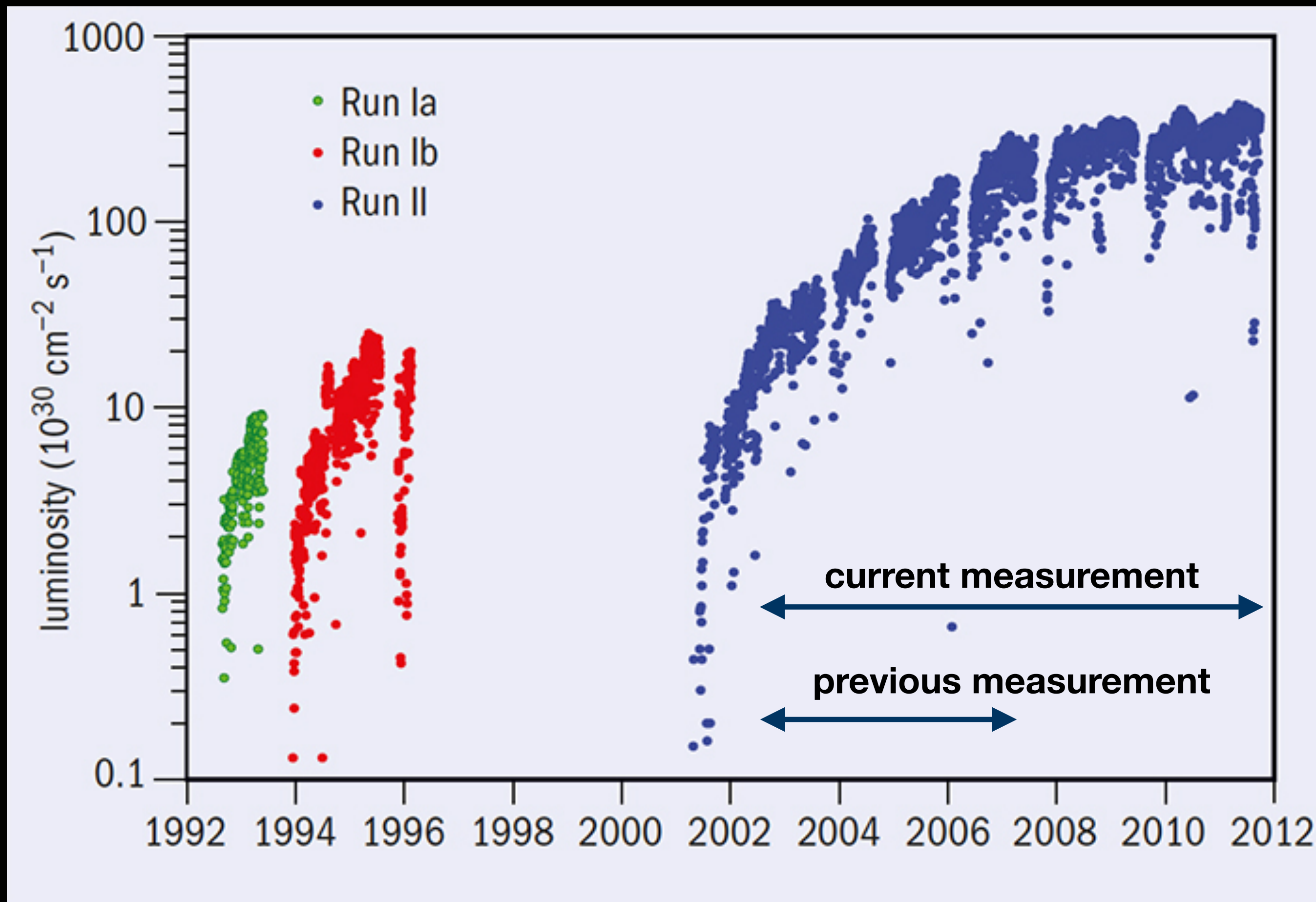

Measurement uses complete Tevatron Run II data set

4x the integrated luminosity of the previous measurement

Higher $\langle \mu \rangle$: peaks at 3

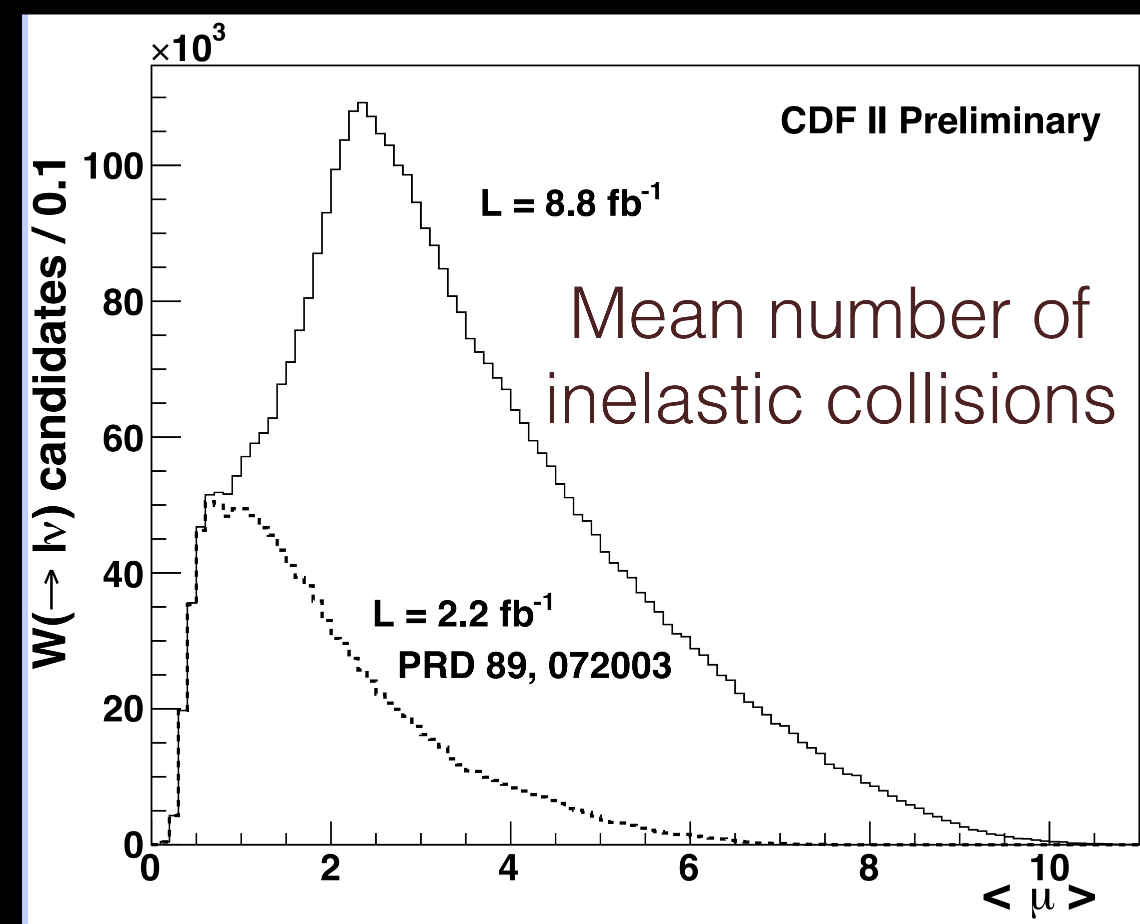

CDF II measurement of the W boson mass

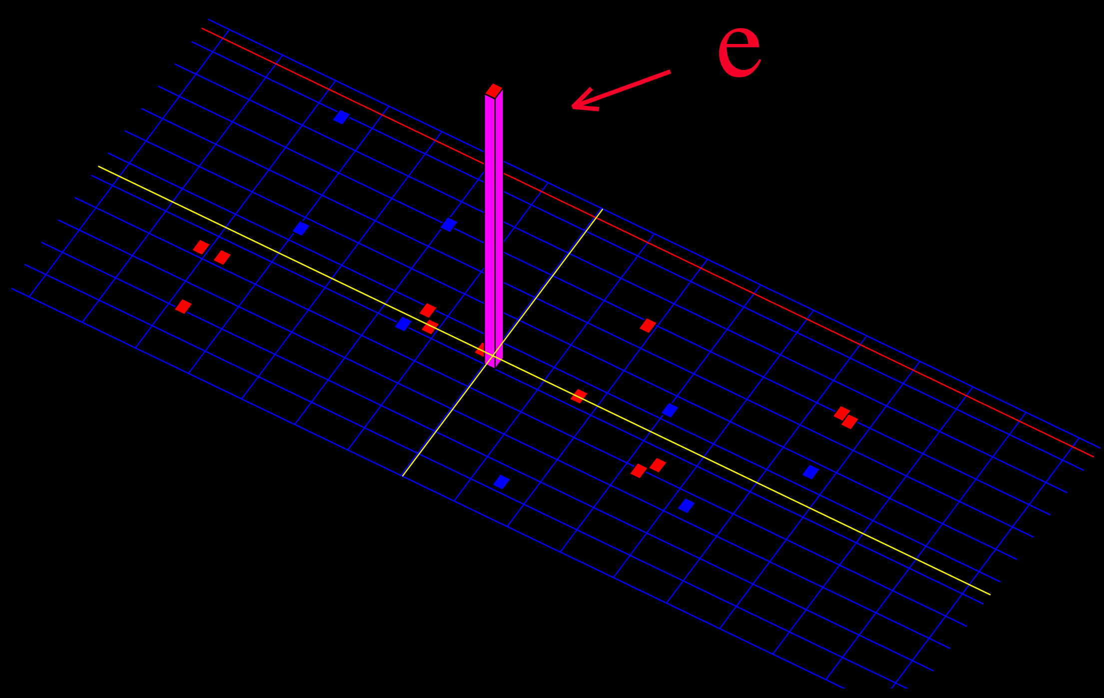

W bosons identified in their decays to $e\nu$ and $\mu\nu$

Mass measured by fitting template distributions of transverse momentum and mass

$$m_T = \sqrt{2 p_T^l \not{p}_T \, (1 - \cos \Delta\phi)}$$

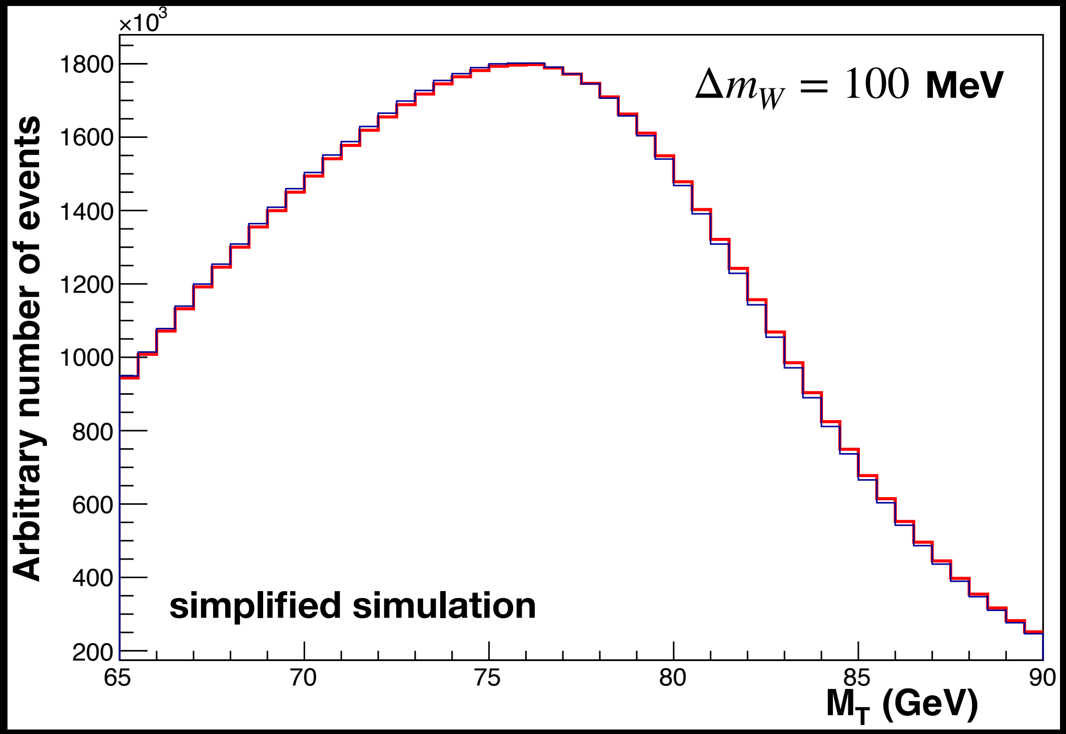

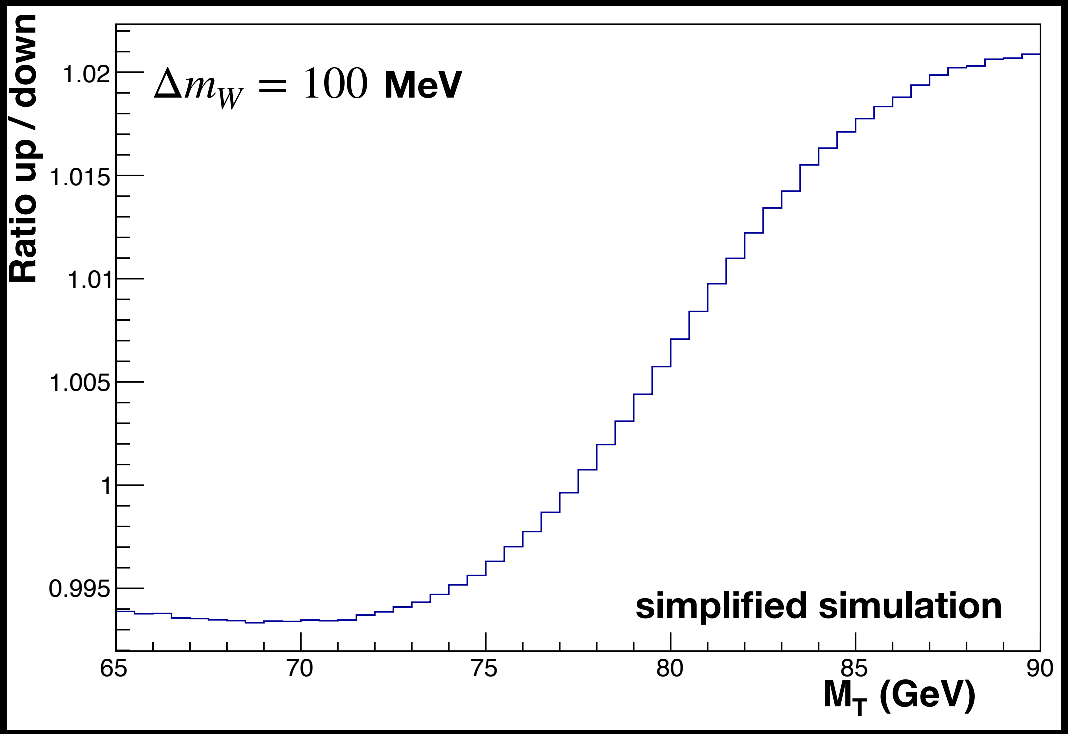

Calibrations

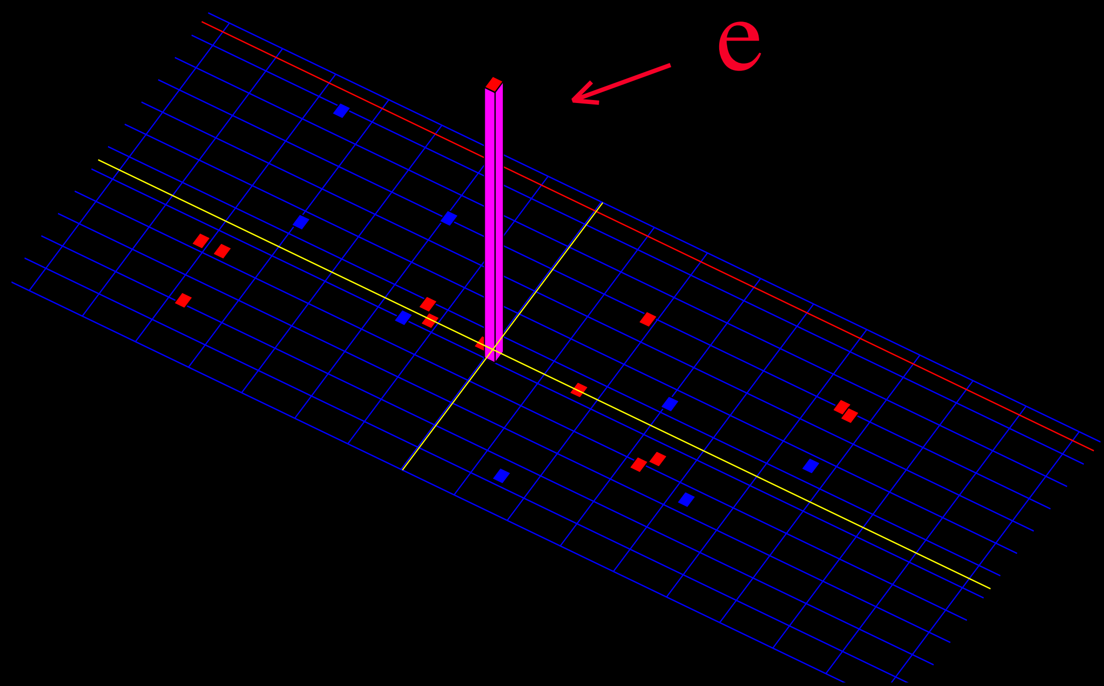

Measurement requires precise calibrations and momentum scale and resoution

Charged lepton scale

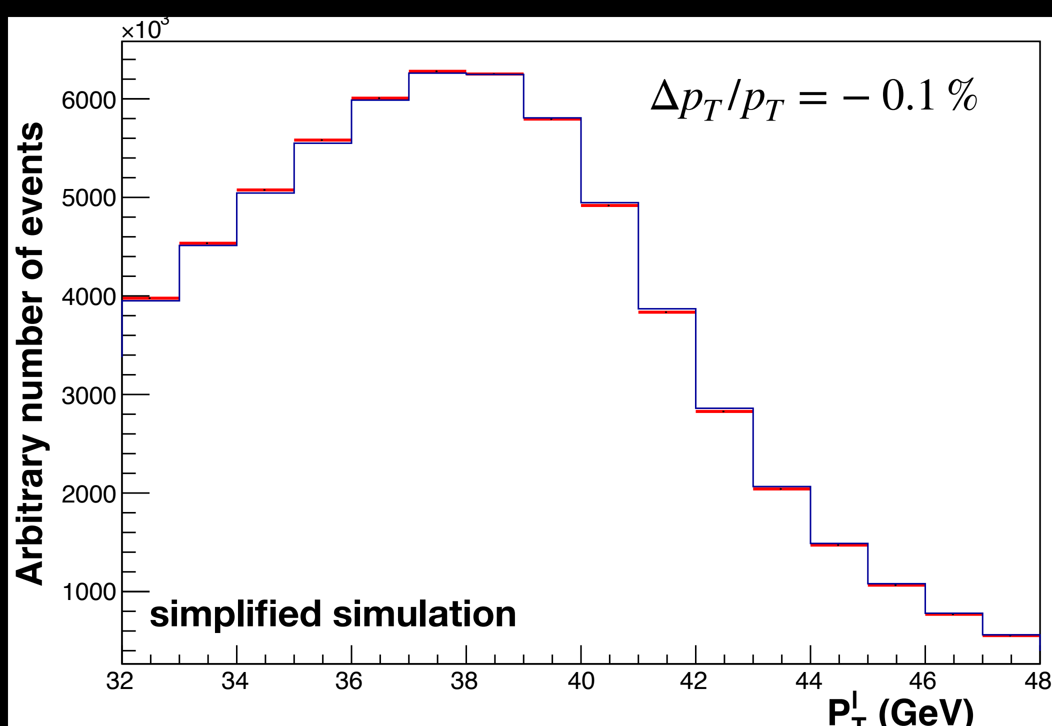

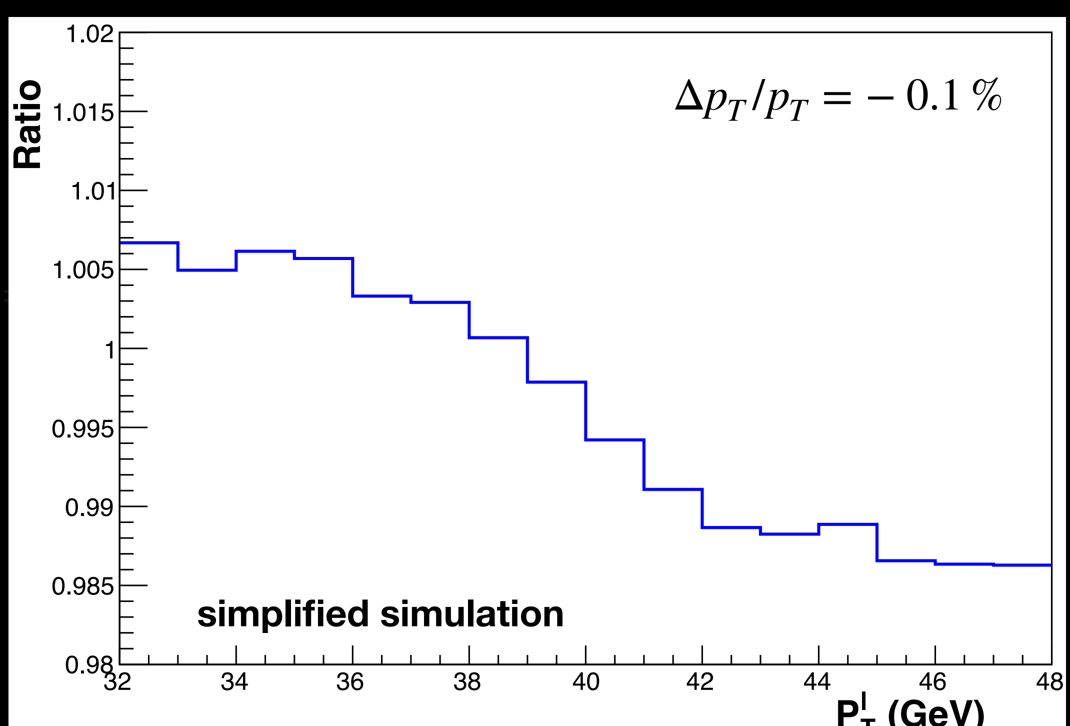

Calibrations

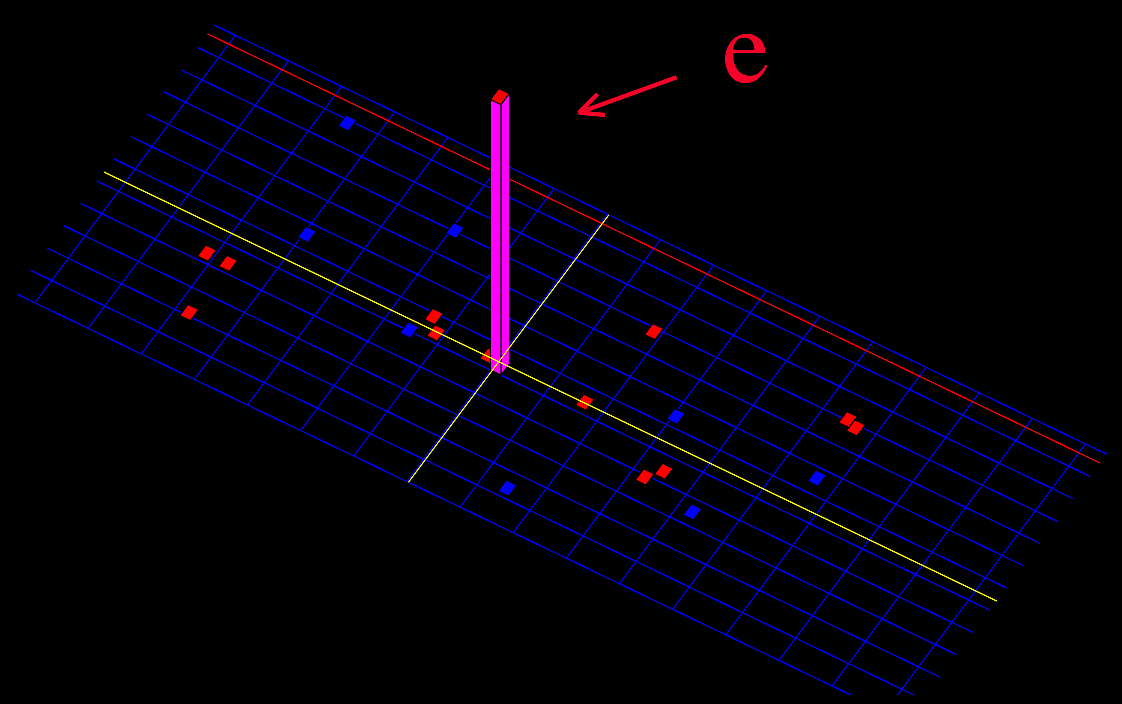

Measurement requires precise calibrations and momentum scale and resoution

$$\vec{\not{p}}_T = -(\vec{p}_T^{\,l} + \vec{u}_T)$$

Recoil scale

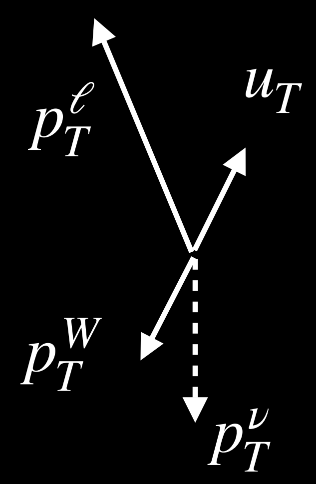

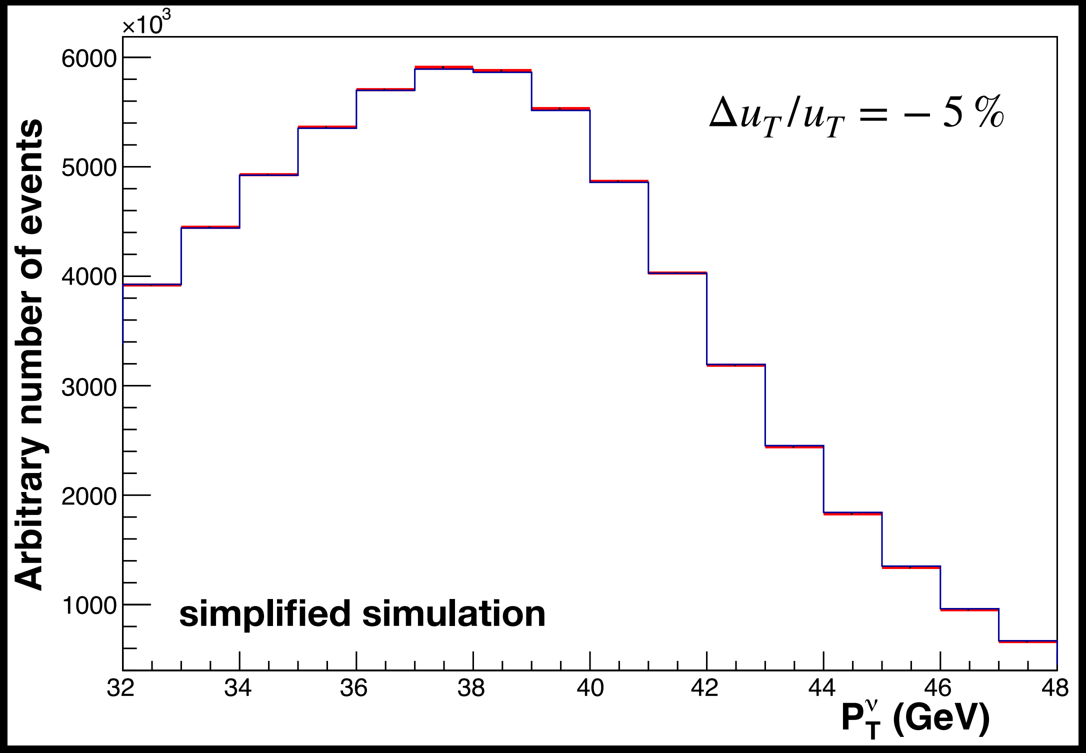

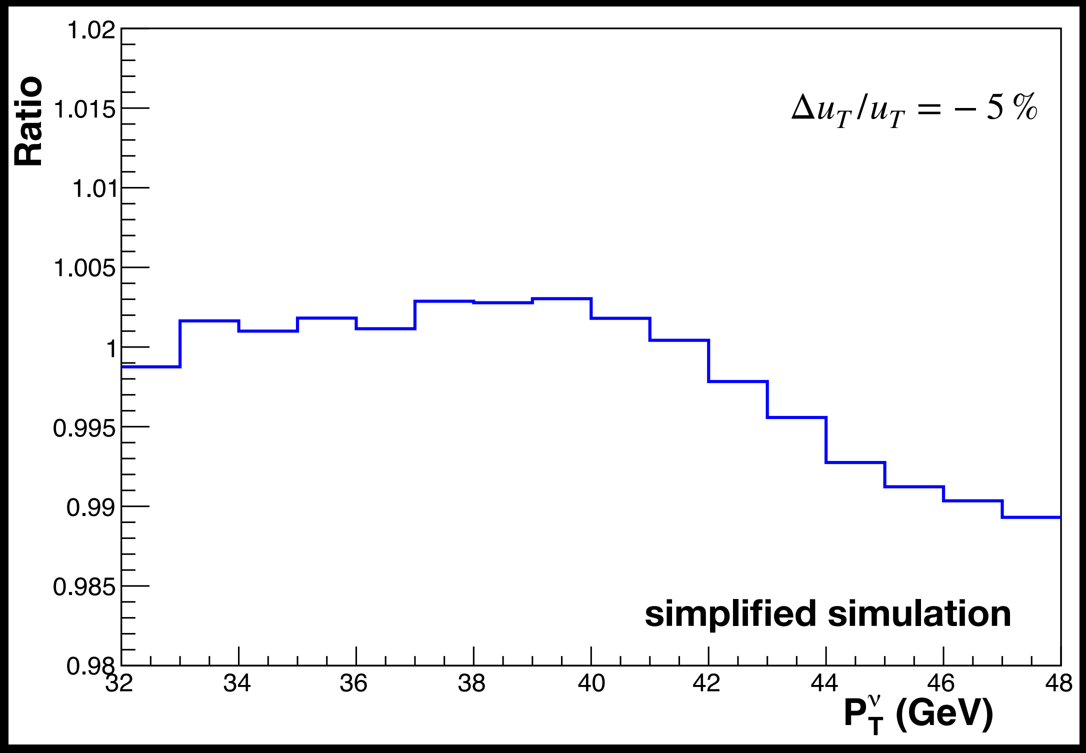

Detector simulation

Developed custom simulation for analysis
Models ionization energy loss, multiple scattering, bremsstrahlung, photon conversion, Compton scattering

Acceptance map for muon detectors

Parameterized GEANT4 model of electromagnetic calorimeter showers
Includes shower losses due to finite calorimeter thickness

Kotwal & CH, NIMA 729, 25 (2013)

Hit-level model of central outer tracker
Layer-by-layer resolution functions and efficiencies

Material map of inner silicon detector
Includes radiation lengths and Bethe-Bloch terms

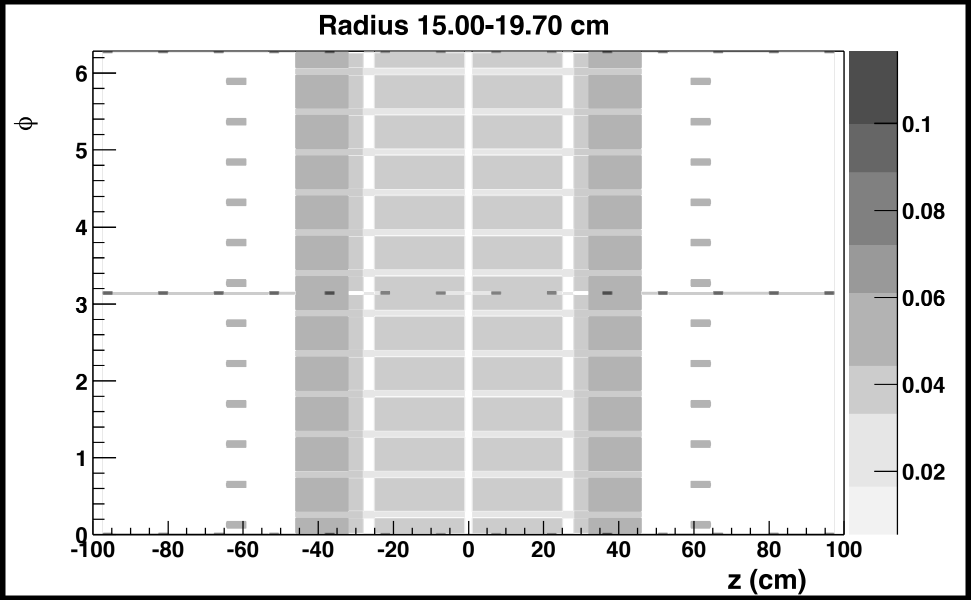

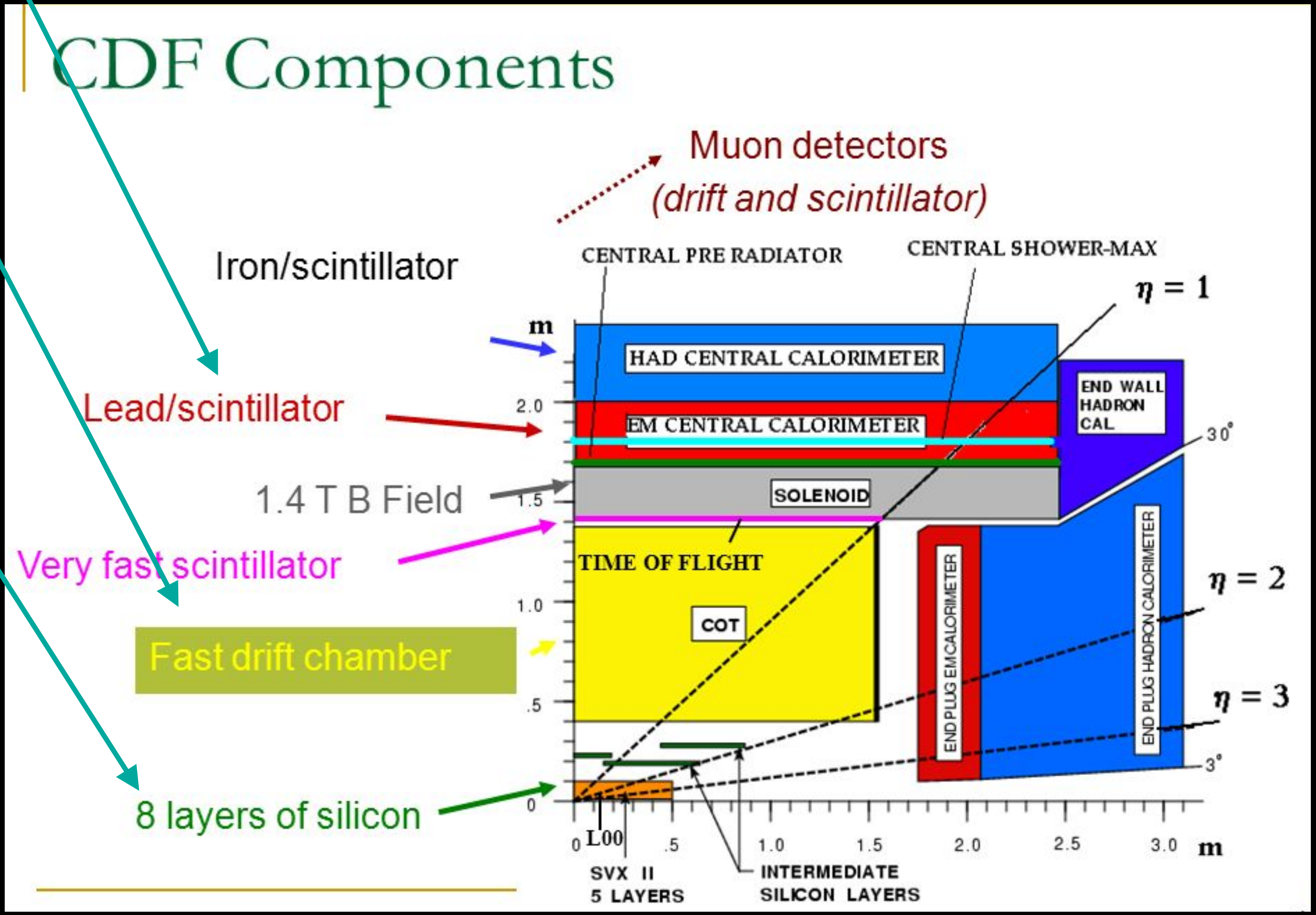

Muon momentum calibration

First step is to align the drift chamber (the “central outer tracker” or COT)

Two degrees of freedom (shift & rotation) for each of 2520 cells made up of twelve sense wires constrained using hit residuals from cosmic-ray tracks

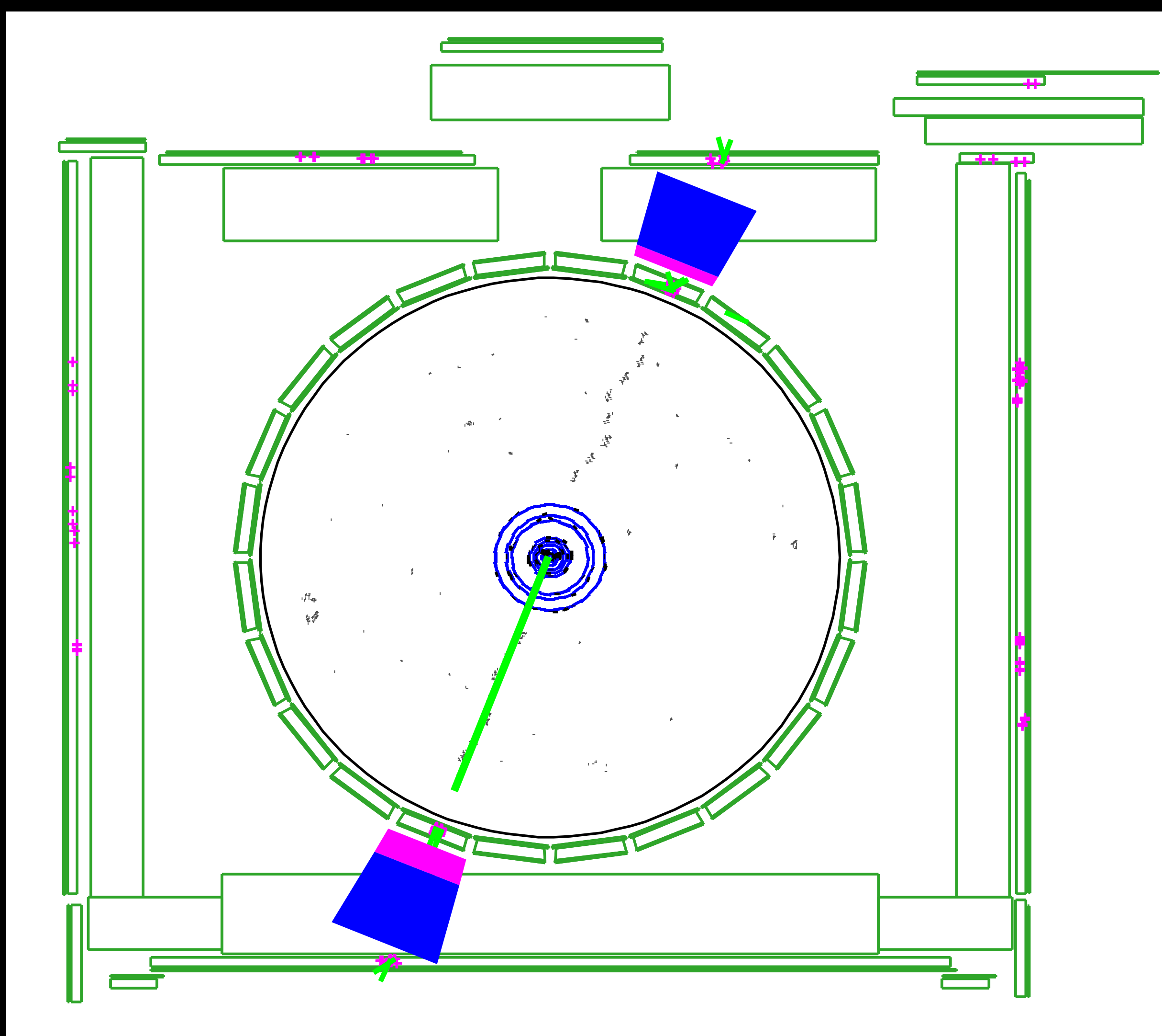

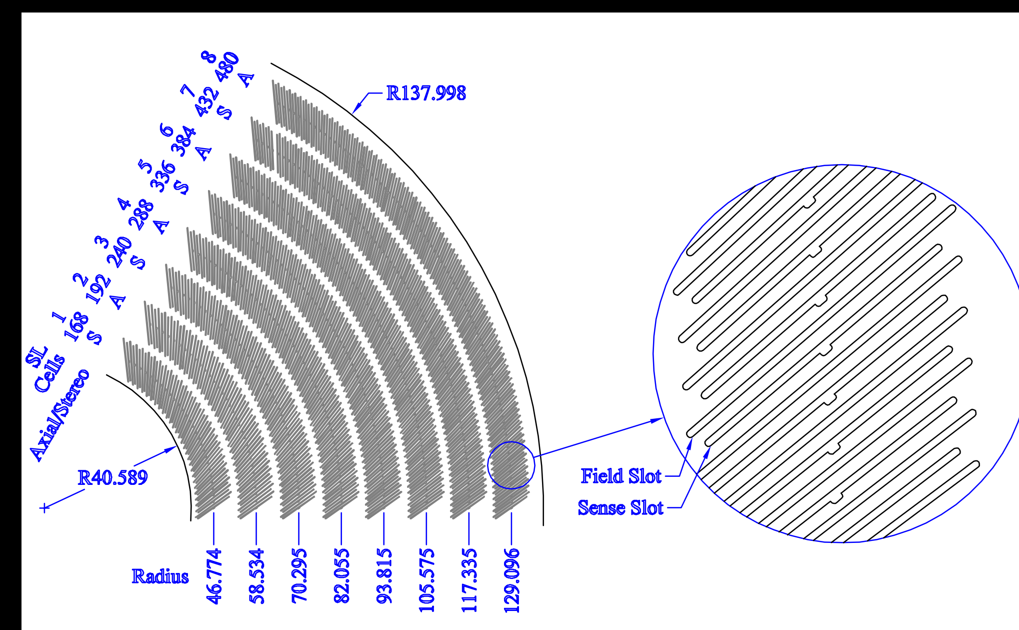

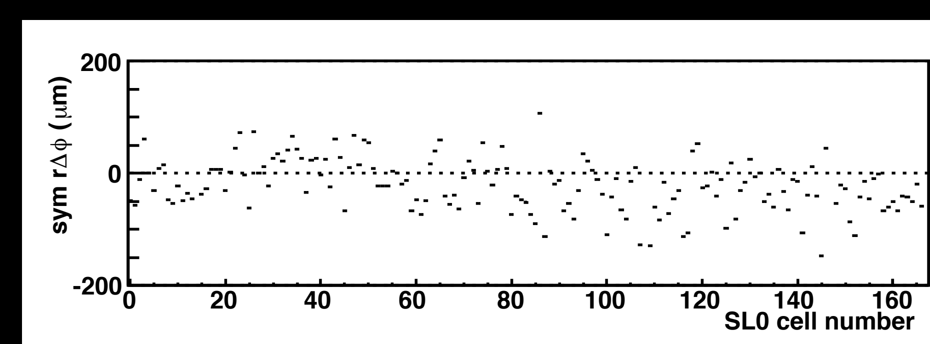

Kotwal & CH, NIMA 762, 85 (2014)

Muon momentum calibration

First step is to align the drift chamber (the “central outer tracker” or COT)

Two parameters for the electrostatic deflection of the wire within the chamber constrained using difference between fit parameters of incoming and outgoing cosmic-ray tracks

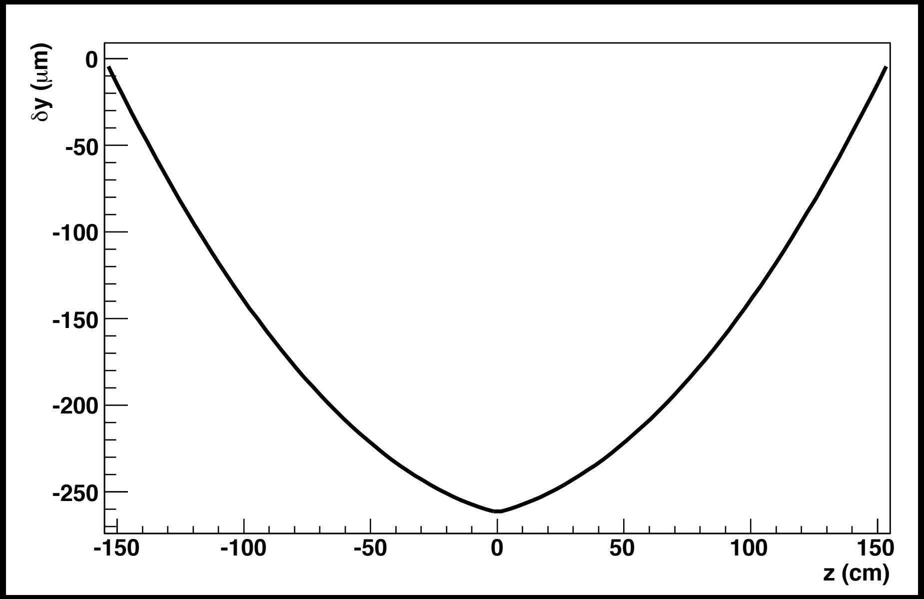

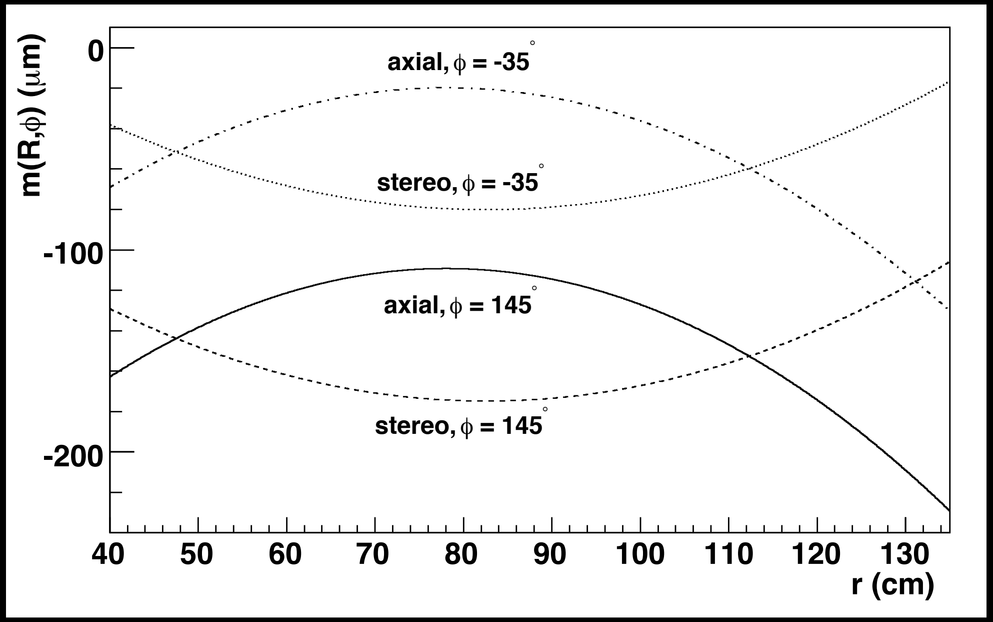

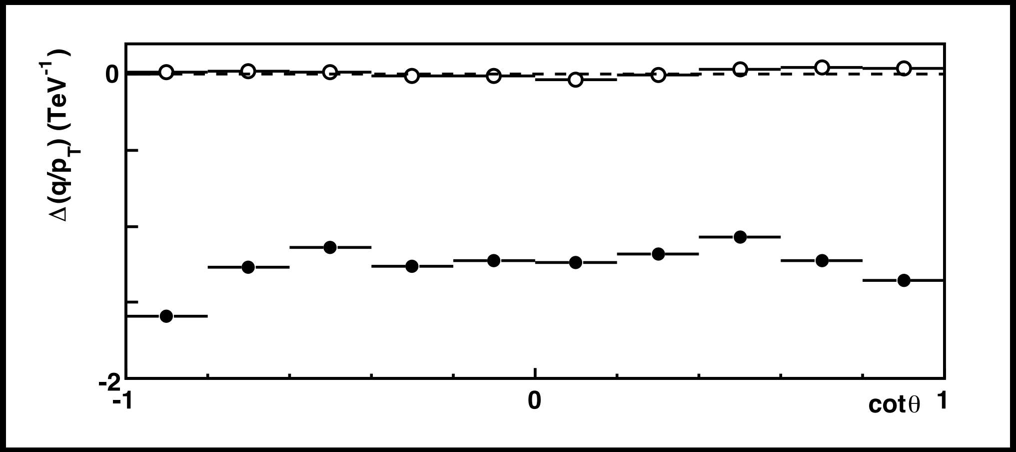

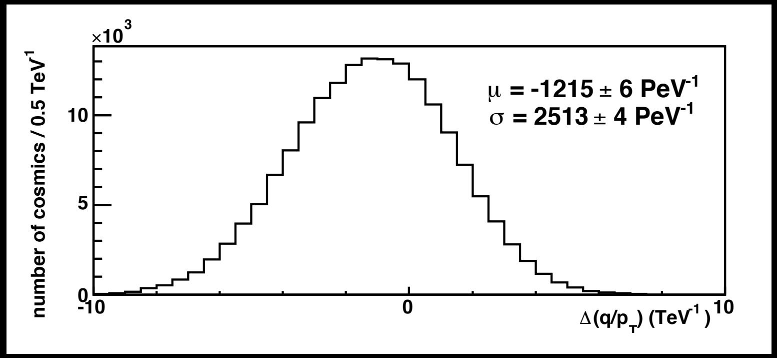

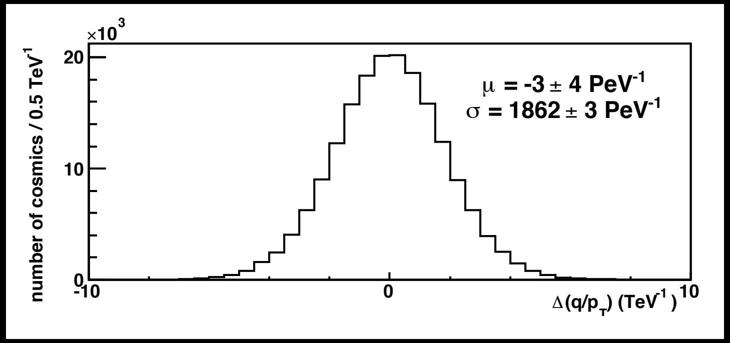

Muon momentum calibration

Second step is to calibrate the momentum scale using J/ψ decays to muons

Simulation:
Adjust kinematics to match the data
Model resonance shape using hit-level simulation and NLO form factor for QED radiation

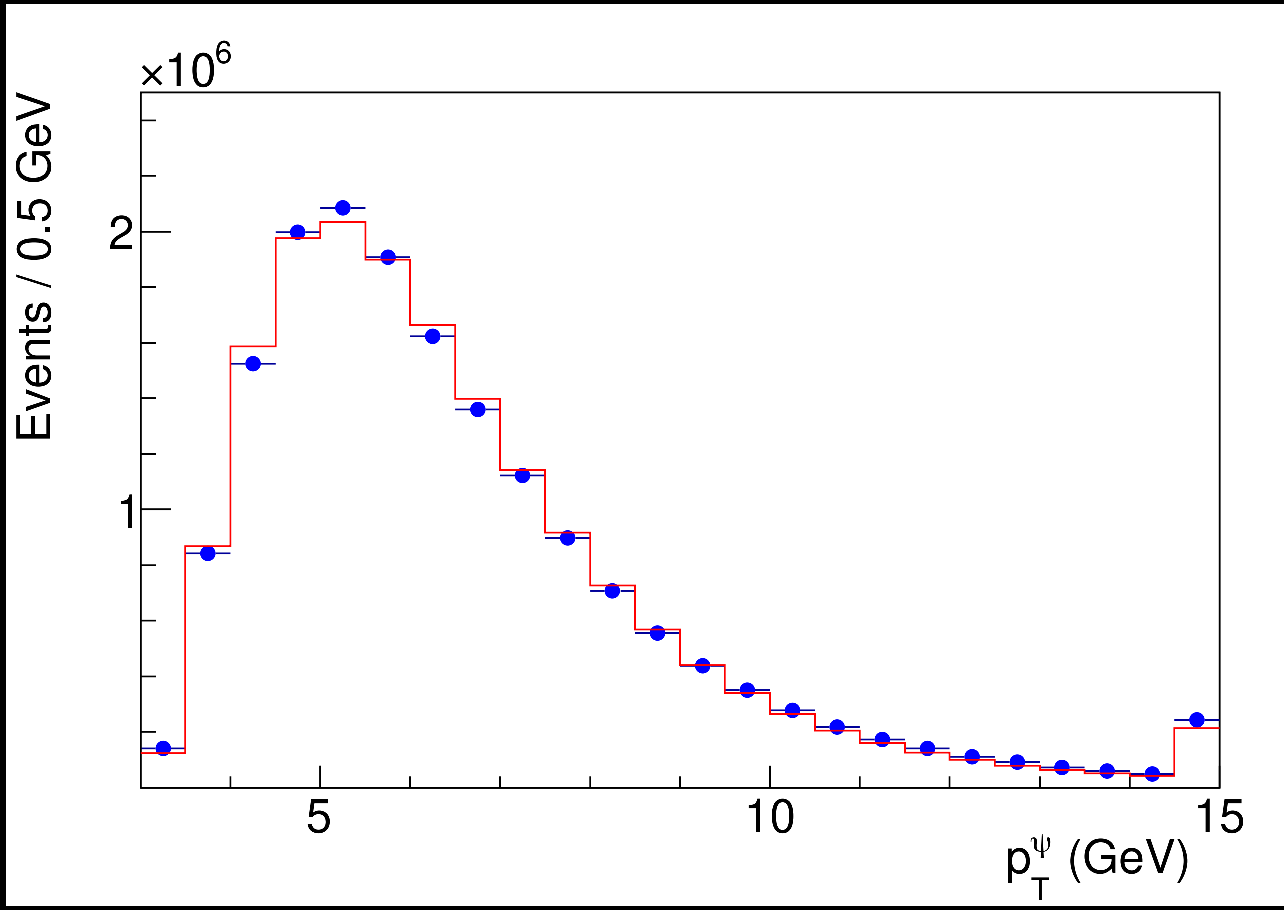

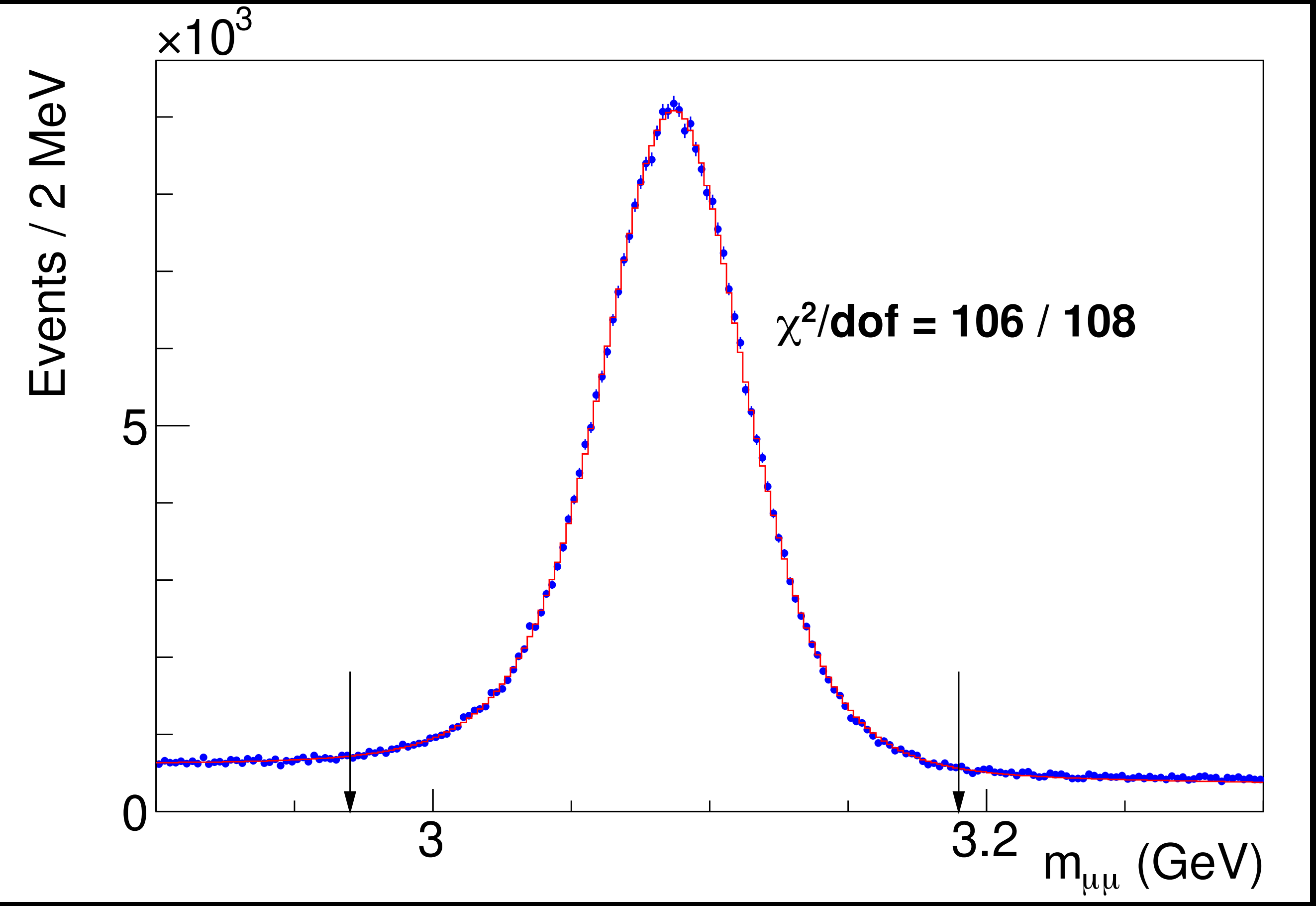

Muon momentum calibration

Second step is to calibrate the momentum scale using J/ψ decays to muons

Simulation corrections:

Correct the length scale of the tracker with mass measurement as a function of $\Delta \cot \theta$

Correct the amount of upstream material with mass measurement as a function of p_T^{-1}

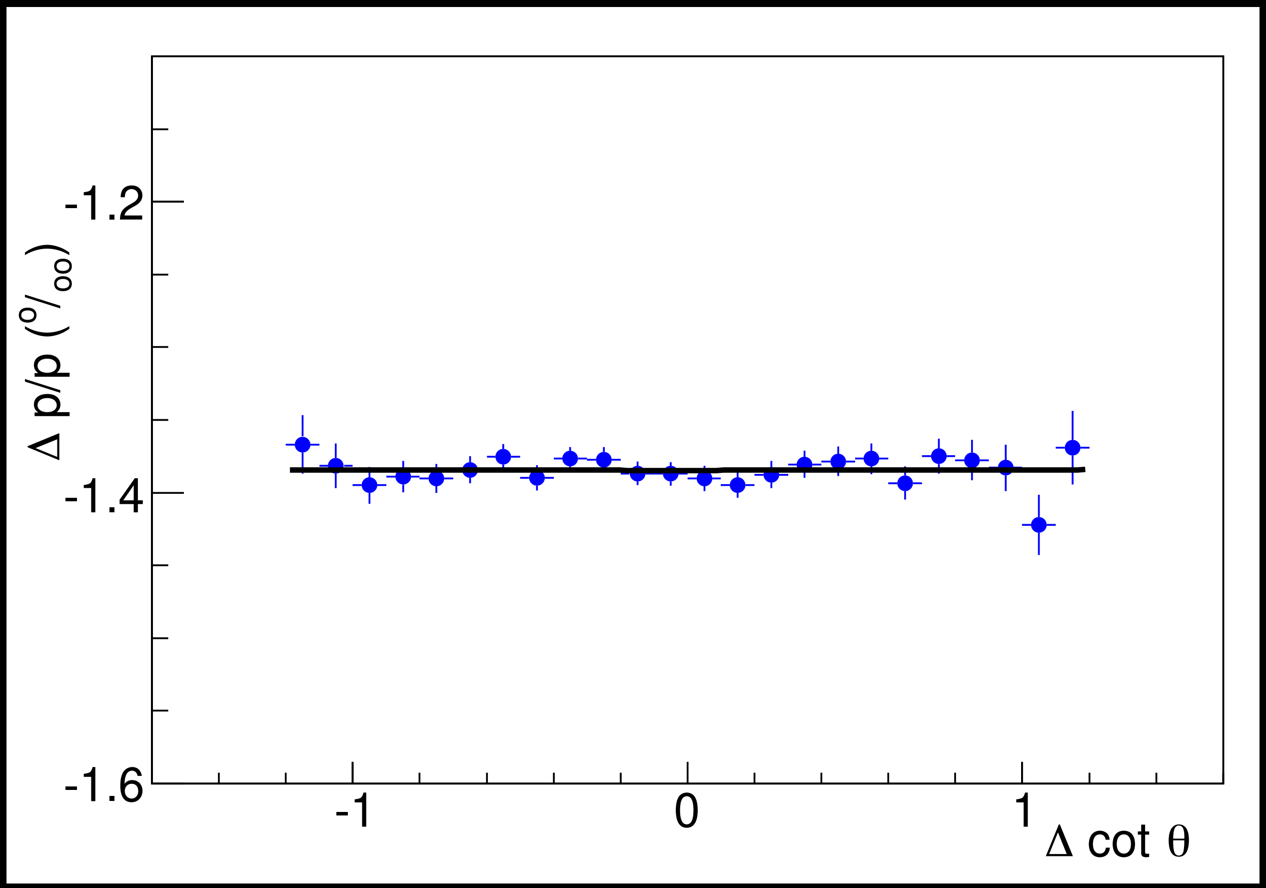

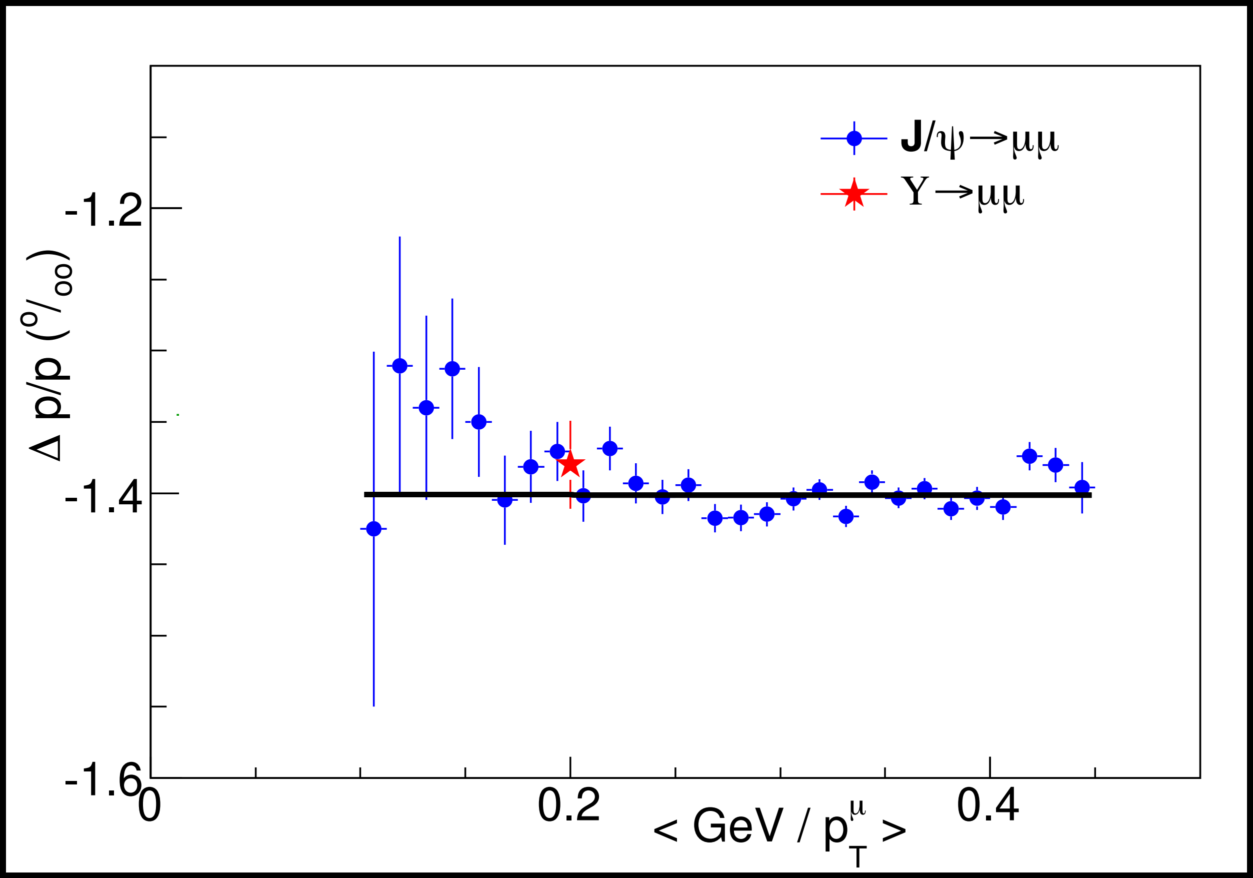

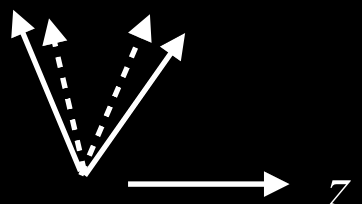

Muon momentum calibration

Third step is to calibrate the scale using Υ decays to muons

Compare fit results with and without constraining the track to the collision point

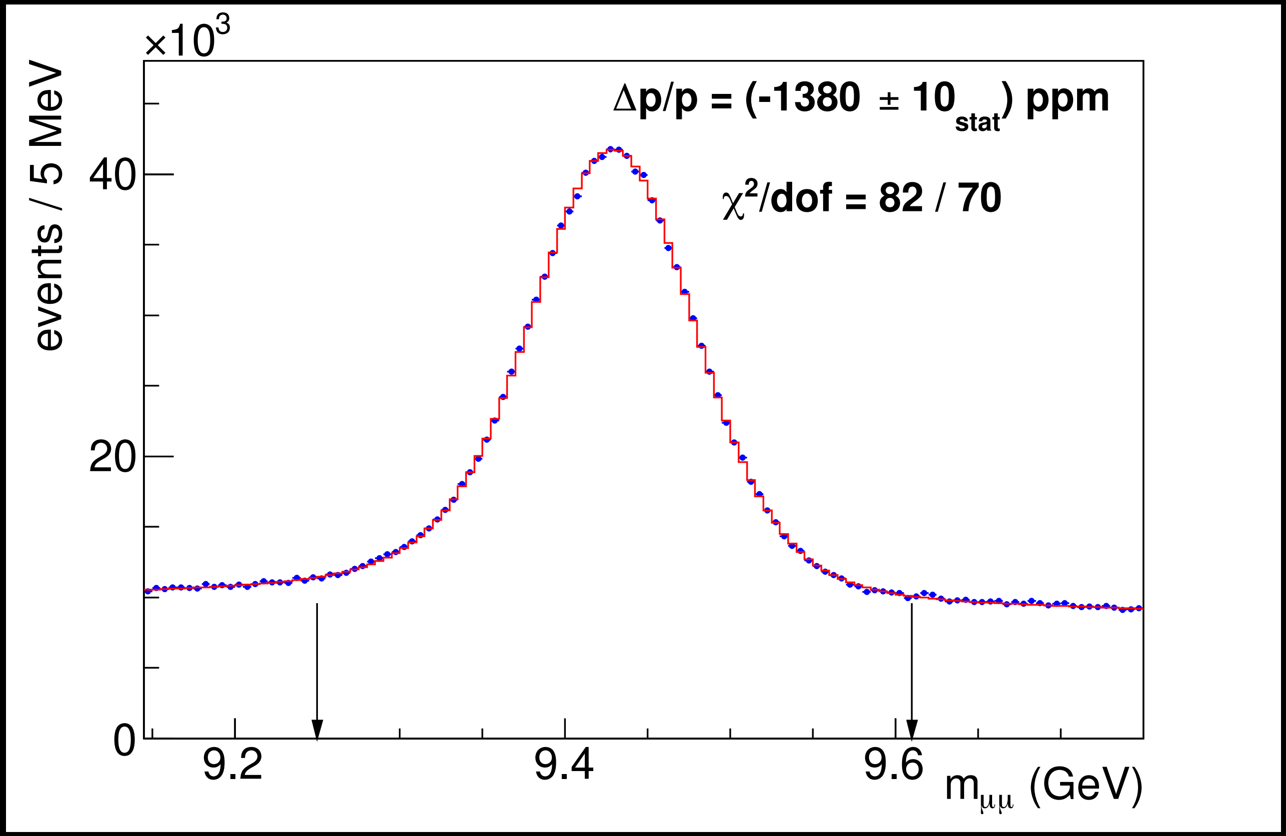

with constraint

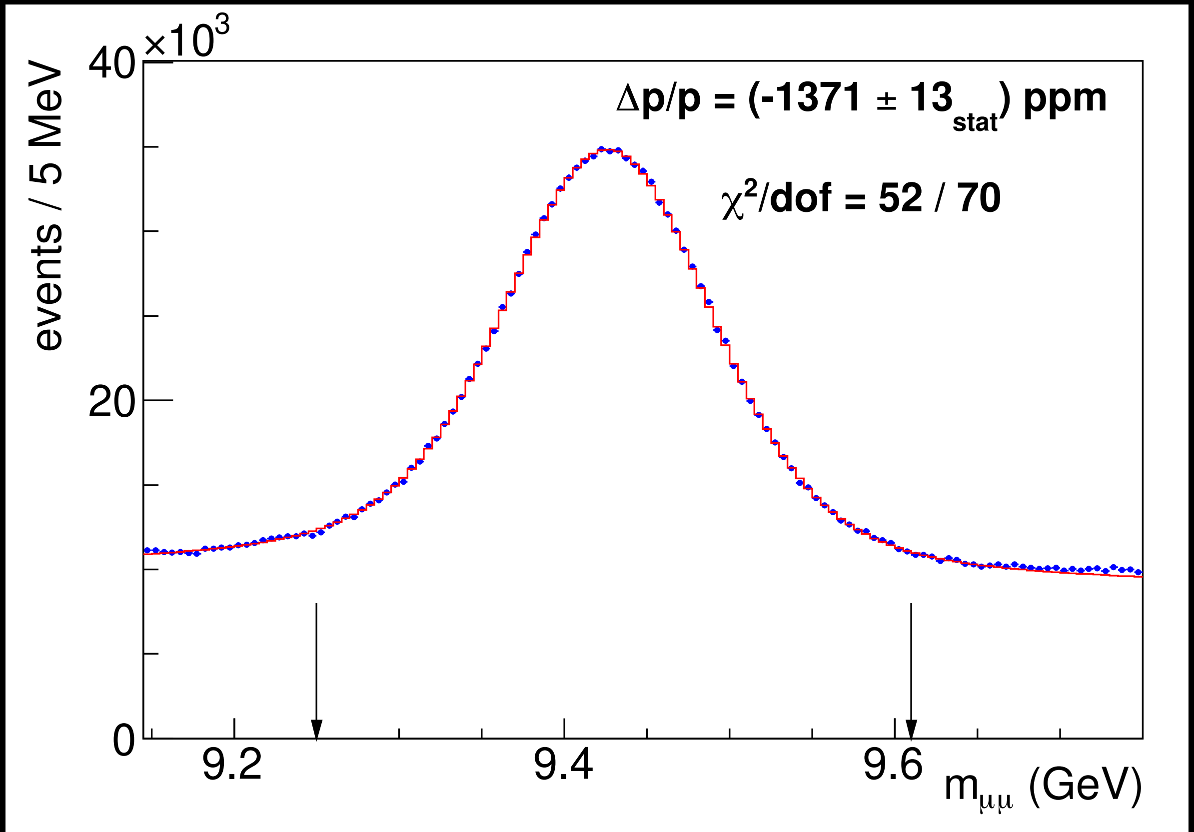

without constraint

Muon momentum calibration

Final step is to measure the Z boson mass

$$M_Z = 91\ 192.0 \pm 6.4_{stat} \pm 4.0_{sys}\ \text{MeV}$$

Result blinded with [-50,50] MeV offset until previous steps were complete
Combine all measurements into a final charged-track momentum scale

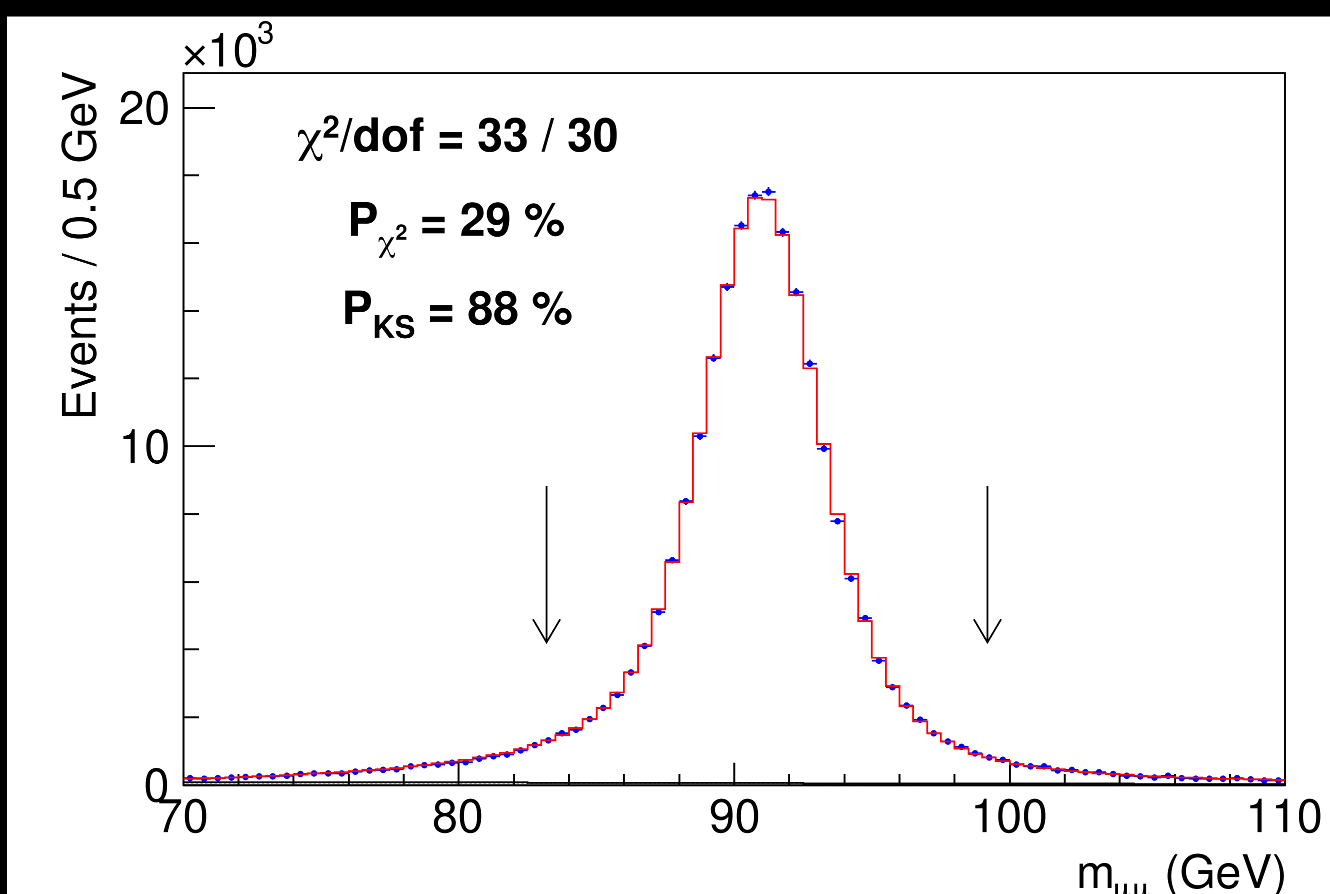

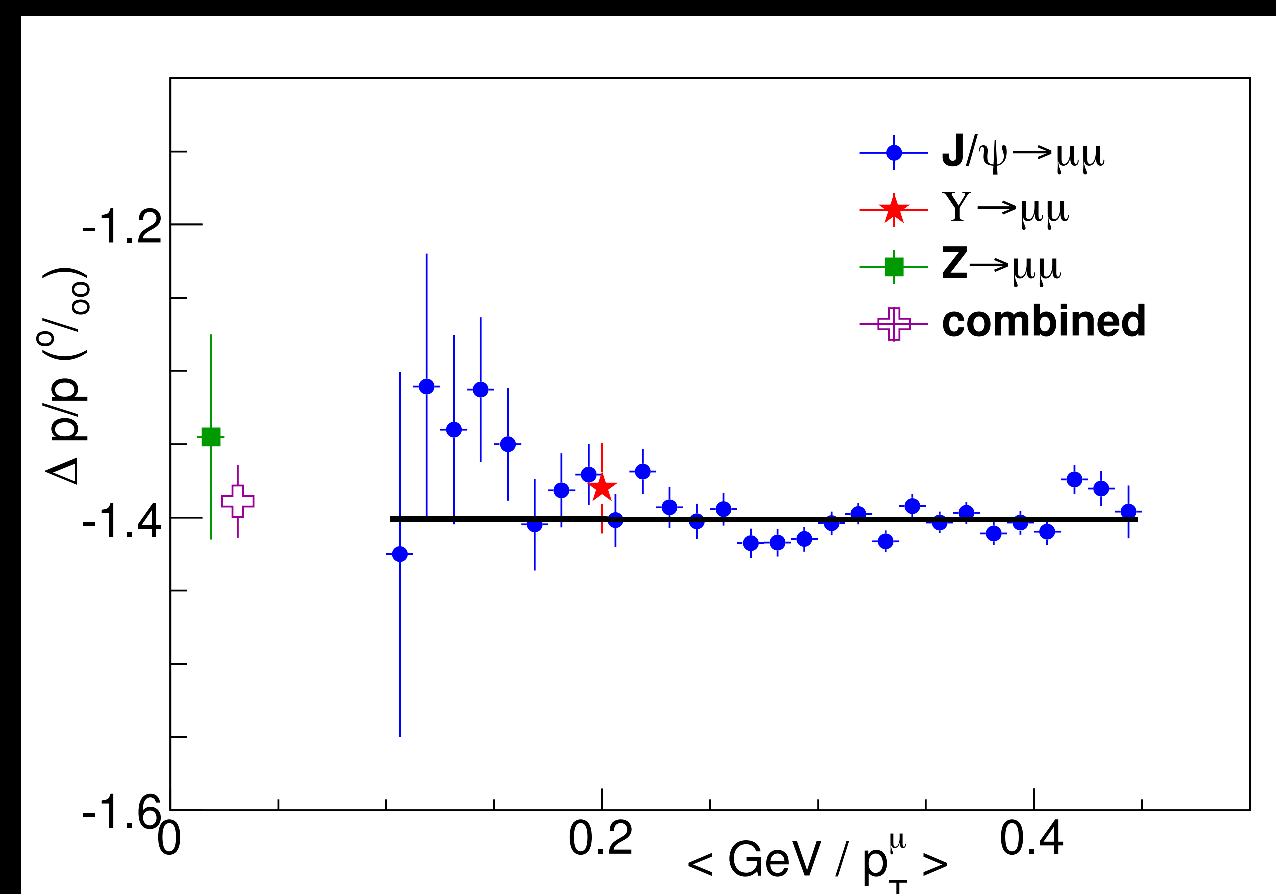

Electron momentum calibration

First step is to transfer the track calibration to the calorimeter (E/p) using W & Z decays

Simulation:
Detailed model of bremsstrahlung and pair production upstream of the drift chamber
Parameterized calorimeter shower deposition based on GEANT4

Kotwal & CH, NIMA 729, 25 (2013)

Tune energy loss due to material upstream of the tracker (high E/p)
Tune shower leakage due to finite calorimeter thickness (low E/p)
Correct for small non-linear calorimeter response

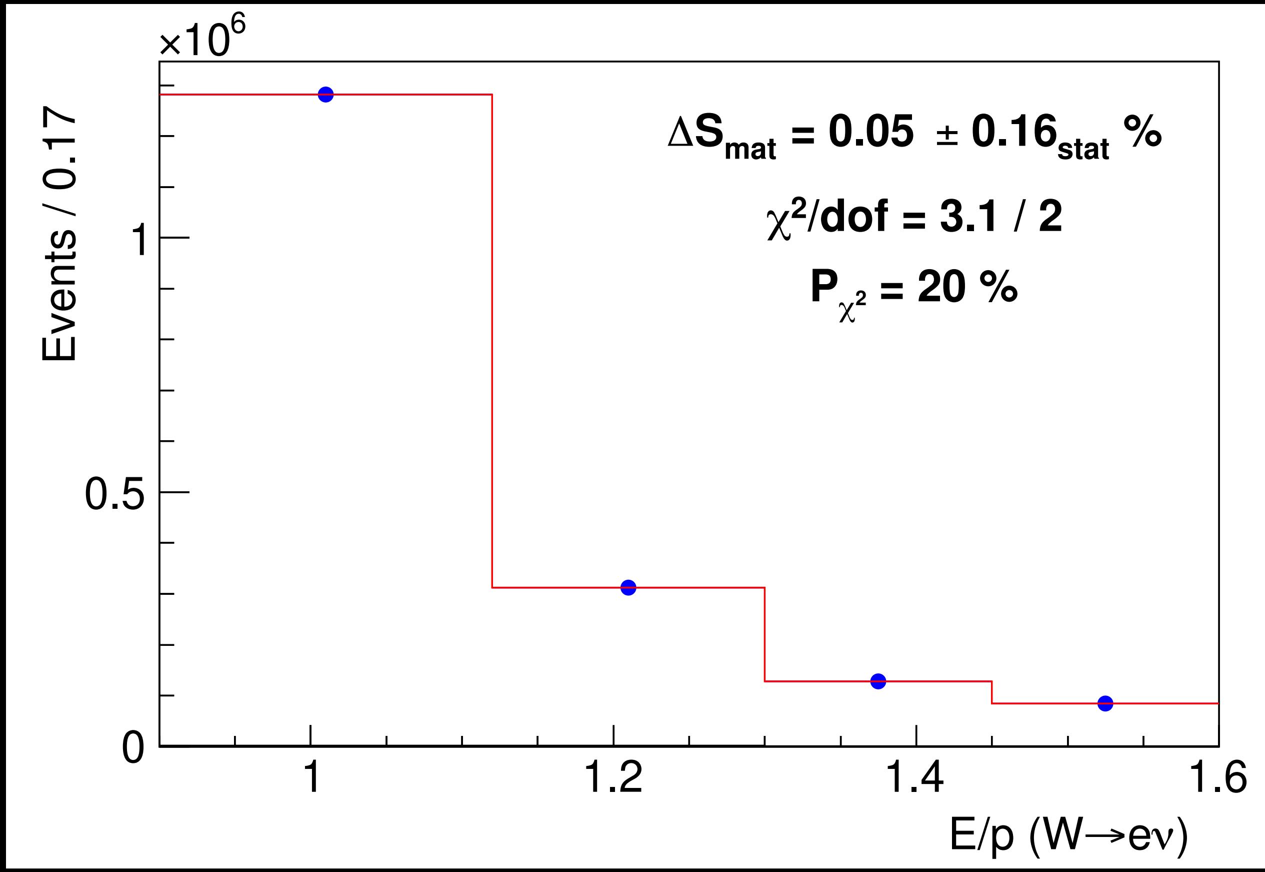

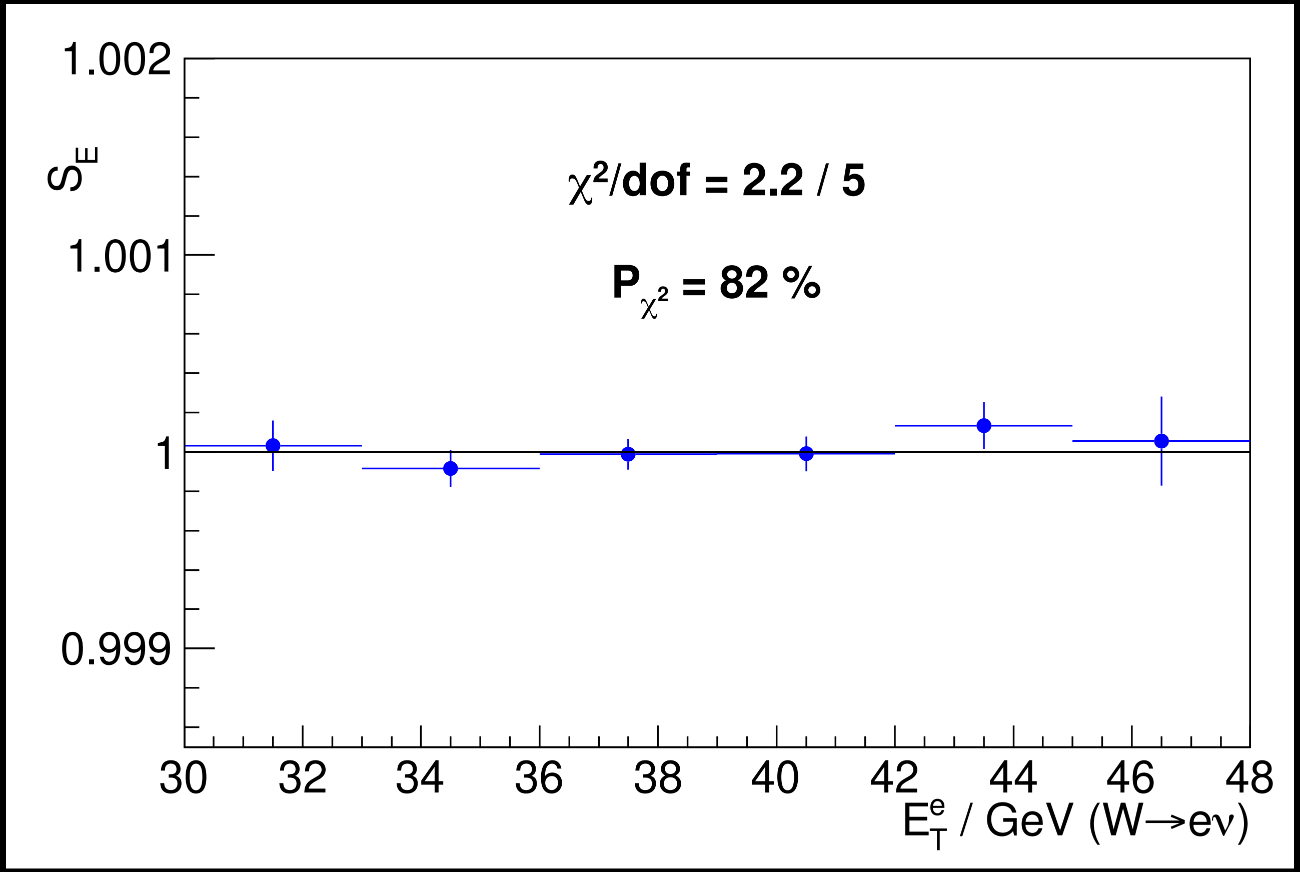

Electron momentum calibration

First step is to transfer the track calibration to the calorimeter (E/p) using W & Z decays

Data corrections:

Use mean E/p to remove time dependence & response variations in tower

Fit ratio of calorimeter energy to track momentum to correct each tower in η

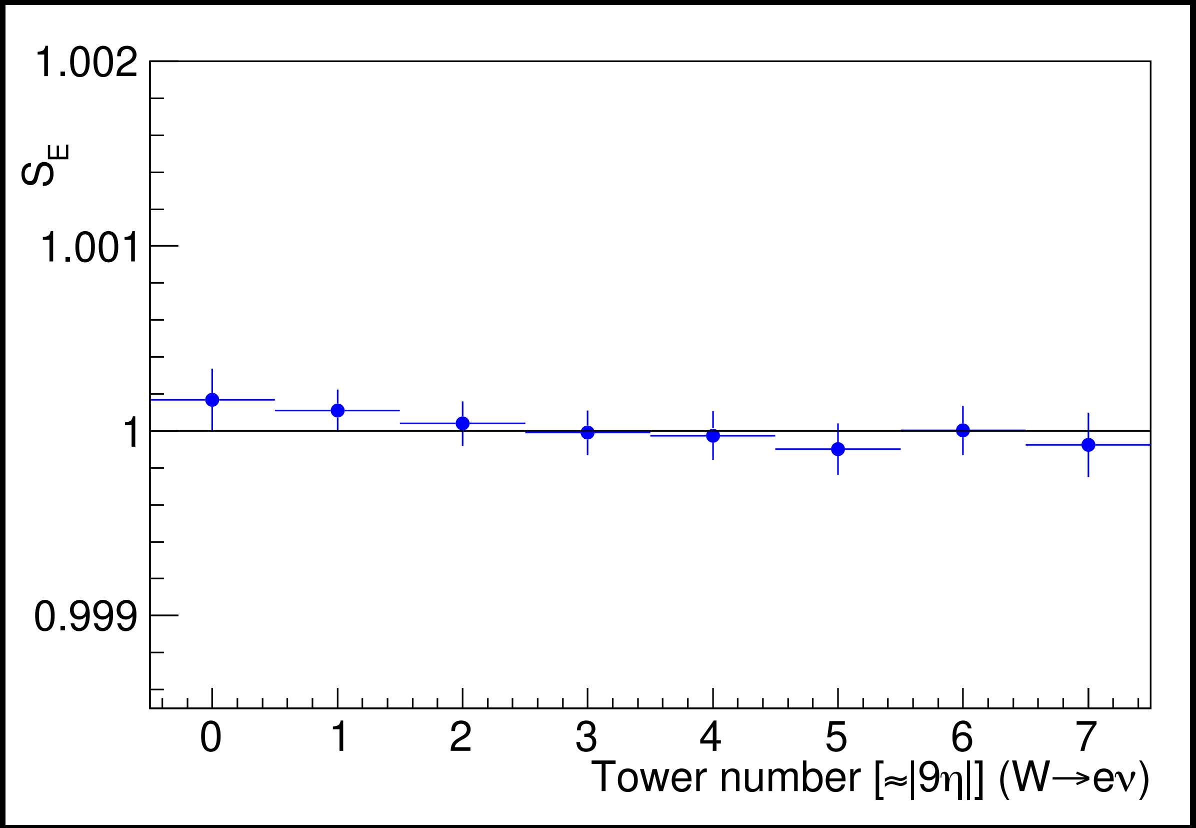

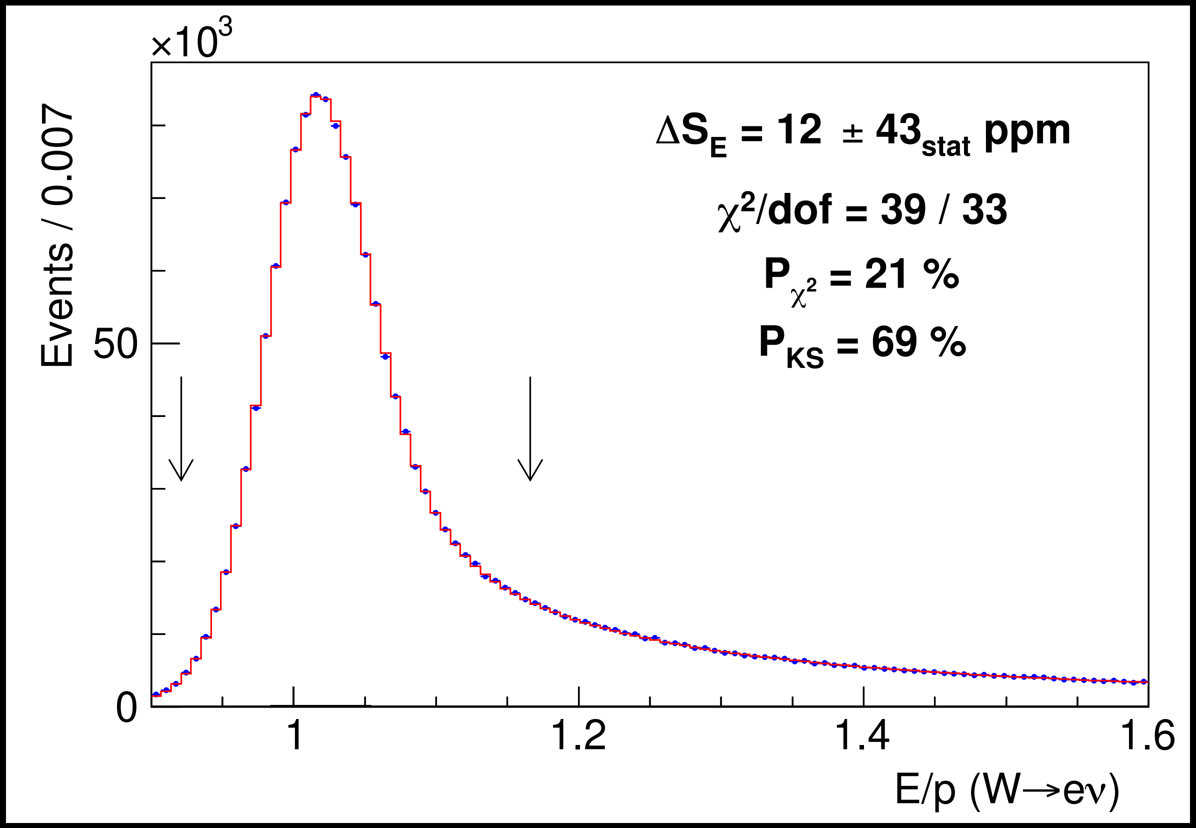

Electron momentum calibration

Second step is the measurement of the Z boson mass

$$M_Z = 91\ 194.3 \pm 13.8_{stat} \pm 7.6_{sys} \text{ MeV}$$

As a consistency check measure mass using only track information

e.g. $M_Z = 91\ 215.2 \pm 22.4$ MeV for non-radiative electrons (E/p<1.1)

Same blinding as for muon channel

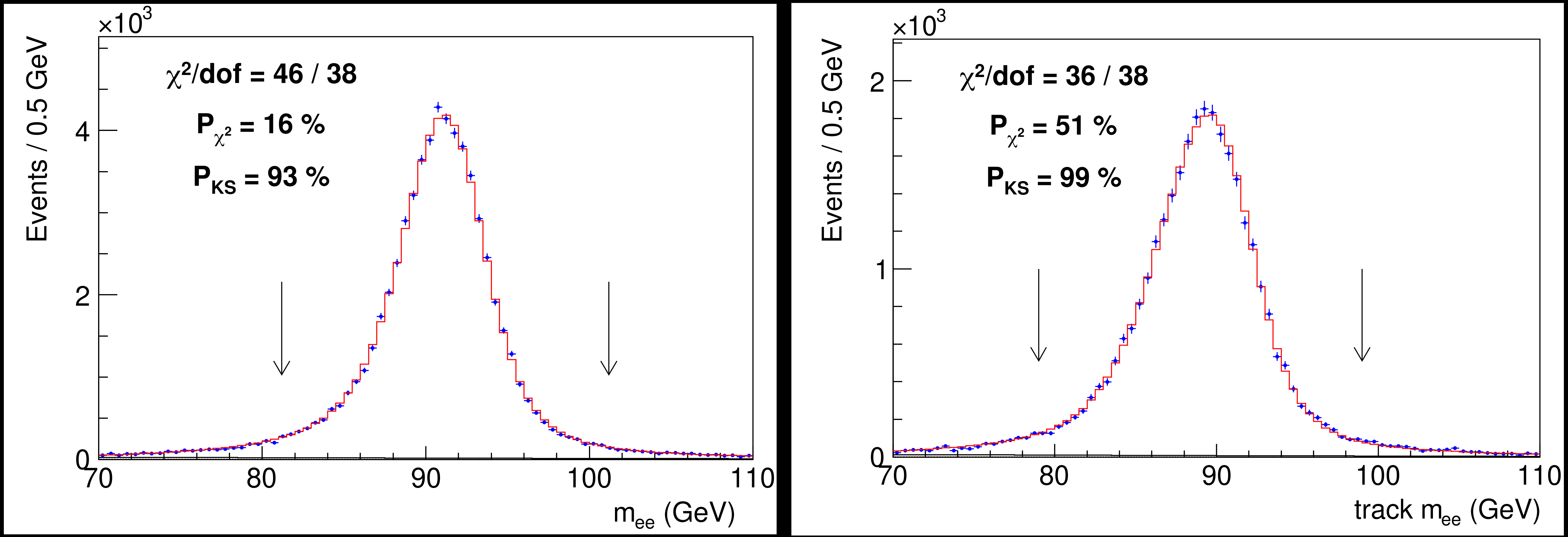

Recoil momentum calibration

First step is the alignment of the calorimeters

- Misalignments relative to the beam axis cause a modulation in the recoil direction
- Alignment performed separately for each run period using minimum-bias data

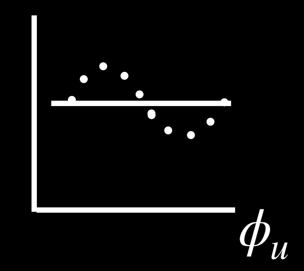

Second step is the reconstruction of the recoil

- Remove towers traversed by identified leptons
- Remove corresponding recoil energy in simulation using towers rotated by 90°
  - *validate using towers rotated by 180°*

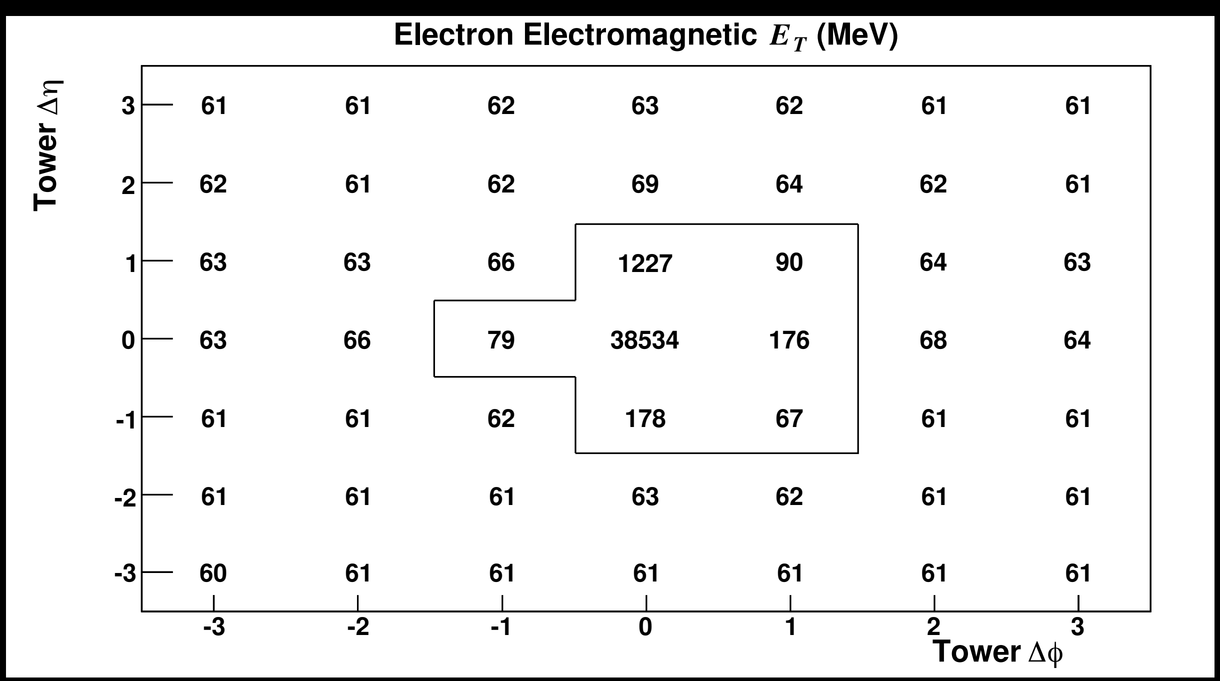

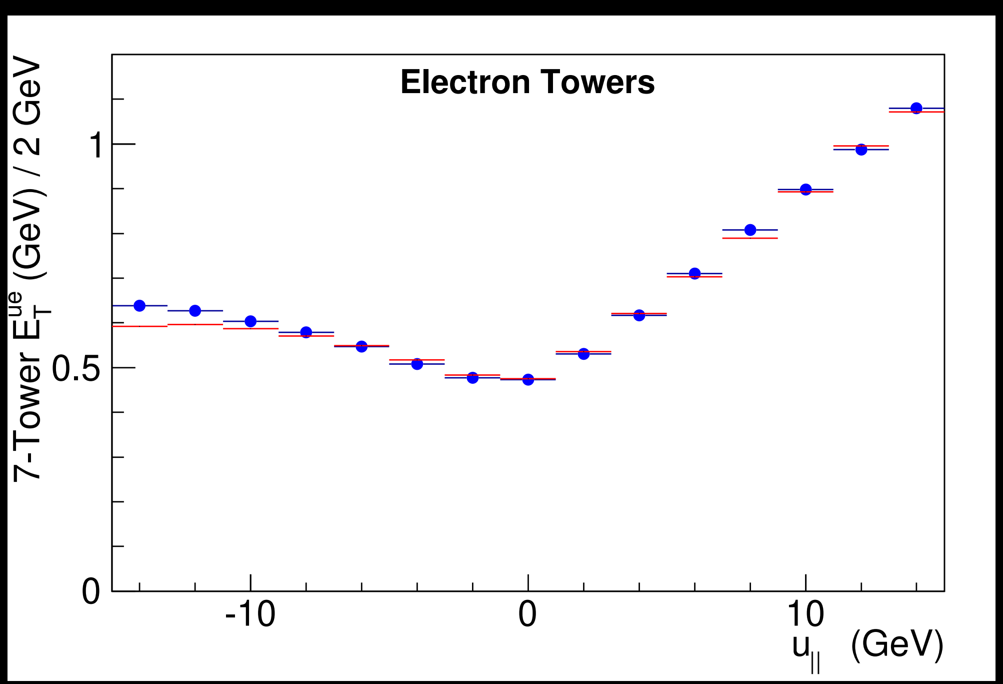

Recoil momentum calibration

Third step is the calibration of the recoil response

Balance recoil against direction of p_T^Z

Check calibration using ratio of recoil magnitude to p_T^Z along direction of p_T^Z (R_{rec})

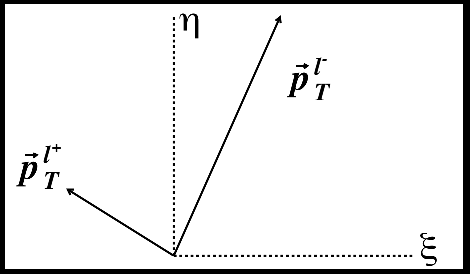

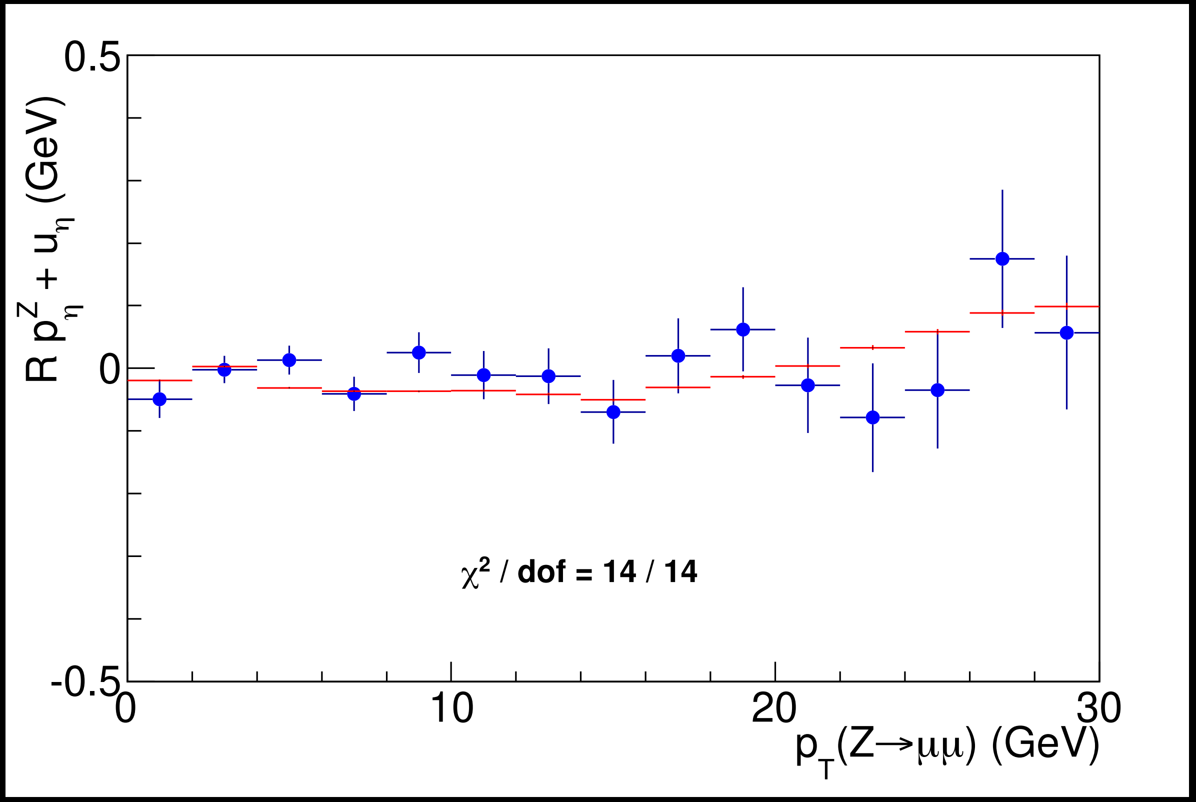

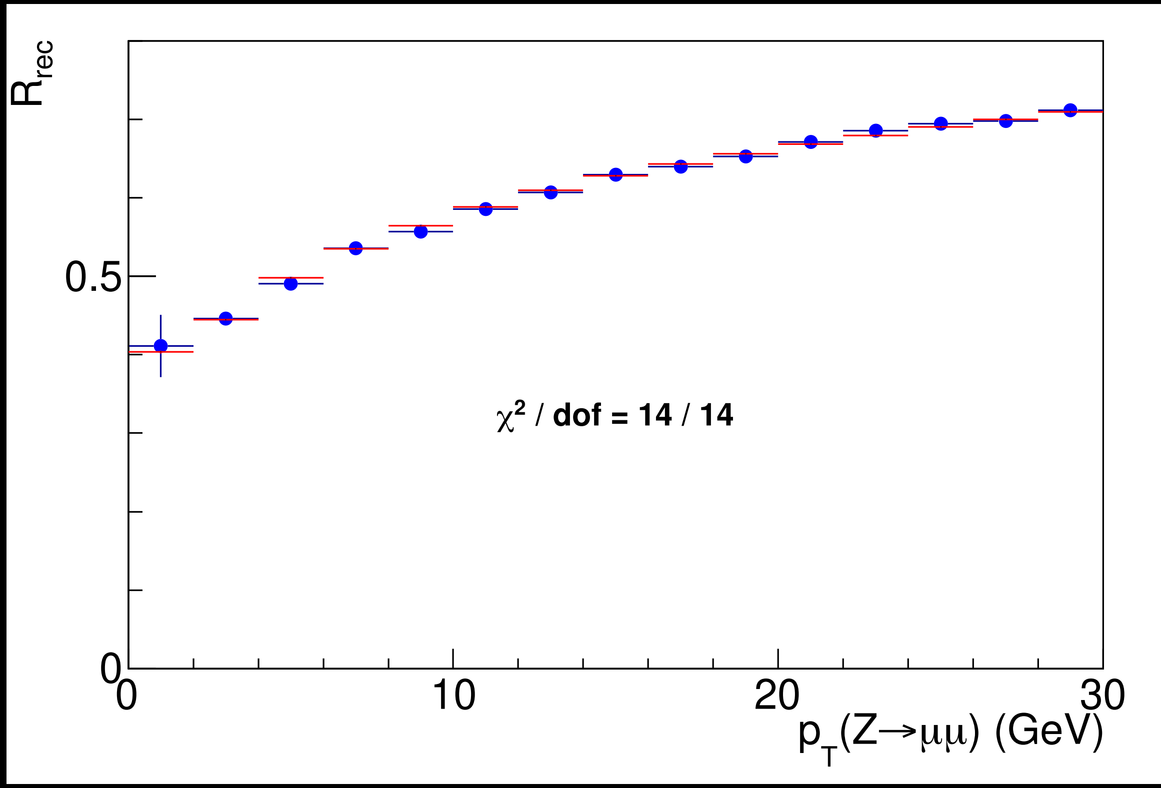

Recoil momentum calibration

Fourth step is the calibration of the recoil resolution

Includes jet-like energy and angular resolution, additional dijet fraction term, and pileup

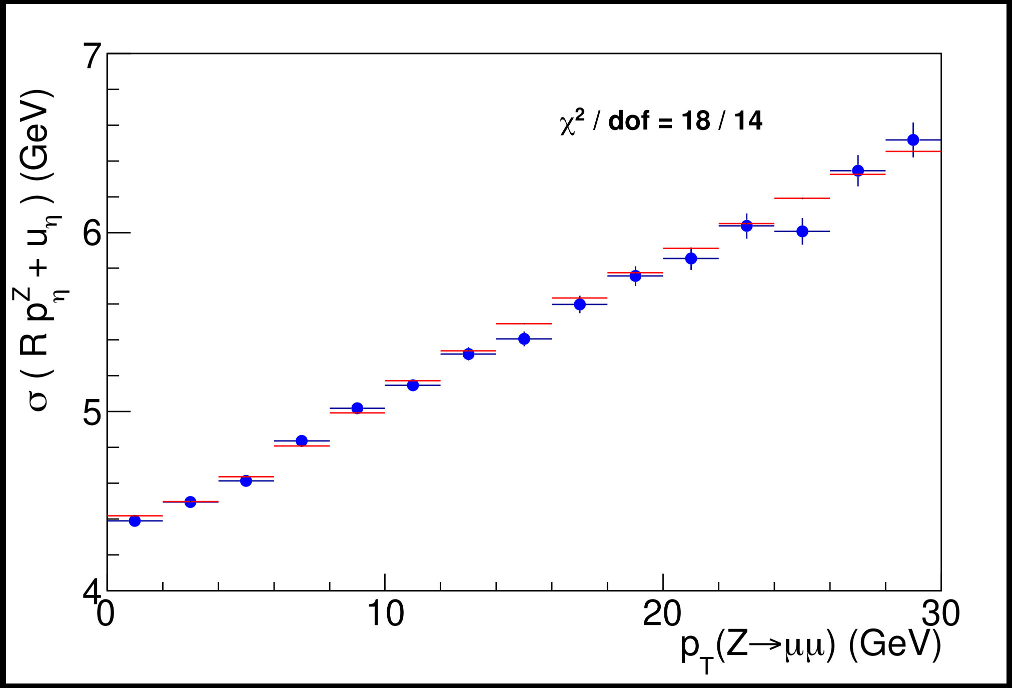

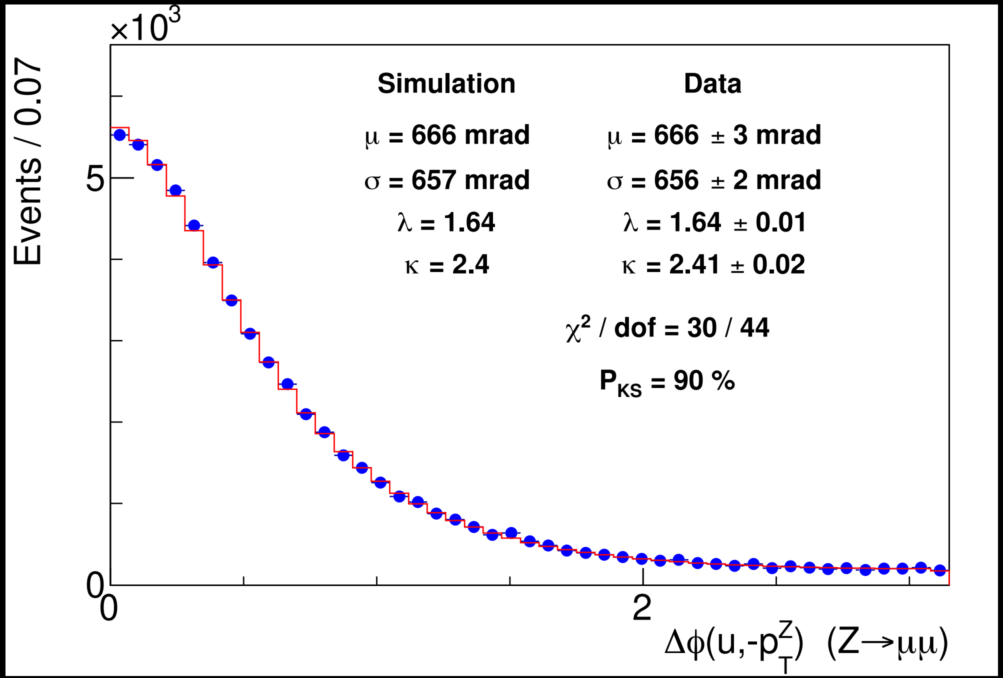

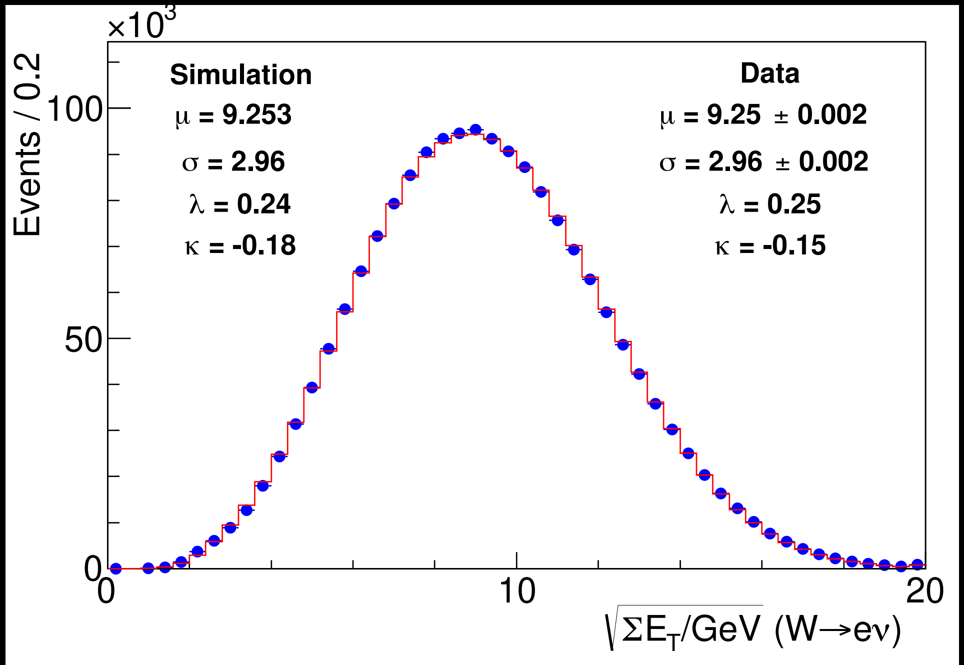

Recoil momentum validation

W boson recoil distributions validate the model

Most important is the recoil projected along the charged-lepton's momentum ($u_{||}$)

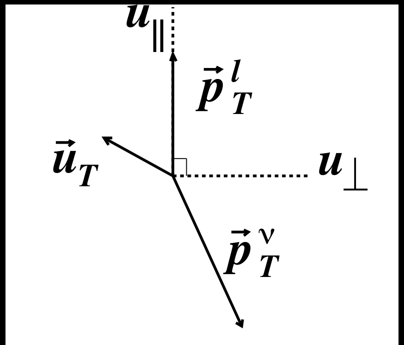

$$m_T \approx 2p_T\sqrt{1 + u_{||}/p_T} \approx 2p_T + u_{||}$$

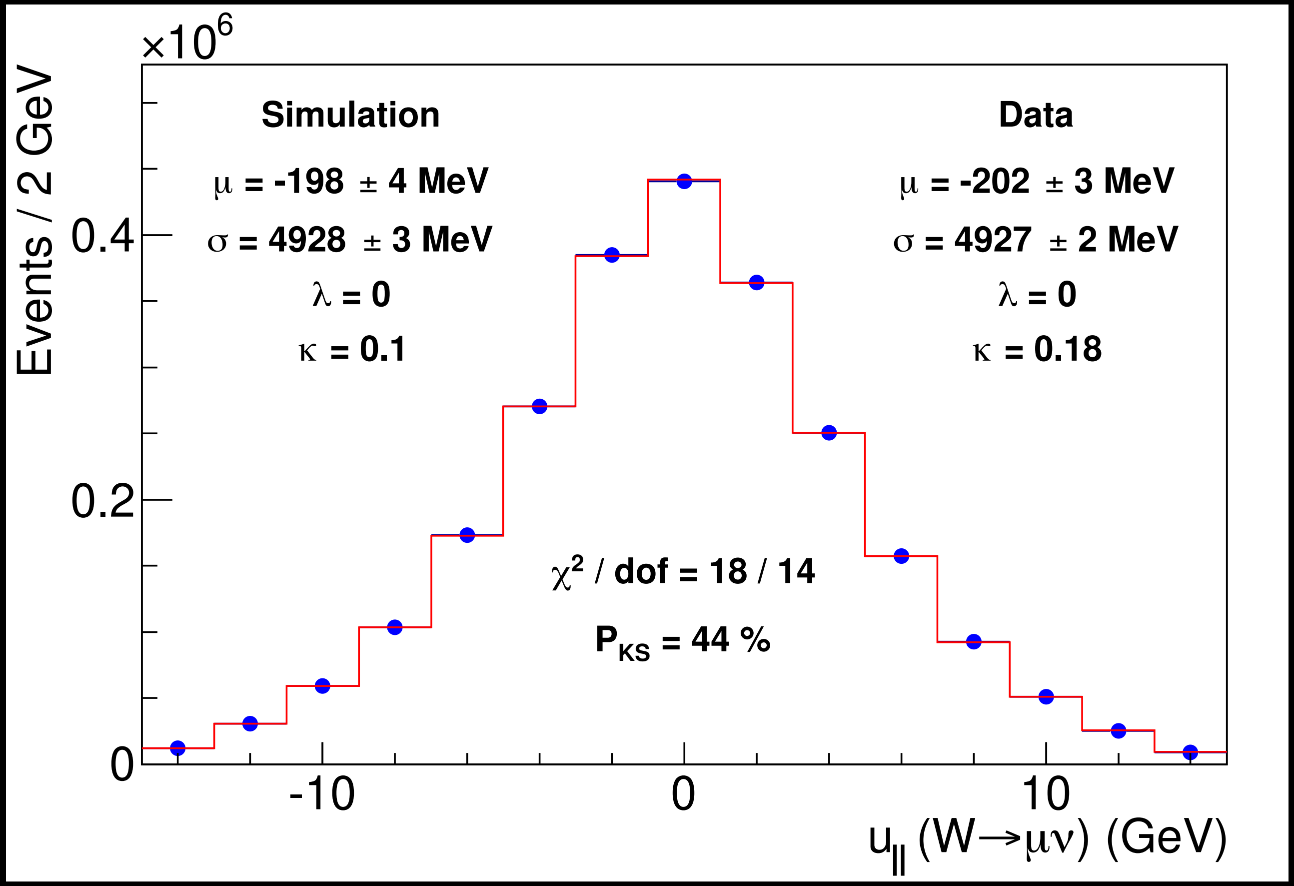

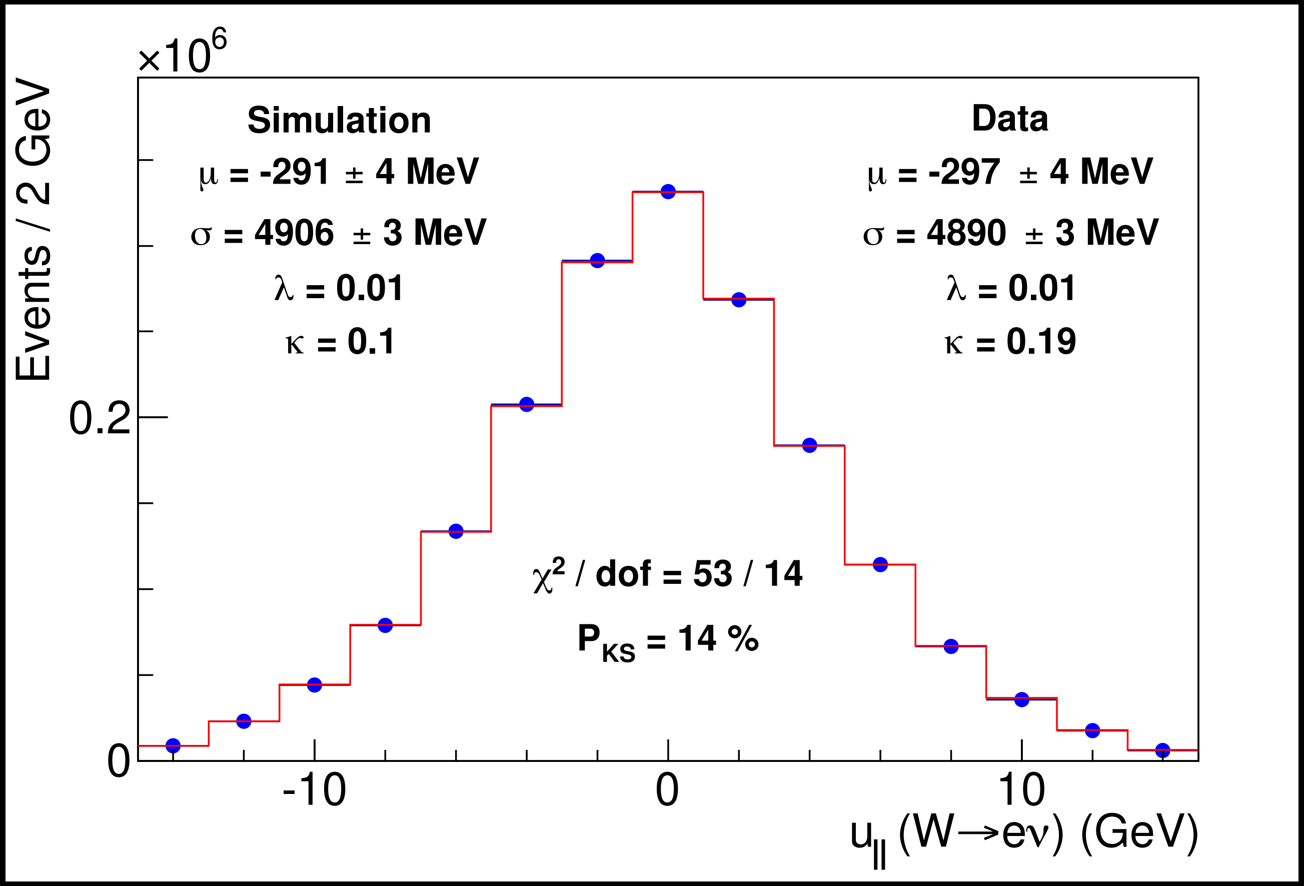

W boson candidates

W boson event selection
Triggers with low momentum thresholds (18 GeV) and very loose lepton id

Offline id also loose, efficiencies vary by 2% as hadronic recoil direction changes

No lepton isolation requirement in trigger or offline selection

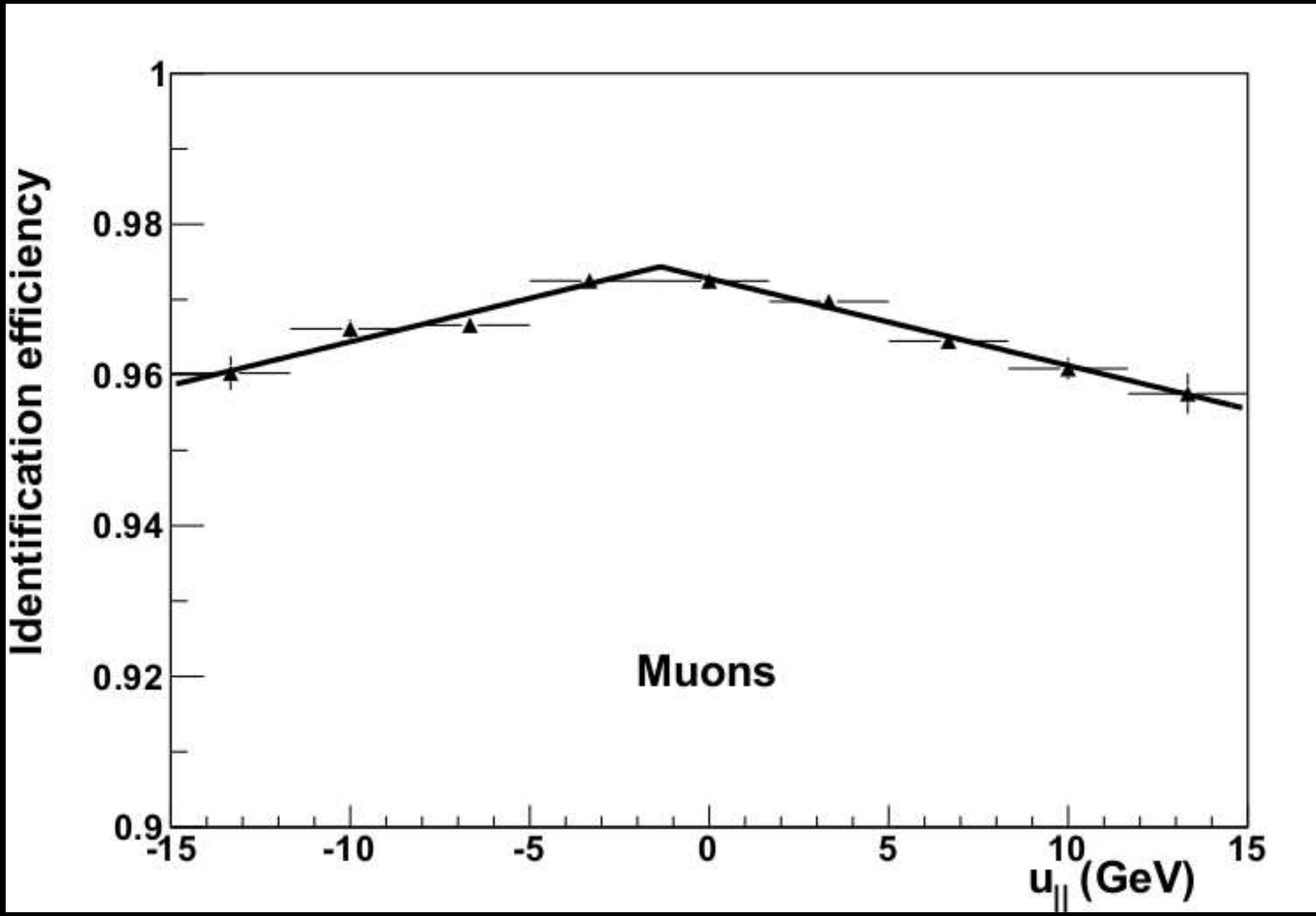

Background suppressed by stringent hadronic recoil requirement
u_T < 15 GeV

Other kinematic requirements
Lepton and missing p_T in the range 30-55 GeV
Transverse mass in the range 60-100 GeV

2.4 M $W \rightarrow \mu\nu$ candidates
1.8 M $W \rightarrow e\nu$ candidates

Backgrounds

Electroweak backgrounds modelled with fast simulation tuned with data and full simulation
Cross-checked with full simulation tuned to data

Largest background is $Z \to \mu\mu$ with one unreconstructed muon: **7.4% of data sample**
$W \to \tau\nu$ background is ~1% in each channel: largest background in electron sample

Background from hadrons misreconstructed as leptons estimated using data: 0.2-0.3%

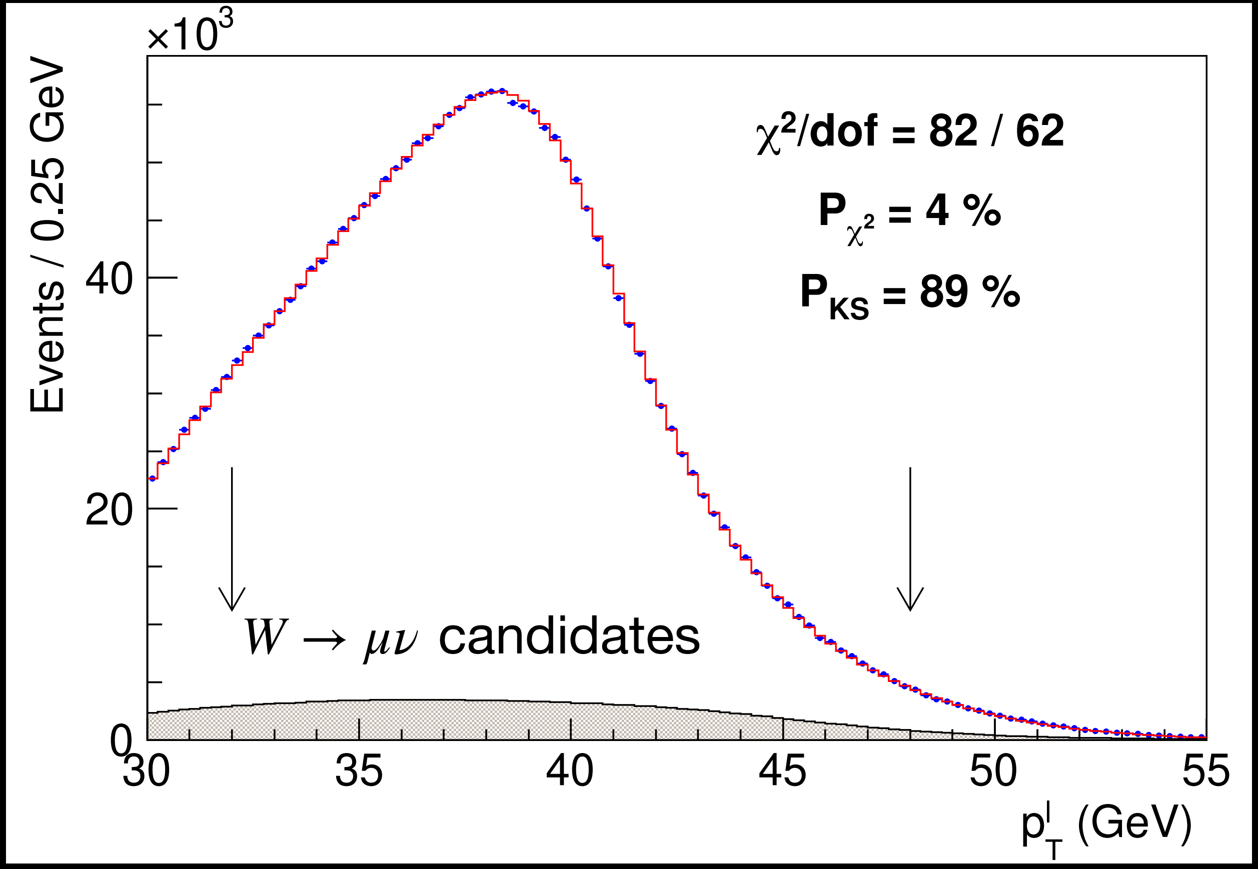

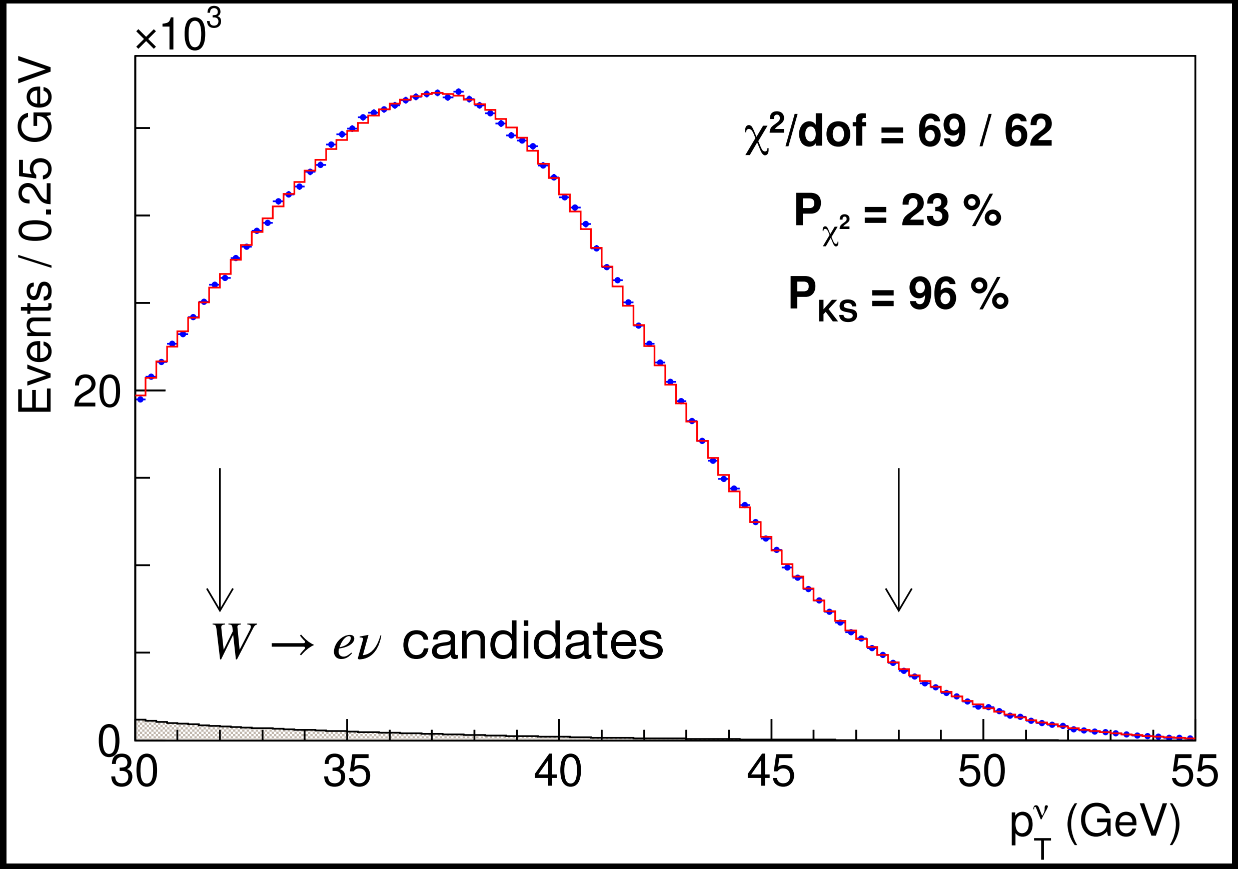

W boson transverse momentum

Boson p_T impacts the p_T distributions of the decay leptons

Resbos used to generate events with non-perturbative parameters and NNLL resummation to model the region of low boson p_T

Z boson p_T used to constrain the non-perturbative parameter g_2 and the perturbative coupling α_s

Resbos models W boson p_T well

uncertainty estimated using DYQT and constrained with data

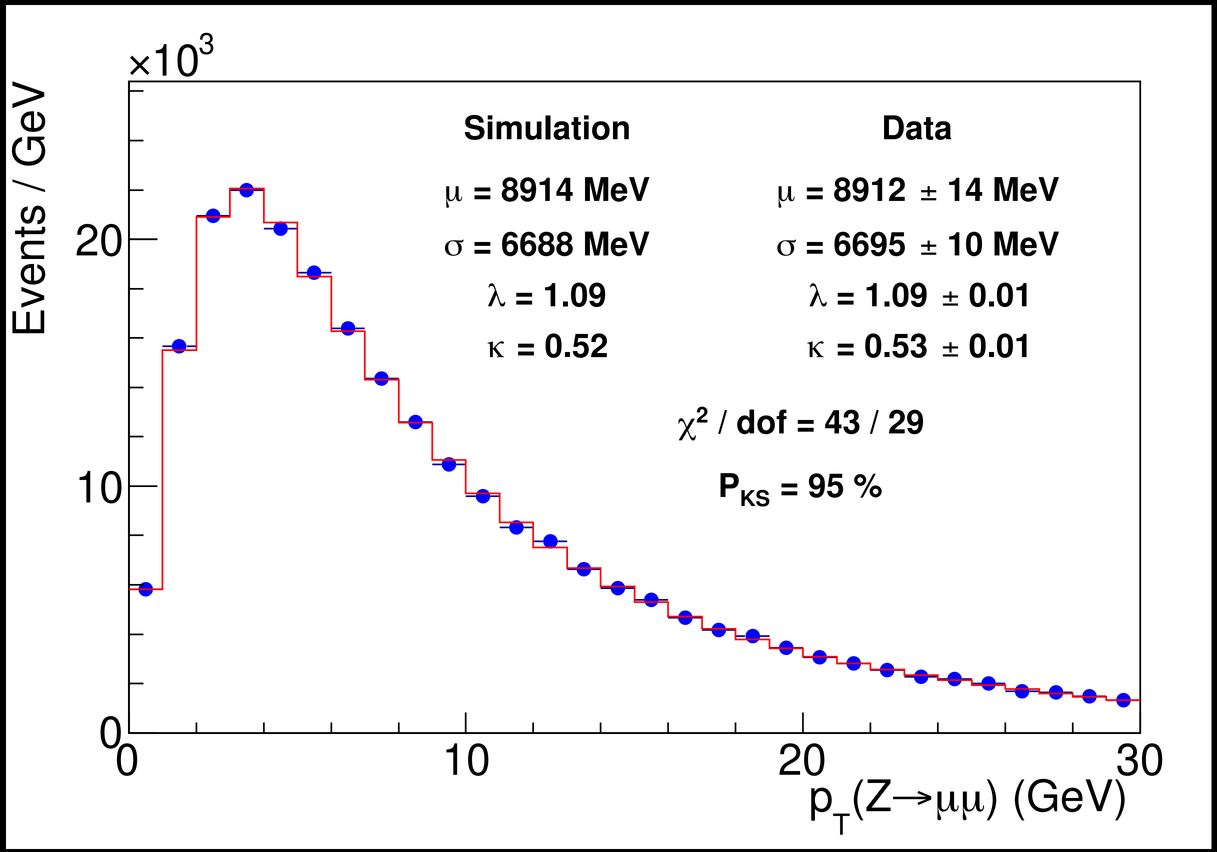

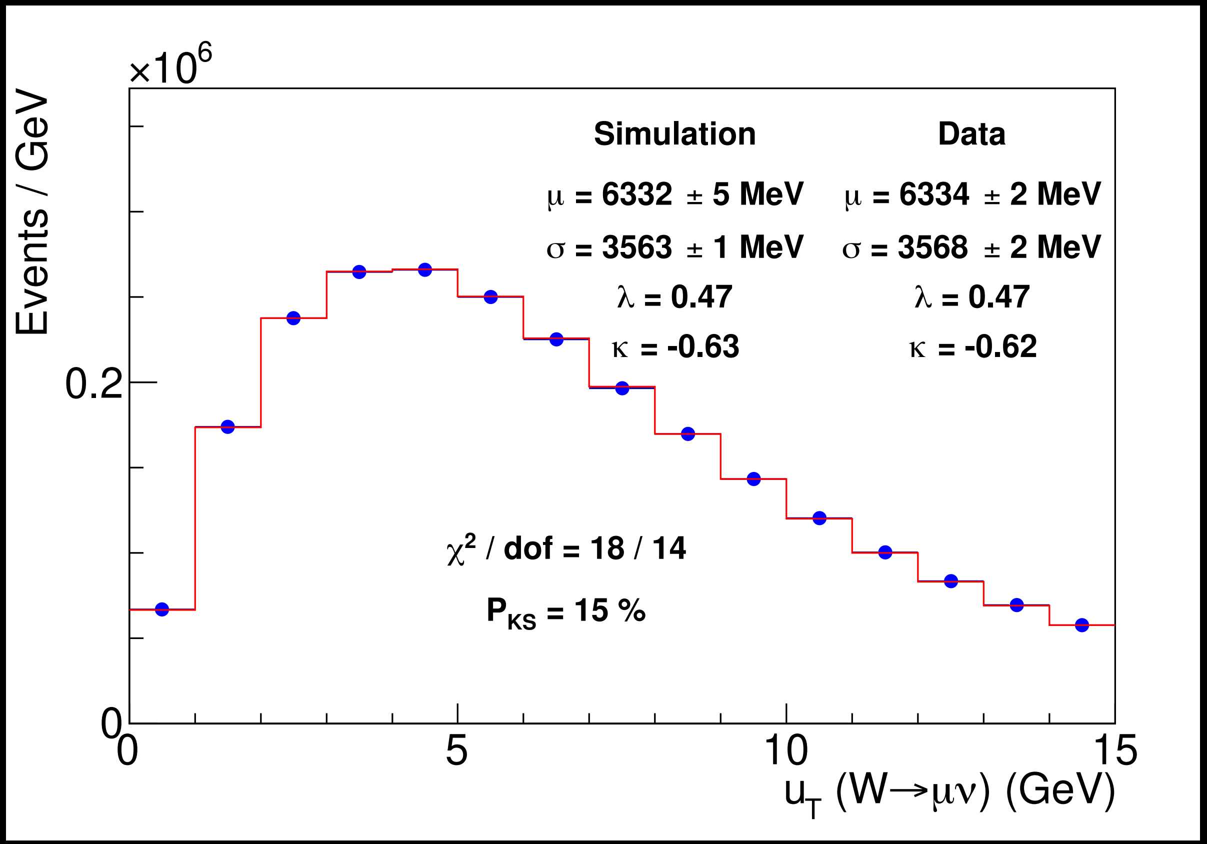

W boson production and decay

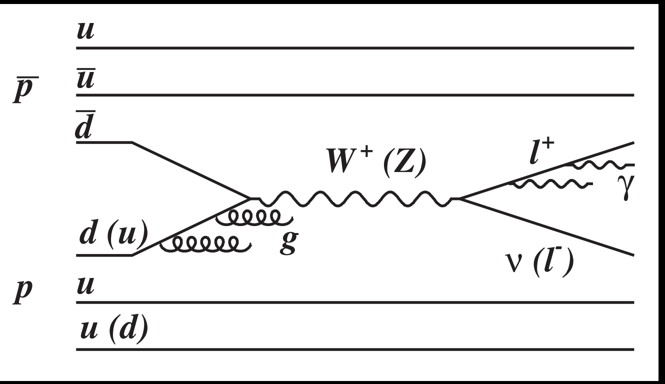

Parton distributions impact the measurement through lepton acceptance

Restriction in η reduces the fraction of low-p_T leptons

Small correction applied to update to NNPDF3.1 NNLO PDF

The set with the most W charge asymmetry measurements at the time

Uncertainty determined using a principal component analysis on the replica set

Measurement sensitive to ~15 eigenvectors

Leading 25 eigenvectors used to estimate uncertainty (3.9 MeV)

Three general NNLO PDF sets (NNPDF3.1, CT18, and MMHT14) have a range of ± 2.1 MeV from mean

Photos resummation with ME corrections used to model final-state photon radiation

validated by studying the average radiation in EM towers around the charged lepton, and with the Z mass measurement

W boson mass measurement

Result blinded by [-50,50] MeV offset until all previous steps complete

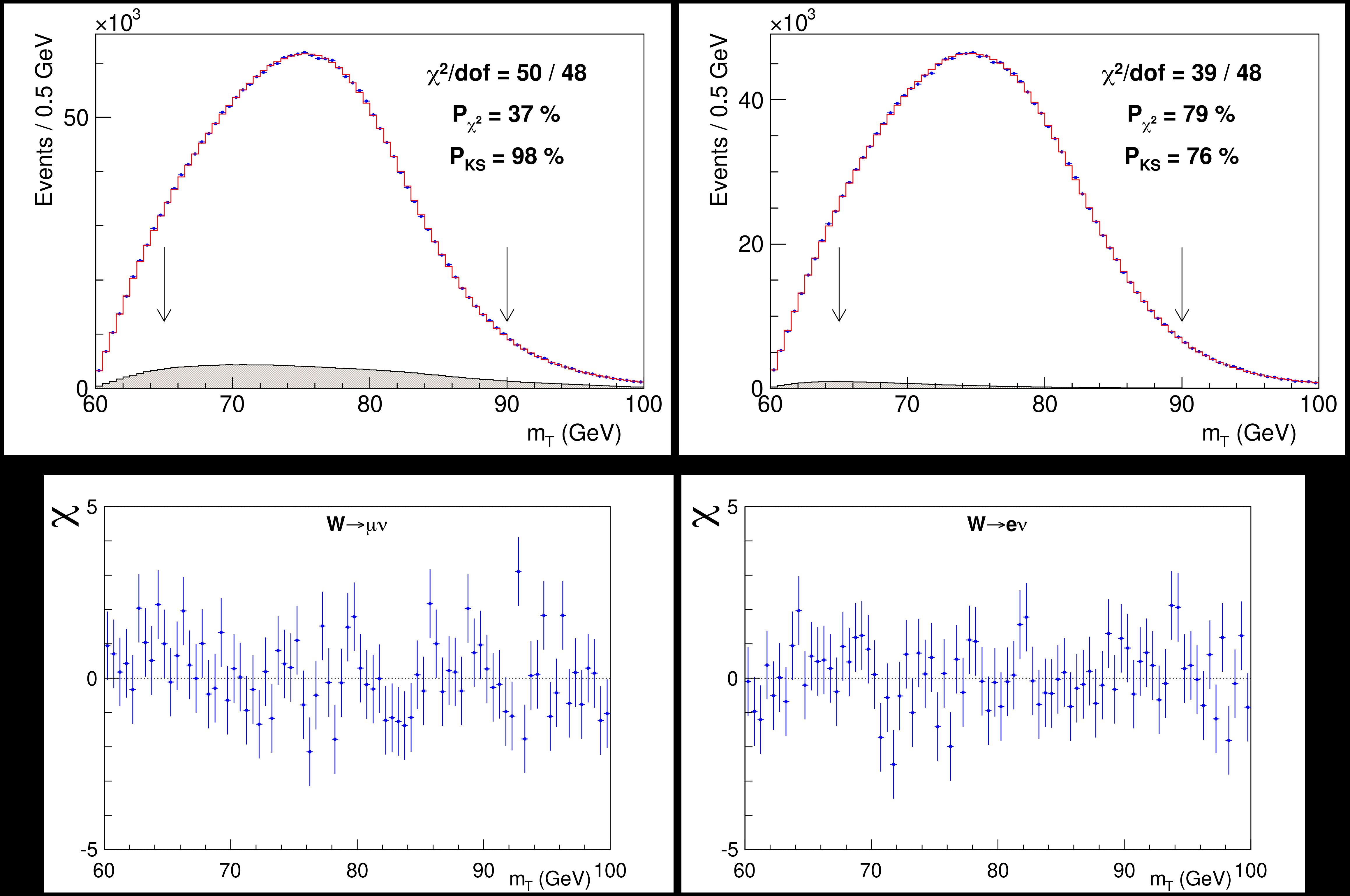

Mass measurement with p_T^ℓ distribution

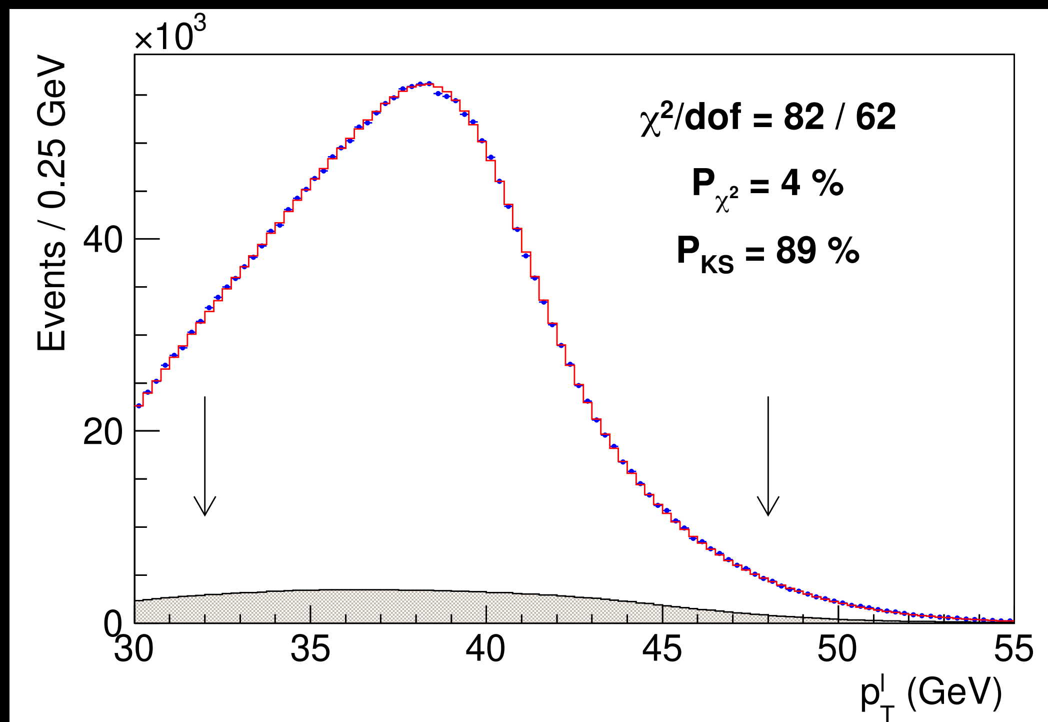

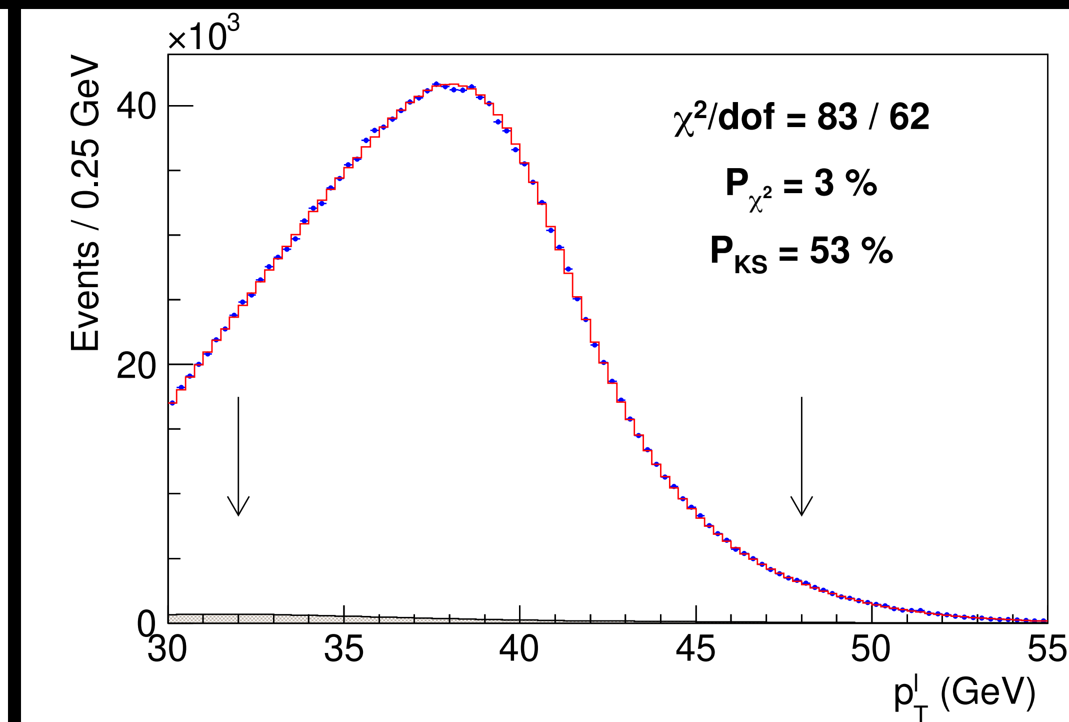

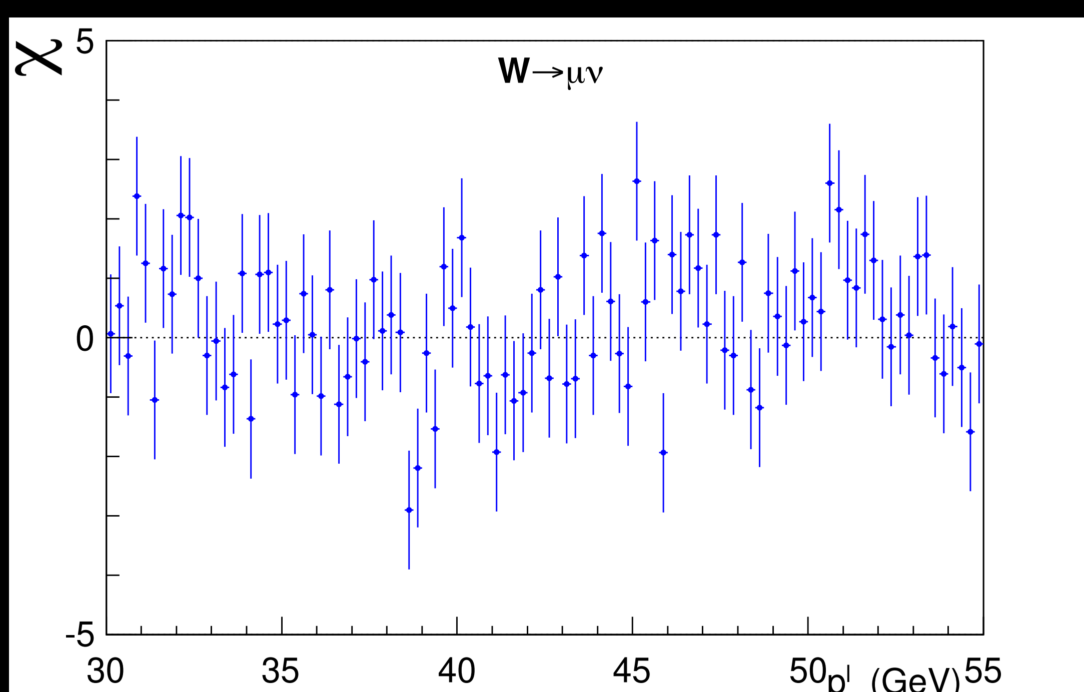

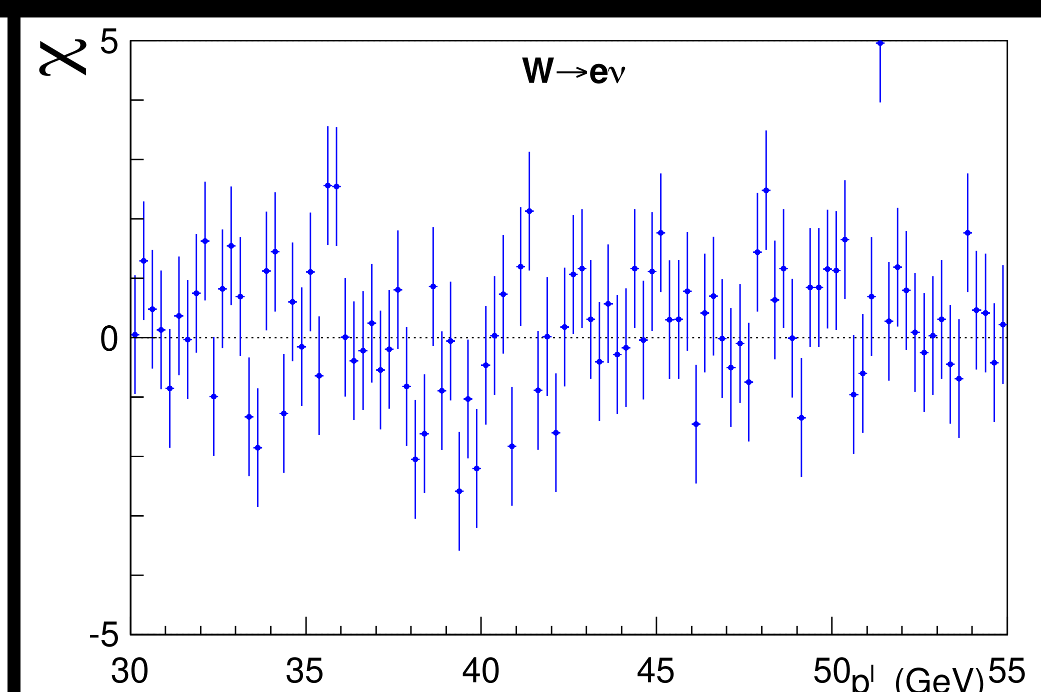

Mass measurement with p_T^ν distribution

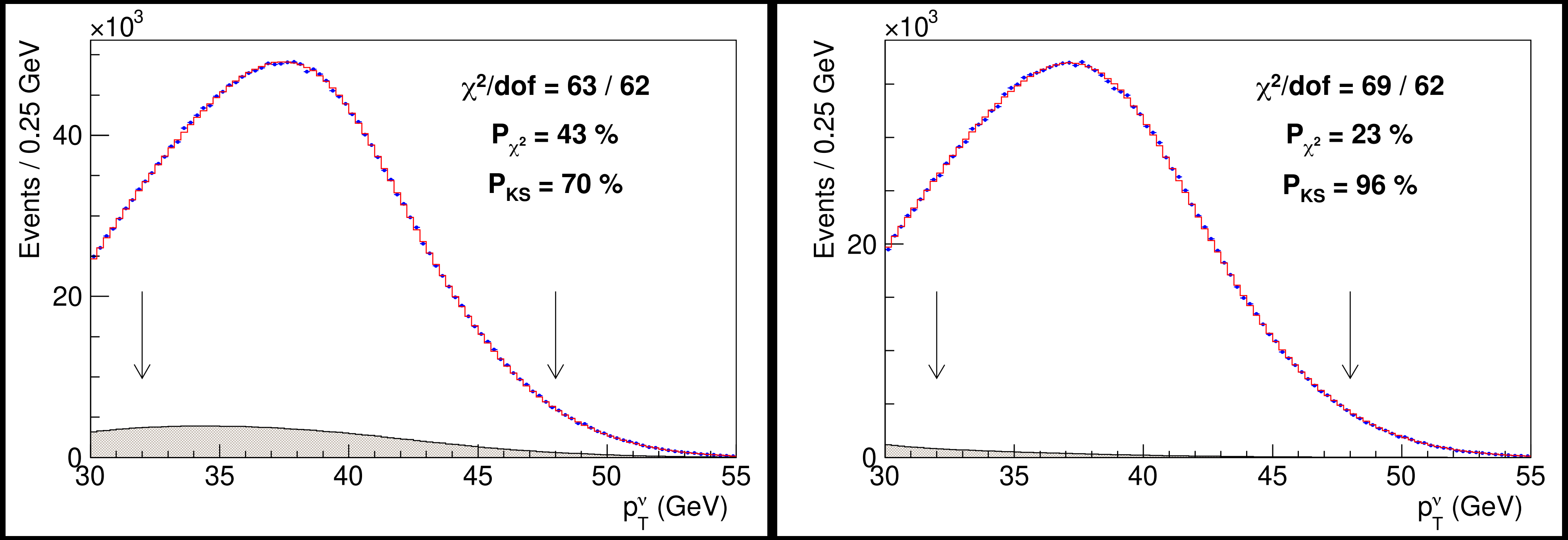

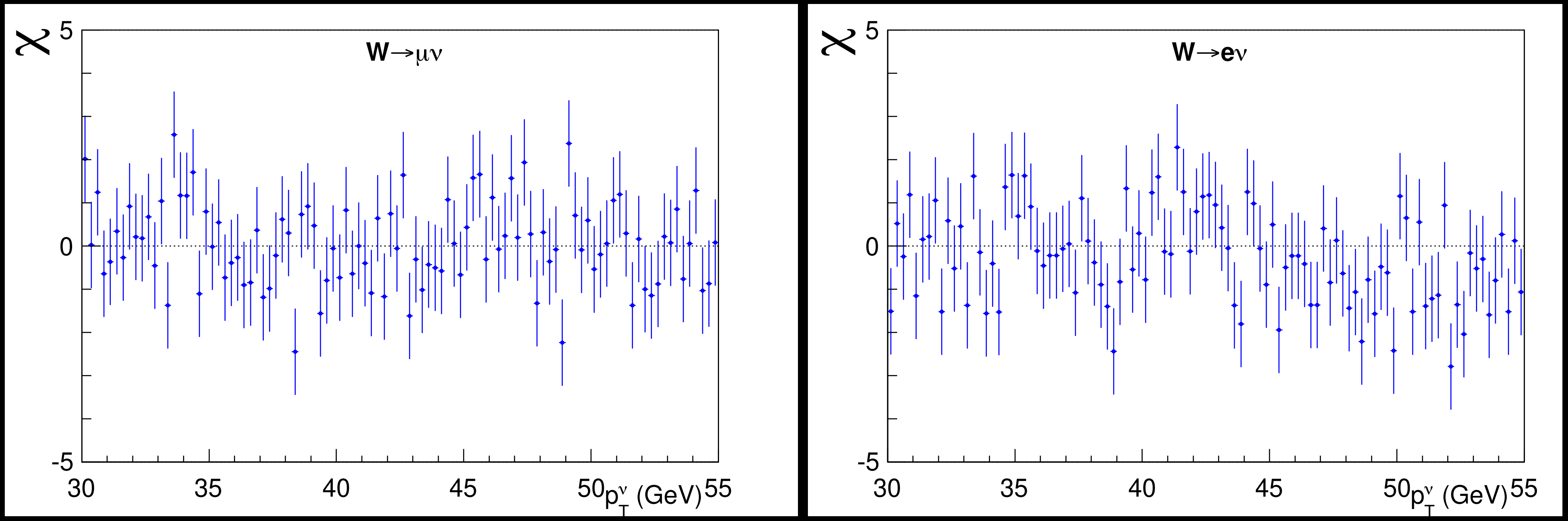

W boson mass measurement

Combination	m_T fit		p_T^ℓ fit		p_T^ν fit		Value (MeV)	χ^2/dof	Probability (%)
	Electrons	Muons	Electrons	Muons	Electrons	Muons			
m_T	✓	✓					$80\ 439.0 \pm 9.8$	1.2 / 1	28
p_T^ℓ			✓	✓			$80\ 421.2 \pm 11.9$	0.9 / 1	36
p_T^ν					✓	✓	$80\ 427.7 \pm 13.8$	0.0 / 1	91
m_T & p_T^ℓ	✓	✓	✓	✓			$80\ 435.4 \pm 9.5$	4.8 / 3	19
m_T & p_T^ν	✓	✓			✓	✓	$80\ 437.9 \pm 9.7$	2.2 / 3	53
p_T^ℓ & p_T^ν			✓	✓	✓	✓	$80\ 424.1 \pm 10.1$	1.1 / 3	78
Electrons	✓		✓		✓		$80\ 424.6 \pm 13.2$	3.3 / 2	19
Muons		✓		✓		✓	$80\ 437.9 \pm 11.0$	3.6 / 2	17
All	✓	✓	✓	✓	✓	✓	$80\ 433.5 \pm 9.4$	7.4 / 5	20

Fit difference	Muon channel	Electron channel
$M_W(\ell^+) - M_W(\ell^-)$	$-7.8 \pm 18.5_{\text{stat}} \pm 12.7_{\text{COT}}$	$14.7 \pm 21.3_{\text{stat}} \pm 7.7_{\text{stat}}^{\text{E/p}}$ $(0.4 \pm 21.3_{\text{stat}})$
$M_W(\phi_\ell > 0) - M_W(\phi_\ell < 0)$	$24.4 \pm 18.5_{\text{stat}}$	$9.9 \pm 21.3_{\text{stat}} \pm 7.5_{\text{stat}}^{\text{E/p}}$ $(-0.8 \pm 21.3_{\text{stat}})$
$M_Z(\text{run} > 271100) - M_Z(\text{run} < 271100)$	$5.2 \pm 12.2_{\text{stat}}$	$63.2 \pm 29.9_{\text{stat}} \pm 8.2_{\text{stat}}^{\text{E/p}}$ $(-16.0 \pm 29.9_{\text{stat}})$

Summary

W boson mass an important parameter for understanding naturalness

Measurement of W boson mass with <10 MeV precision achieved with complete CDF data set

Result of >20 years of experience with the CDF II detector

0.01% precision required flexibility: all experimental aspects controlled by the analysis team
Reconstruction, alignment, calibration, simulation, analysis

Analysis procedures approved pre-blinding and frozen

Surprising 0.1% deviation from SM motivates expanded study of m_W measurements and procedures

Backup

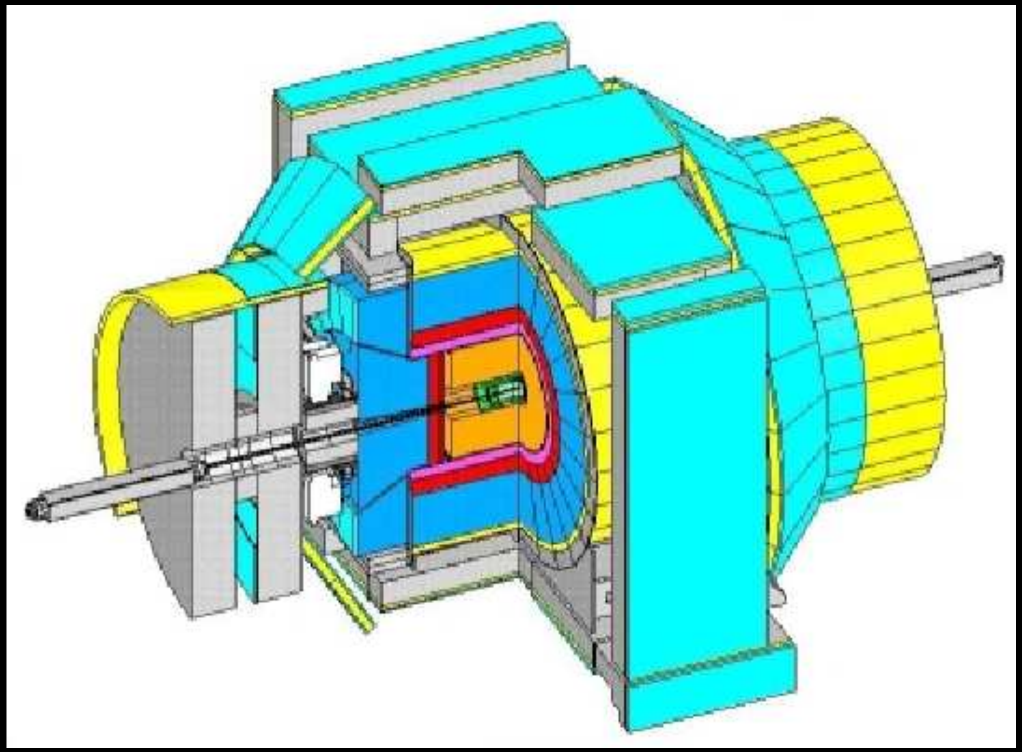

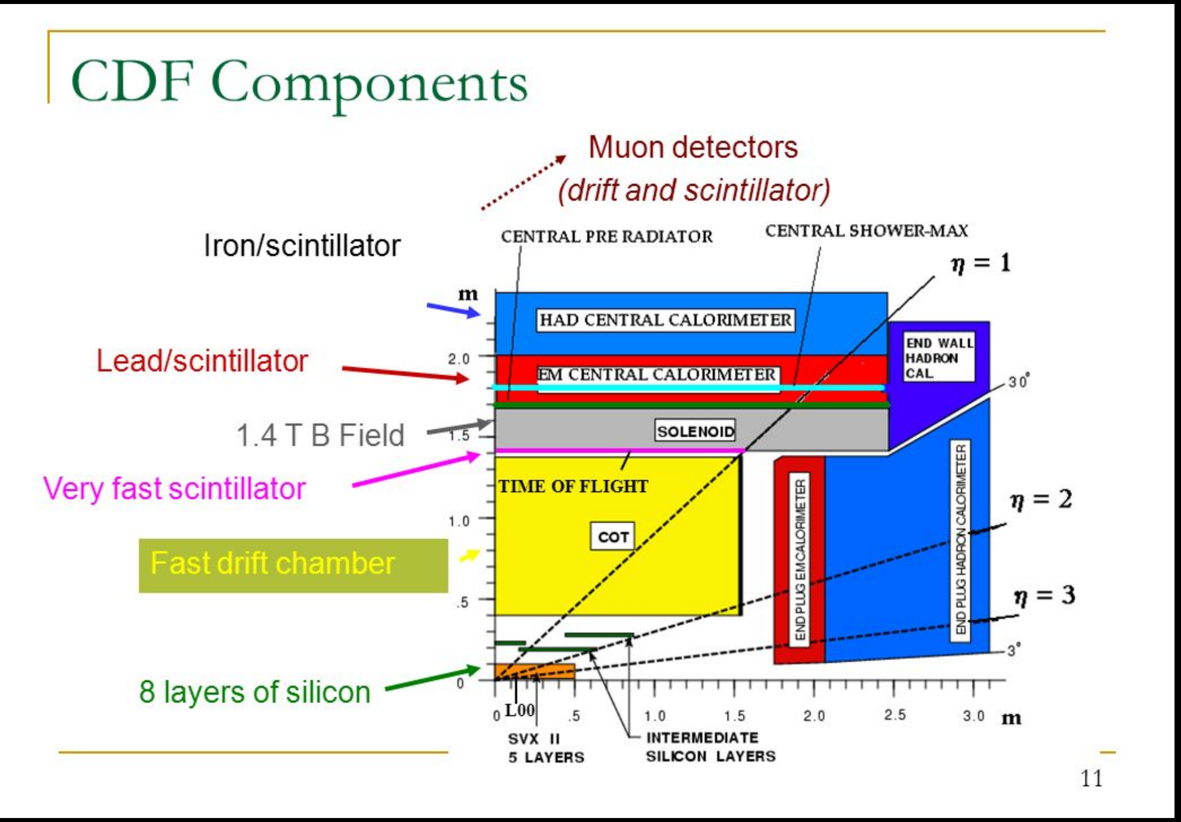
CDF Components
Muon detectors
(drift and scintillator)
Iron/scintillator
CENTRAL PRE RADIATOR
CENTRAL SHOWER-MAX
η = 1
HAD CENTRAL CALORIMETER
EM CENTRAL CALORIMETER
END WALL HADRON CAL
Lead/scintillator
1.4 T B Field
SOLENOID
Very fast scintillator
TIME OF FLIGHT
COT
Fast drift chamber
END PLUG EM CALORIMETER
END PLUG HADRON CALORIMETER
30°
η = 2
η = 3
3°
8 layers of silicon
L00
SVX II
5 LAYERS
INTERMEDIATE
SILICON LAYERS
m
0 .5 1.0 1.5 2.0 2.5 3.0 m
11

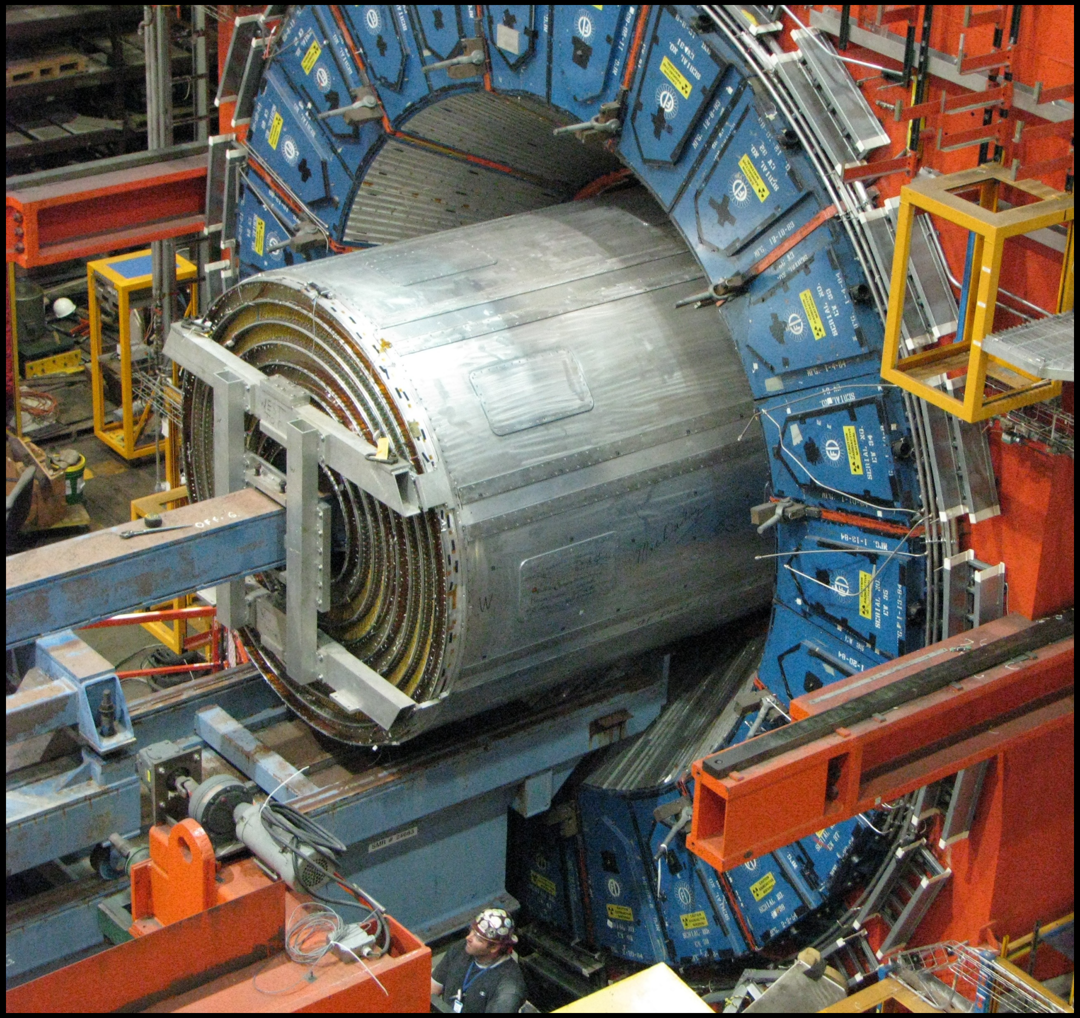

Uncertainties

Source of systematic uncertainty	m_T fit			p_T^ℓ fit			p_T^ν fit		
	Electrons	Muons	Common	Electrons	Muons	Common	Electrons	Muons	Common
Lepton energy scale	5.8	2.1	1.8	5.8	2.1	1.8	5.8	2.1	1.8
Lepton energy resolution	0.9	0.3	-0.3	0.9	0.3	-0.3	0.9	0.3	-0.3
Recoil energy scale	1.8	1.8	1.8	3.5	3.5	3.5	0.7	0.7	0.7
Recoil energy resolution	1.8	1.8	1.8	3.6	3.6	3.6	5.2	5.2	5.2
Lepton $u_{\|\|}$ efficiency	0.5	0.5	0	1.3	1.0	0	2.6	2.1	0
Lepton removal	1.0	1.7	0	0	0	0	2.0	3.4	0
Backgrounds	2.6	3.9	0	6.6	6.4	0	6.4	6.8	0
p_T^Z model	0.7	0.7	0.7	2.3	2.3	2.3	0.9	0.9	0.9
p_T^W/p_T^Z model	0.8	0.8	0.8	2.3	2.3	2.3	0.9	0.9	0.9
Parton distributions	3.9	3.9	3.9	3.9	3.9	3.9	3.9	3.9	3.9
QED radiation	2.7	2.7	2.7	2.7	2.7	2.7	2.7	2.7	2.7
Statistical	10.3	9.2	0	10.7	9.6	0	14.5	13.1	0
Total	13.5	11.8	5.8	16.0	14.1	7.9	18.8	17.1	7.4

Background fractions

Source	Fraction (%)	δM_W (MeV) m_T fit	p_T^μ fit	p_T^ν fit
$Z/\gamma^* \to \mu\mu$	7.37 ± 0.10	1.6 (0.7)	3.6 (0.3)	0.1 (1.5)
$W \to \tau\nu$	0.880 ± 0.004	0.1 (0.0)	0.1 (0.0)	0.1 (0.0)
Hadronic jets	0.01 ± 0.04	0.1 (0.8)	-0.6 (0.8)	2.4 (0.5)
Decays in flight	0.20 ± 0.14	1.3 (3.1)	1.3 (5.0)	-5.2 (3.2)
Cosmic rays	0.01 ± 0.01	0.3 (0.0)	0.5 (0.0)	0.3 (0.3)
Total	8.47 ± 0.18	2.1 (3.3)	3.9 (5.1)	5.7 (3.6)

Source	Fraction (%)	δM_W (MeV) m_T fit	p_T^e fit	p_T^ν fit
$Z/\gamma^* \to ee$	0.134 ± 0.003	0.2 (0.3)	0.3 (0.0)	0.0 (0.6)
$W \to \tau\nu$	0.94 ± 0.01	0.6 (0.0)	0.6 (0.0)	0.6 (0.0)
Hadronic jets	0.34 ± 0.08	2.2 (1.2)	0.9 (6.5)	6.2 (-1.1)
Total	1.41 ± 0.08	2.3 (1.2)	1.1 (6.5)	6.2 (1.3)

Initial state LO & NLO

W^+ initial	Type	Pythia LO	Madgraph LO	Madgraph NLO
u dbar	v-v	81.7%	82.0%	82.7%
dbar u	s-s	8.9%	9.0%	8.8%
u sbar	v-s	1.6%	1.9%	1.8%
sbar u	s-s	0.3%	0.3%	0.3%
c sbar	s-s	2.9%	2.9%	-
sbar c	s-s	2.9%	2.9%	-
c dbar	s-v	0.7%	0.7%	-
dbar c	s-s	0.2%	0.2%	-
u g	v-g		-	3.7%
g dbar	g-v		-	1.8%
g u	g-s		-	0.4%
dbar g	s-g		-	0.5%
g sbar	g-s		-	0.02%
sbar g	s-g		-	0.02%

Recoil in W & Z events

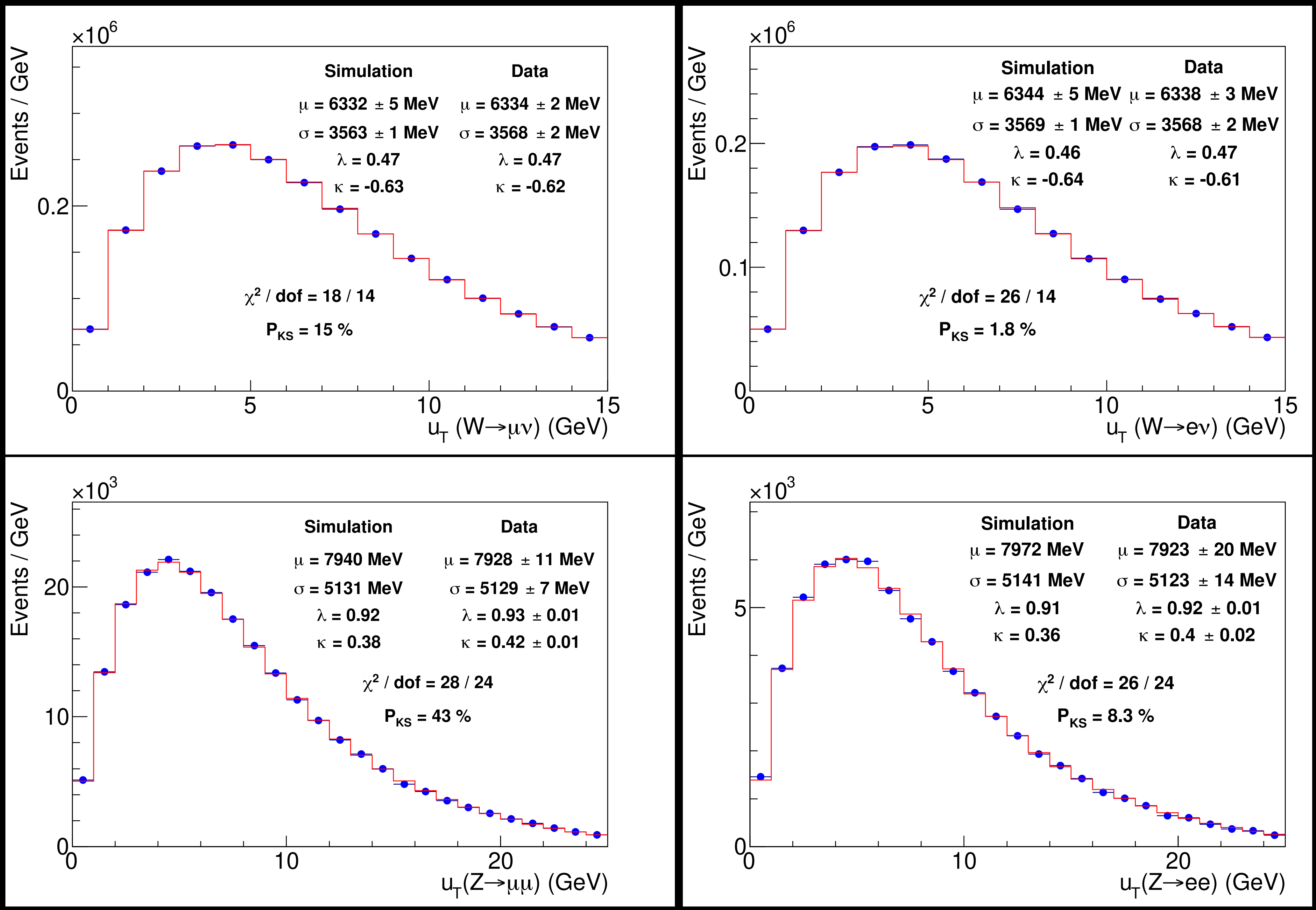

Recoil projections in W events

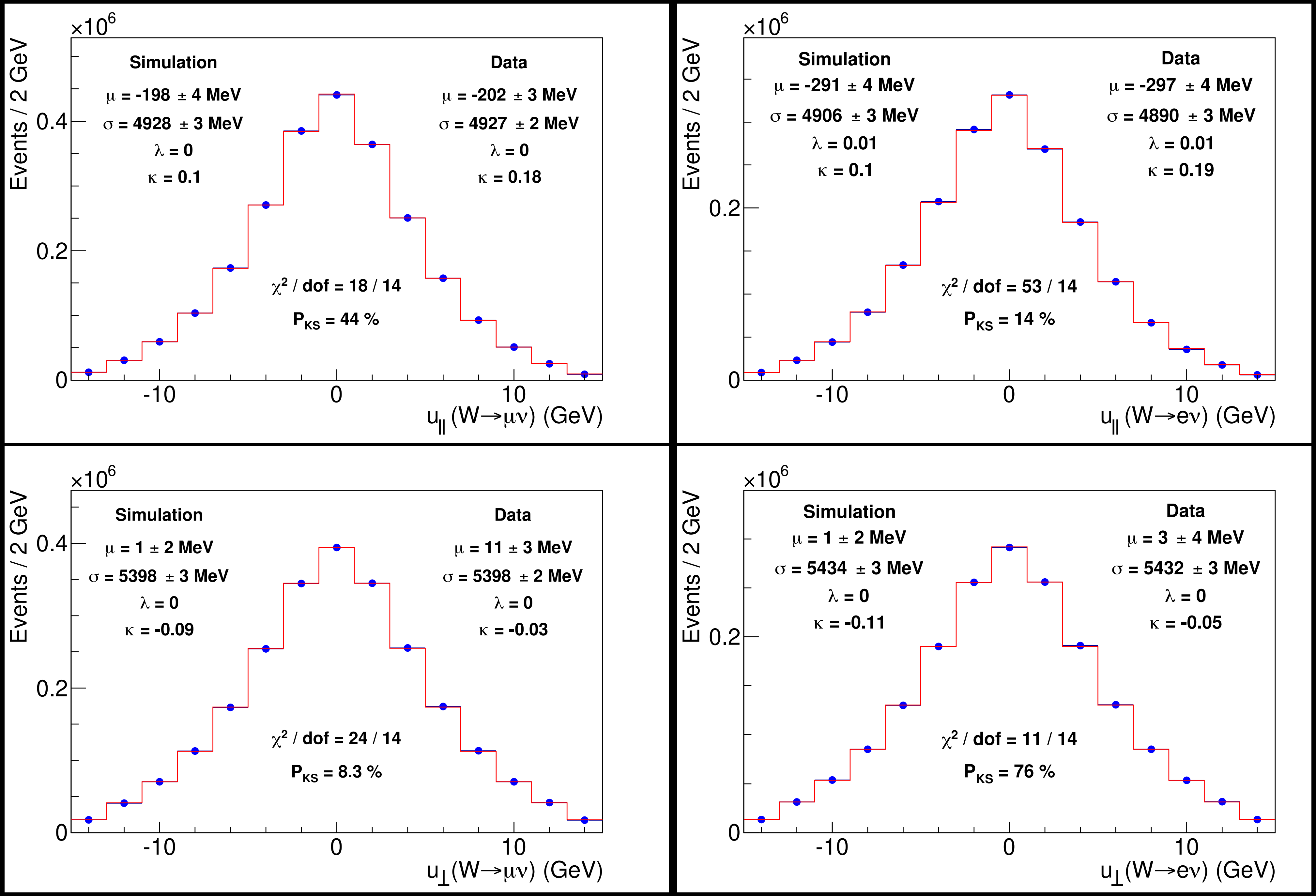

Recoil model parameters

Parameter	Description	Source	m_T	p_T^{ℓ}	p_T^{ν}
a	average response	Fig. S23	−1.6	−2.9	−0.2
b	response non-linearity	Fig. S23	−0.8	−2.0	0.7
Response			1.8	3.5	0.7
N_V	spectator interactions	Fig. S24	0.5	−3.2	3.6
s_{had}	sampling resolution	Fig. S24	0.3	0.3	0.8
$f_{\pi^0}^{4}$	EM fluctuations at low u_T	Fig. S25	−0.3	−0.2	−1.0
$f_{\pi^0}^{15}$	EM fluctuations at high u_T	Fig. S25	−0.3	−0.3	−0.2
α	angular resolution at low u_T	Fig. S26	1.4	0.1	2.5
β	angular resolution at intermediate u_T	Fig. S26	0.2	0.1	0.7
γ	angular resolution at high u_T	Fig. S26	0.3	0.3	0.7
f_2^a	average dijet component	Fig. S27	0.1	−1.1	0.8
f_2^s	variation of dijet component with u_T	Fig. S27	−0.1	−0.2	−0.1
k_ξ	average dijet resolution	Fig. S28	−0.1	0.1	−0.3
δ_ξ	fluctuations in dijet resolution	Fig. S28	−0.2	0.2	−1.1
A_ξ	higher-order term in dijet resolution	Fig. S28	0.1	−1.0	0.7
μ_ξ	—"—	Fig. S28	−0.5	−0.4	−0.9
ϵ_ξ	—"—	Fig. S28	0.1	−0.2	0.4
S_ξ^+	—"—	Fig. S28	0.5	−0.4	1.4
S_ξ^-	—"—	Fig. S28	−0.3	−0.2	−0.5
q_ξ	—"—	Fig. S28	−0.2	0.0	0.2
Resolution			1.8	3.6	5.2

Z mass fits using tracker or calorimeter

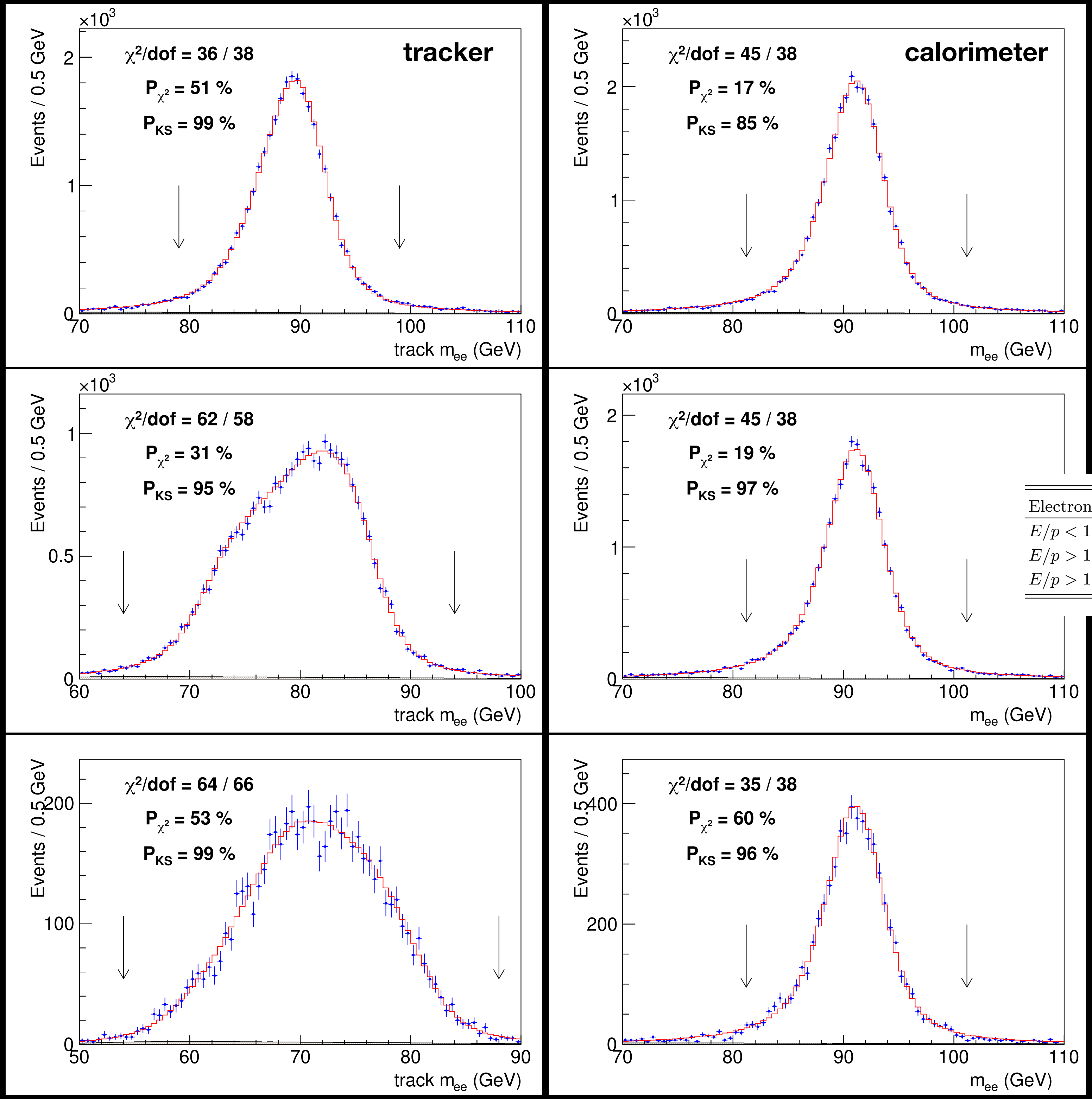

Electrons	Calorimeter	Track
$E/p < 1.1$ only	$91\,190.9 \pm 19.7$	$91\,215.2 \pm 22.4$
$E/p > 1.1$ and $E/p < 1.1$	$91\,201.1 \pm 21.5$	$91\,259.9 \pm 39.0$
$E/p > 1.1$ only	$91\,184.5 \pm 46.4$	$91\,167.7 \pm 109.9$

Recoil reconstruction in muon channel

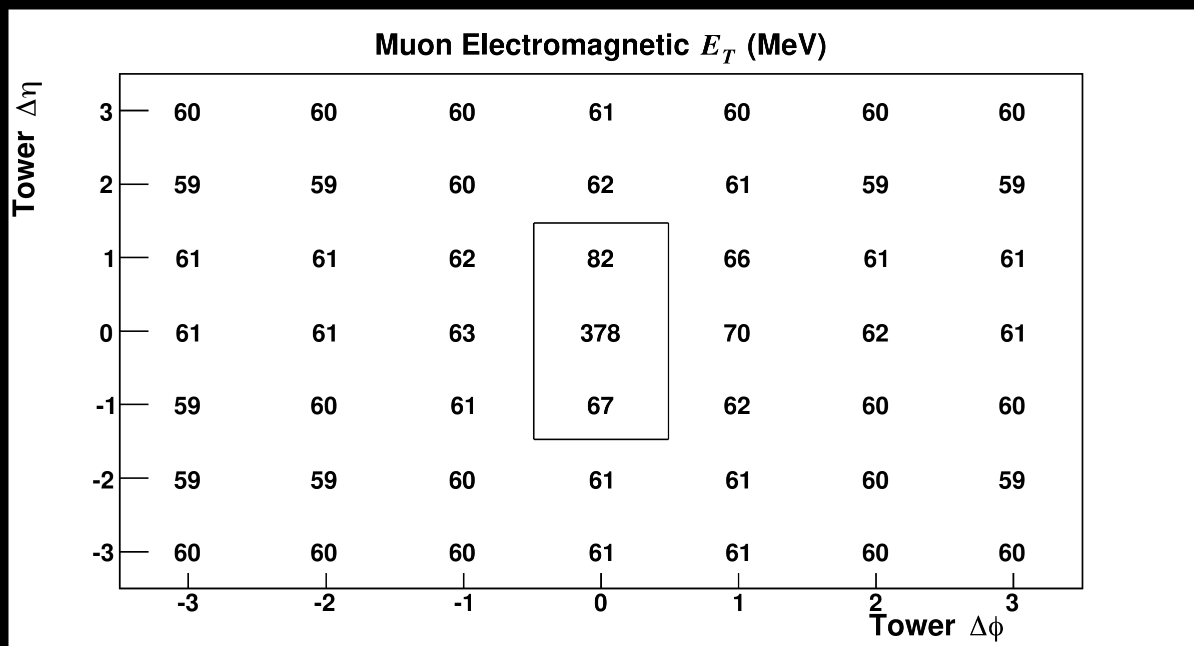

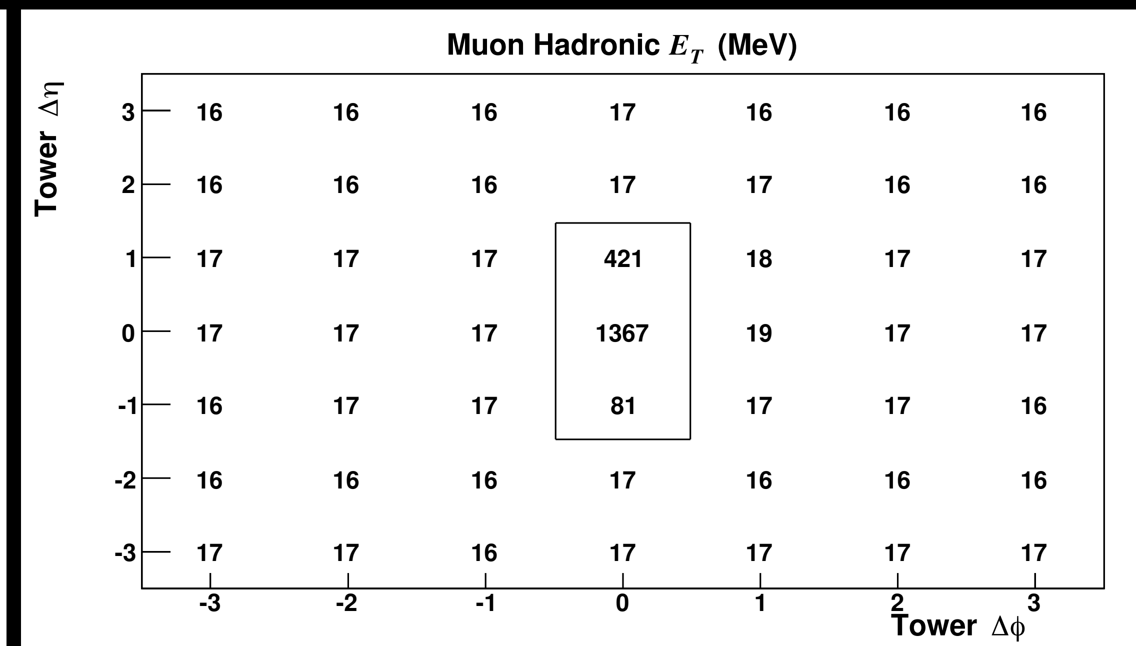

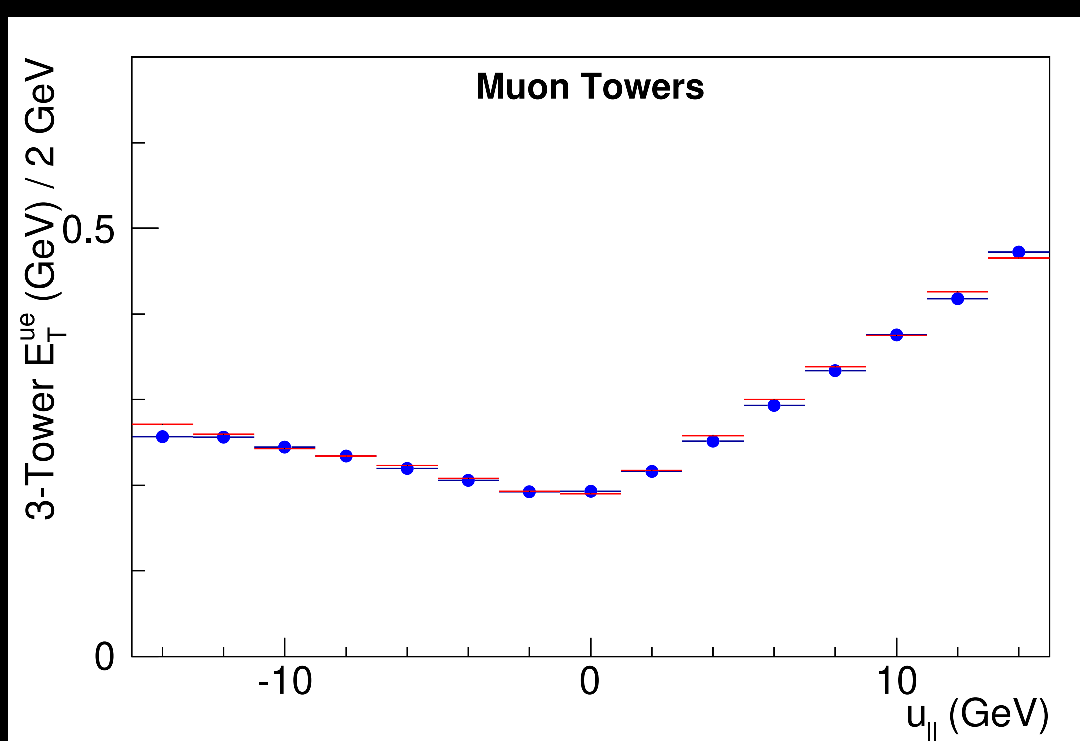

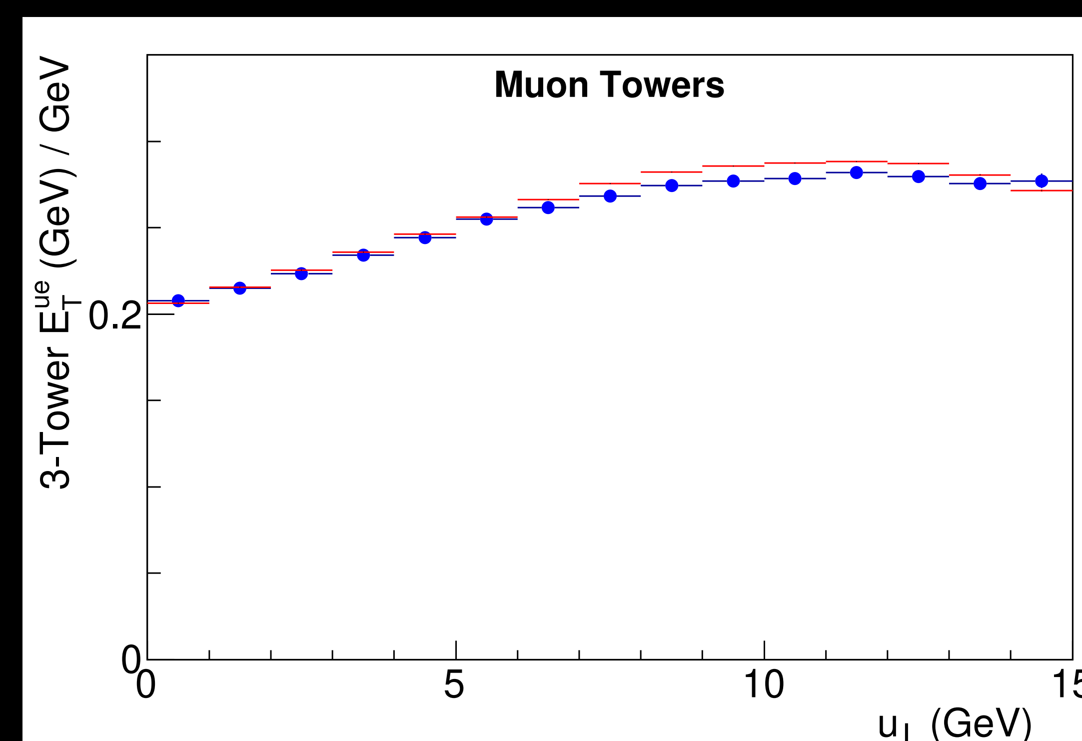

Electron momentum calibration

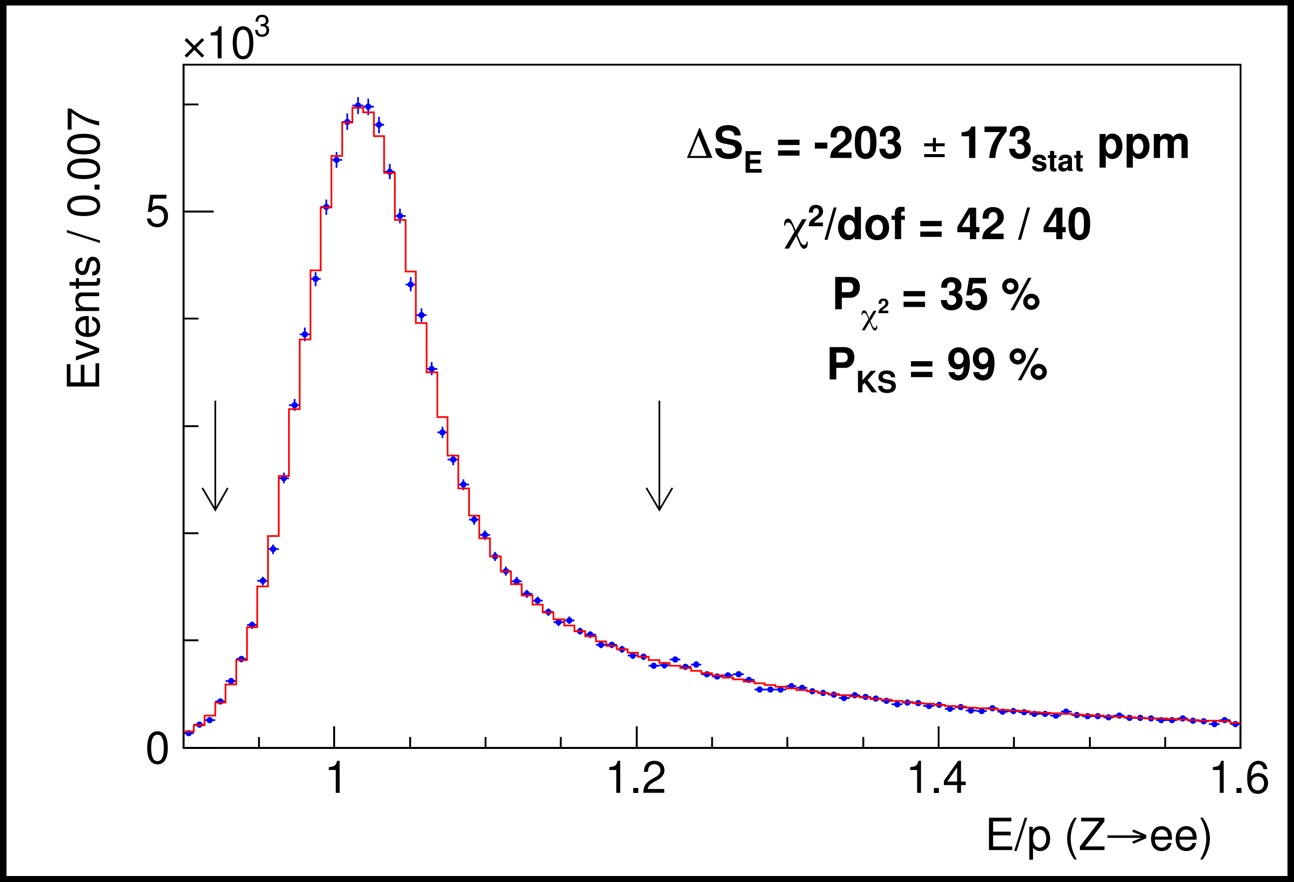

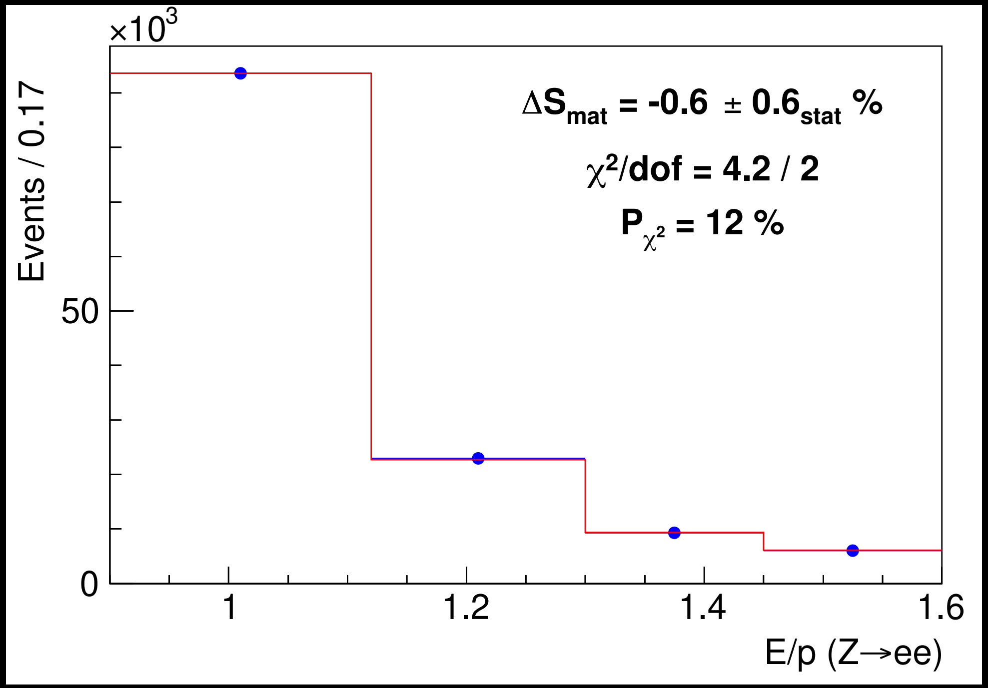

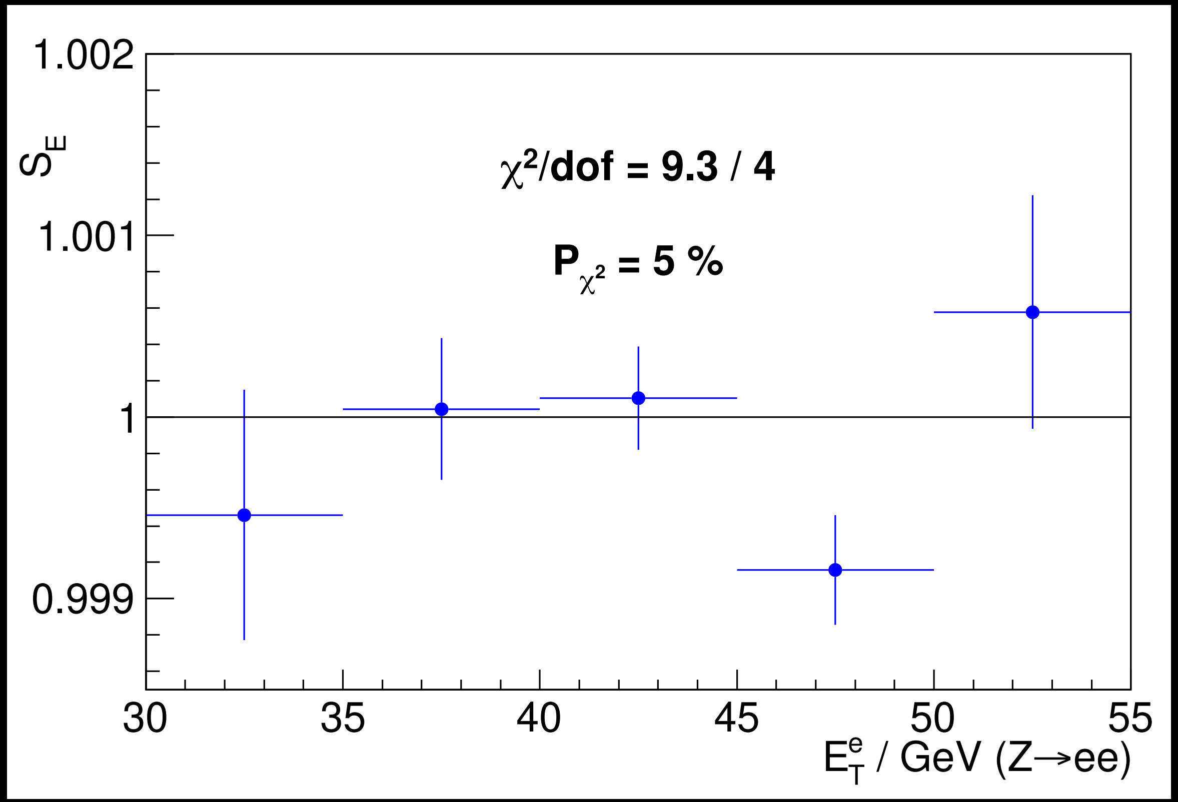

Electroweak observables at dimension 6

$$\boxed{Q_{HWB}, Q_{HD}}, \boxed{Q_{H\ell}^{(1)}, Q_{H\ell}^{(3)}, Q_{Hq}^{(1)}, Q_{Hq}^{(3)}, Q_{He}, Q_{Hu}, Q_{Hd}}, \boxed{Q_{\ell\ell}}$$

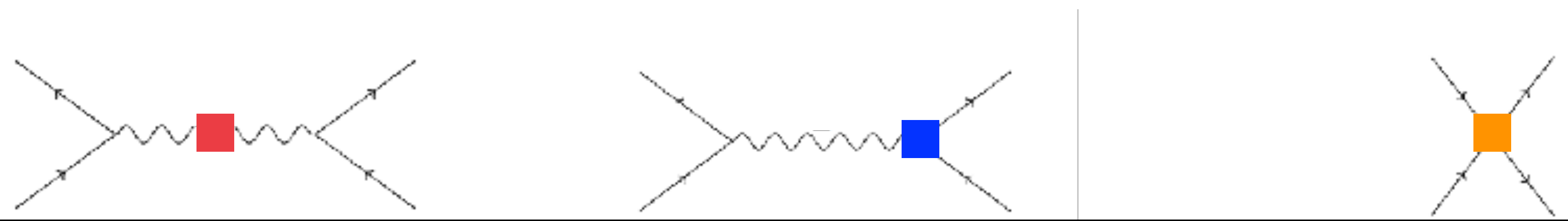

Parameter	Input Value
$\hat{m}_Z$	91.1875 ± 0.0021
$\hat{G}_F$	$1.1663787(6) \times 10^{-5}$
$\hat{\alpha}_{ew}$	$1/137.035999074(94)$

$$\frac{\delta m_W^2}{\hat{m}_W^2} = \hat{\Delta}\left[4\,C_{HWB} + \frac{c_{\hat{\theta}}}{s_{\hat{\theta}}}C_{HD} + 4\frac{s_{\hat{\theta}}}{c_{\hat{\theta}}}C_{H\ell}^{(3)} - 2\frac{s_{\hat{\theta}}}{c_{\hat{\theta}}}C_{\ell\,\ell}\right]$$

Observable	Experimental Value	Ref.	SM Theoretical Value	Ref.
$\hat{m}_Z$[GeV]	91.1875 ± 0.0021	[19]	–	–
$\hat{m}_W$[GeV]	80.385 ± 0.015	[49]	80.365 ± 0.004	[50]
Γ_Z[GeV]	2.4952 ± 0.0023	[19]	2.4942 ± 0.0005	[48]
R_ℓ^0	20.767 ± 0.025	[19]	20.751 ± 0.005	[48]
R_c^0	0.1721 ± 0.0030	[19]	0.17223 ± 0.00005	[48]
R_b^0	0.21629 ± 0.00066	[19]	0.21580 ± 0.00015	[48]
σ_h^0 [nb]	41.540 ± 0.037	[19]	41.488 ± 0.006	[48]
$A_{\rm FB}^\ell$	0.0171 ± 0.0010	[19]	0.01616 ± 0.00008	[32]
$A_{\rm FB}^c$	0.0707 ± 0.0035	[19]	0.0735 ± 0.0002	[32]
$A_{\rm FB}^b$	0.0992 ± 0.0016	[19]	0.1029 ± 0.0003	[32]